Biomechanics of the pelvic floor musculature

Štěpán Janda

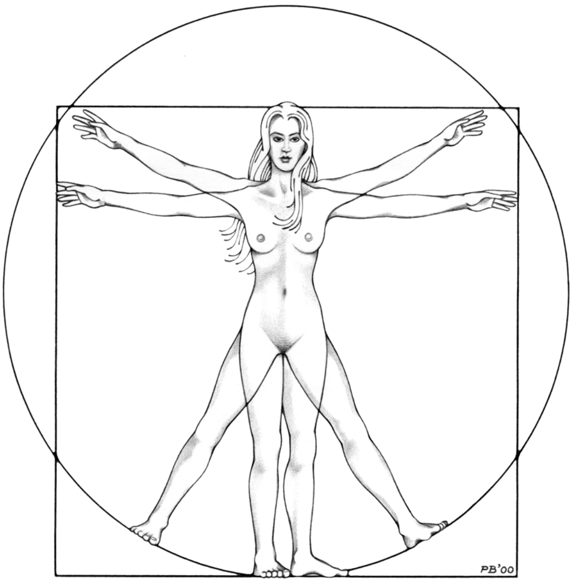

Biomechanics of the pelvic floor musculature

Proefschrift

ter verkrijging van de graad van doctor
aan de Technische Universiteit Delft,
op gezag van de Rector Magnificus prof.dr.ir. J.T. Fokkema,
voorzitter van het College voor Promoties,
in het openbaar te verdedigen op maandag 30 januari 2006 om 15:30 uur
door

Štěpán JANDA

inženýr
Fakulta strojní
České vysoké učení technické v Praze
geboren te Jablonec nad Nisou, Tsjechië.

Dit proefschrift is goedgekeurd door de promotoren:

Prof. dr. F.C.T. van der Helm	Technische Universiteit Delft
Prof. dr. ir. H.G. Stassen	Technische Universiteit Delft

Toegevoegd promotor:

Dr. S. de Blok	Technische Universiteit Delft

Samenstelling promotiecommissie:

Rector Magnificus	voorzitter
Prof. dr. F.C.T. van der Helm	TU Delft, promotor
Prof. dr. ir. H.G. Stassen	TU Delft, promotor
Dr. S. de Blok	TU Delft, toegevoegd promotor
Prof. dr. H.A.M. Brölmann	VU Amsterdam
Prof. dr. P.A.J.B.M. Huijing	U-Twente/VU Amsterdam
Prof. dr. ir. F. van Keulen	TU Delft
Prof. dr. P.J. Prendergast	Trinity College Dublin, Ierland
Prof. dr. A.M. Vossepoel	TU Delft, reservelid

Title:	Biomechanics of the pelvic floor musculature
Author:	Štěpán Janda
Subject headings:	Pelvic floor, finite element modelling, genital prolapse, MRI, EMG
Cover:	The 3D geometrical model of the pelvic floor muscles based on the experimental data set from the MRI measurements.
Cover design:	Štěpán Janda

Email:	s.janda@gmail.com

ISBN 90-9020334-6

To my family

TABLE OF CONTENTS

Chapter 1

GENERAL INTRODUCTION

1.1 INTRODUCTION

One of the long-term problems of vaginal childbearing is the traumatic injury to the support structures of the vagina and uterus. While these injuries are not at first obvious, as time passes these problems become evident by the tendency of the vagina and uterus to prolapse down to and sometimes through the vaginal opening in about 10% of women. This descent of the vagina tends to cause the bladder to protrude into the vagina (cystocele) and/or rectum to protrude into the vagina (rectocele). These prolapse problems seem to be accelerated by smoking, chronic lung disease and menopause. Sufferers tend to complain of pelvic pressure, pain, urinary or faecal incontinence or complete prolapse of the vagina. Surgery is frequently required to correct prolapse problems. Hysterectomy (removing of the uterus) is usually included in the management plan. In severe cases, synthetic mesh material or natural fascia may be used to "patch" injured support tissue.

The life-time risk of needing surgery for genital prolapse in the U.S.A. is 11%. Among these women, one in every four needs a second operation (Olsen et al., 1997). Among women with documented prolapse, 76% had a defect in the support of the posterior compartment (rectocele) (Olsen et al., 1997). Various surgical procedures have been advocated for repair of pelvic floor organ prolapse depending on the site of the defect (Richardson et al., 1976, Hurt, 1997). Prolapse can recur postoperatively in up to 34% of cases (Shull et al., 1994). It is possible that the recurrences may be the results of failure to identify the causative lesion in the pelvic floor before operation (Hoyte et al., 2000). In the Netherlands about 20% of new patients sent to outpatient gynaecology clinics present with symptomatic pelvic organ prolapse (National Medical Registration) and more than 1.000.000 patients with incontinence (29 % of females between 45 and 70 years old, 6 % urge-incontinence and 23 % combined incontinence). Despite the common occurrence of genital prolapse, the structural defects responsible for its formation remain poorly understood.

Many research groups and national or international pelvic floor societies were established recently in order to obtain more knowledge and to improve treatment in the pelvic floor. A new development has been done in minimally invasive techniques (laparoscopic surgery) used during surgery of the pelvic floor. However, the success of the surgery has not improved. There is a little knowledge about biomechanics, forces, stresses and pressure in the pelvic floor. Therefore, research in this field is necessary in order to obtain basic knowledge about the pelvic floor and pelvic floor disorders. Our research goal is to study the complex biomechanical behaviour of the pelvic floor muscles and to investigate the effectiveness of reconstructive surgery.

1.2 FUNDAMENTALS OF THE FEMALE PELVIC FLOOR ANATOMY

1.2.1 DIAPHRAGMA PELVIS AND DIVISION OF THE M. LEVATOR ANI

The levator ani, with its superior and inferior fascial covering, constitutes the pelvic diaphragm (see Figure 1.1). In pronograde four-legged animals, it functions primarily as a tail wagger. When humans assumed an upright posture, they lost the tail as a functioning appendage, and the levator ani took on an entirely different purpose. The comparative anatomy of this evolution has functional significance and relevance to the physiology of the pelvis.

The width of the pelvic floor compartment (see Figure 1.1) is only about one-third that of the abdomen (Power, 1948). The viscera in the pelvis occupies most of the pelvic floor and separate the peritoneum from the pelvic diaphragm. The viscera are actually embedded in a mass of connective tissue that forms the layers of the endopelvic fascia. The pelvic diaphragm is a thin muscular layer (2 to 6 mm in thickness). In fact, the vagina forms the one weak spot on the pelvic floor, and it is only in the vagina that hernias, such as cystocele, rectocele, and prolapse, occur (Nichols and Randall, 1996).

The levator ani is composed of three general portions (see Figure 1.1), each named according to its origin of insertion. The medial and anterior division is the pubococcygeus, which, from the gynaecologist's clinical point of view, is the most significant component of the levator ani.

Originating on the face of the pubis, approximately 1.5 cm either side of centre, a substantial portion of the levator ani sweeps downward and posteriorly along the sides of the urethra, vagina, perineal body, and rectum. These muscles appear to have clinically significant attachments to the connective tissue along the side of the urethra, the vagina, the rectum, and the upper portion of the perineal body. Because these attachments vary considerably in strength and integrity, the support and protection that they provide to both internal and external genitalia vary as well. There appear to be specific bundles of pubococcygeus fibres that extend medially. These bundles contribute to the posterolateral investment of the urethra (pubourethralis) and provide a slinglike posterior support to the rectum (puborectalis).

The puborectalis may be a distinct development of the most medial portion of the pubococcygeus. It is often believed, that the puborectalis is a distinct muscle intimately associated anteriorly, but distinctly separated posteriorly from the pubococcygeus. The two muscles appear to have a common origin, although the pubococcygeus arises on a higher plane. The puborectalis arises from the lowest portion of the symphysis pubis and from the deep layers of the triangular ligament. It passes downward and backward on either side of the vagina and lateral aspect of the rectum, with the two sides coming together again at the levator plate. It is continuous with the deep external anal sphincter. It fuses posteriorly in the midline, providing muscular support for the anorectal junction. Thus the puborectalis serves an important role in rectal continence.

The right and left muscle bellies of the pubococcygei fuse in the midline posterior to the rectum and continue to the coccyx. The rectum, vagina, and urethra pass through the levator hiatus, and both the rectum and the vagina rest on the levator plate. The normal horizontal position of this supporting levator plate accounts for the normal horizontal axis of the upper vagina. If the levator ani muscle is defective, the plate inclines downward and the hiatus sags.

Although the importance of the levator plate in providing pelvic support has been recognised and defined (Hadra, 1888; Halban and Tandler, 1907), the rectal distention and the absence of muscle tone in cadavers made it difficult to demonstrate the function of the plate. Berglas and Rubin (1953), however, were able to demonstrate this plate in the living and to relate its pathologic displacement with various degrees of genital prolapse. They did so by injecting contrast material in the vagina, uterus, and rectum. Radiograms taken of various patients while resting and while straining clearly showed the position of the normal plate as well as tipping of the plate in patients with genital prolapse.

In the standing patient, the horizontal levator plate extends from the coccyx toward the midportion of the pubic symphysis, but does not reach it. The anterior margin of the plate is separated from the posterior margin of the pubis by the levator or genital hiatus. When the supports of the plate are damaged and it tips, not only do the organs above it "slide downhill", but also the anteroposterior diameter of the hiatus increases significantly, providing a larger portal for the egress of prolapsing organs (Nichols and Randall, 1996).

The intermediate portion of the levator ani, the iliococcygeus, is somewhat thinner and flatter than the pubococcygeus and measures between 0.05 and 1 cm in thickness. Originating from the surface of the obturarius internus fascia, this muscle inserts along the lateral margin of the coccyx and lower sacrum. Contrary to popular belief, the iliococcygeus is often convex (dome shape) rather than concave (basin shape), because fat within the ischiorectal fossa pushes on the soft belly of the muscle (Quinby, 1954). This pressure occurs when the woman is sitting or reclining, as these positions exert force on the ischiorectal fat from below. A massive weight reduction that results in a loss of ischiorectal fat decreases the under support of the pelvic diaphragm, thus predisposing the levator muscle to sag, the levator plate to tip, and genital prolapse to develop subsequently (Nichols and Randall, 1996).

The most posterior major division of the levator ani is the coccygeus muscle, which originates in the ischial spine and inserts along the fourth and fifth lateral margins of the coccyx and lower sacrum.

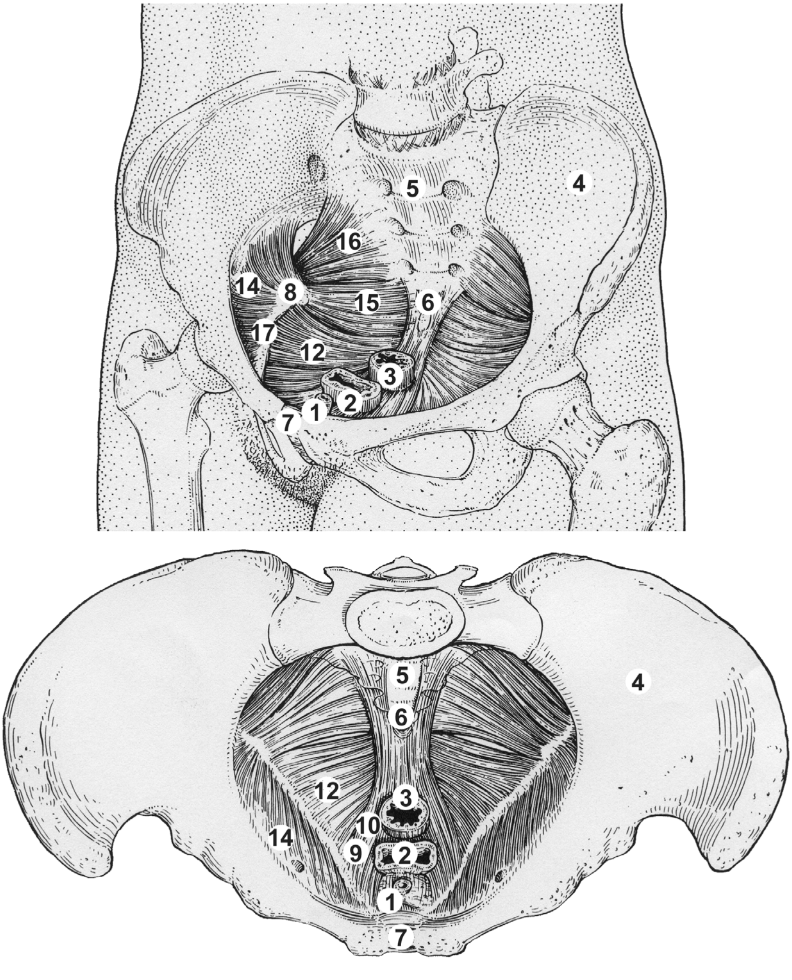

FIGURE 1.1: *Anatomy of the pelvic floor in standing female subject. Oblique view on the top, superior view below. A number of muscles combine with ligaments forms the pelvic floor diaphragm, which support the pelvic floor organs (adapted from Evers et al., 1990). Legend:* ***1*** *- urethra,* ***2*** *- vagina,* ***3*** *- rectum,* ***4*** *- os ilium,* ***5*** *- sacrum,* ***6*** *- coccyx,* ***7*** *- pubic symphysis,* ***8*** *- ischial spine,* ***9*** *- m. pubovaginalis,* ***10*** *- m. puborectalis,* ***9 + 10*** *- m. pubococcygeus ,* ***12*** *- m. ileococcygeus,* ***12*** *- m. levator ani,* ***14*** *- m obturatorius internus,* ***15*** *- m. coccygeus,* ***16*** *- m. piriformis,* ***17*** *- arcus tendineus*

1.2.2 Pelvic floor organs and structures

Female pelvis organs are readily distensible within certain maximal limits. Bladder, vagina, and rectum distend quite independently in the course of their normal functions, and each rather quickly resumes its usual or resting shape, dimension, and relationship when distension is no longer necessary. Functioning in concert, they reinforce one another. The histological components that permit such a range of activity include combinations of varying amounts of smooth muscle, striated muscle, elastic tissue, and collagen.

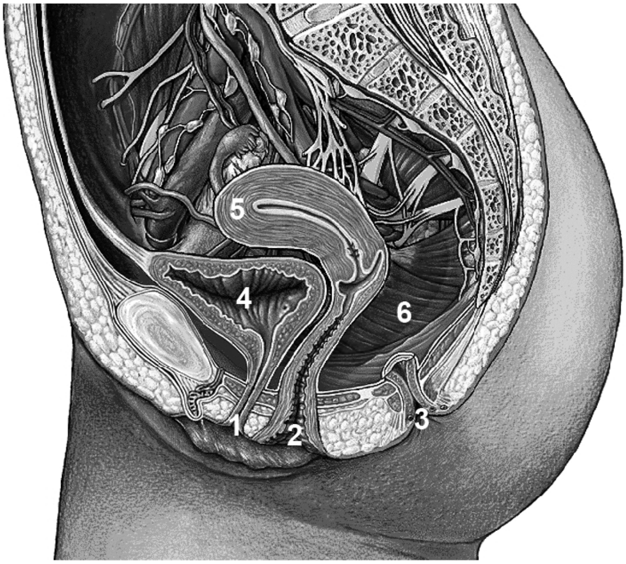

Figure 1.2: *Anatomy of the pelvic floor in standing female subject. Medial view (adapted from ADAM Student Atlas of Anatomy). Legend: **1** - urethra, **2** - vagina, **3** - rectum, **4** - bladder, **5** - uterus, **6** - diaphragma pelvis*

Bladder

The bladder (see Figure 1.2) is the urine reservoir crucial for proper lower urinary function (continence and micturation). The bladder lies posterior to the pubic bones, separated from the pubic bones by the retropubic space, which contains areolar tissue, veins and, near the bladder base, supportive ligaments. With distension the bladder rises over the upper border of the pubic bone, with the bladder base or trigonum in a relatively fixed position. The wall of the bladder consists of three layers: an inner layer of mucous membrane, a smooth muscle layer and an outer adventitial layer, in some regions covered by peritoneum.

VAGINA

The vagina (see Figure 1.2) transverses the pelvic floor in a sagittal oblique plane. The vagina is a fibromuscular sheath extending from the uterine cervix to the vestibule. The length is approximately 7.5 cm anterior and 8.5 cm posterior. The walls are collapsed with the lumen flattened in the anteroposterior plane (H-shape). The smooth muscle coat primarily has a longitudinal orientation.

UTERUS

The uterus (see Figure 1.2) is a midline visceral organ, pear-shaped and mainly horizontal in orientation. The upper two-thirds constitutes the body and the lower one-third the uterine cervix. In general the cervix is tilted forward from the coronal plane: anteversion, while the body is slightly flexed on the cervix: anteflexion. The uterus is above the pelvic diaphragm.

SMOOTH MUSCLE

Smooth muscle has the least complex histological structure of all muscle types. It is composed of elongated, tapering, isolated, or small groups of cells. Each cell has one centrally located nucleus. The cells vary greatly in length. It possesses no visible cross-striations. Smooth muscle cells are arranged in bundles and layers and in many sites are associated with elastic or connective tissue. Smooth muscle tissue is also referred to as involuntary muscle because most smooth contractions occur without voluntary control. The speed of contraction in smooth muscles is very slow compared with skeletal muscle, and the duration is often prolonged (Keele and Neil, 1971).

SKELETAL MUSCLE

In contrast to smooth muscle, it is composed of elongate, multinucleate, cylindrical structures called fibres that bear alternating dark and light cross-markings of striations. The striations are caused by the presence of intracellular fibrils. Skeletal muscle is also referred to as voluntary muscle because its contractions are under voluntary control. The striated and smooth muscles have complementary activities that permit and contribute to functional changes within the limitations of the pelvic supporting tissues. For more information about the skeletal muscle see Section 1.4 on page 11.

ARCUS TENDINEUS

The arcus tendineus lies on side of the pelvis (see Figure 1.1). The arcus tendineus of the levator ani runs from the back side of the pubis to the ischial spine. The arcus tendineus of the levator ani provides a soft tissue attachment for the connective tissue bundle of fibres attaches to the anterior vaginal sulcus.

Perineal body

The perineal body is a pyramidal fibromuscular node located midline between urogenital region and the anal sphincter. At this center numerous striated muscles and fascia converge and interlace: the longitudinal muscle of the anorectum, the pubovaginal part of the pubococcygeus muscle, perineal membrane, superficial transverse perineal muscle, bulbospongiose muscle and external anal sphincter. In women the insertion is larger, and the imbrication of the muscle fibers is more pronounced. Therefore, it is often described as the perineal body. The involvement of numerous muscles with their attachments to several parts of the pelvic ring (e.g. anal sphincter is connected to the coccyx by the anococcygeal ligament), give the perineal body an important function in the complex interaction of pelvic floor muscles.

Elastic Tissue

Elastic tissue fibres are constructed in irregular networks that are especially well suited for tissues that are frequently subject to stress. These fibres respond to stress with stretching, but they resist such stretching by a natural tendency to return to their original state, much as a rubber band does. The histogenesis of these fibres is unknown, although they are apparently produced by fibroblastic cells. The quantity of elastic tissue decreases with age (Nichols and Randall, 1996).

Collagen

Like elastic tissue fibres, collagen fibres are arranged in an interlacing meshwork. Unlike elastic tissue fibres, they are limited in stretch (up to 5%). With age they swell, fuse, and become hyalinized. Because they are flexible, they permit movement without stretching, much like a piece of string or rope.

Bone and Cartilage

Bone and cartilage are inflexible, firm, and strong. They resist sudden strain and stress, but respond to prolonged stress and sprain by gradual changes in architecture. This response appears to be both age- and hormone-related.

1.2.3 Anatomic pelvic support systems

There are several different anatomical systems contribute varying degrees of support to the pelvic compartment (Nicols and Randall, 1996):

1) Bone

2) Ligaments and other connective tissue

3) Muscles

Though each of these systems is a separate anatomic unit, they are interrelated, and additional components may exert synergistic, supportive, or even sphincterlike action. It is uncommon for any of these anatomic units to be individually defective, other than by congenital anomaly. These systems can be injured or damaged separately, however, or they can be injured or damaged in various combinations. Damage may be primary, secondary, or both.

1.3 PELVIC ORGAN PROLAPSE

Pelvic organ prolapse (genital prolapse) is a condition in which organs, which are normally supported by the pelvic floor, namely the bladder, bowel and uterus, herniate or protrude into the vagina (see Figure 1.3). This occurs as a result of damage to the muscles and ligaments making up the pelvic floor support.

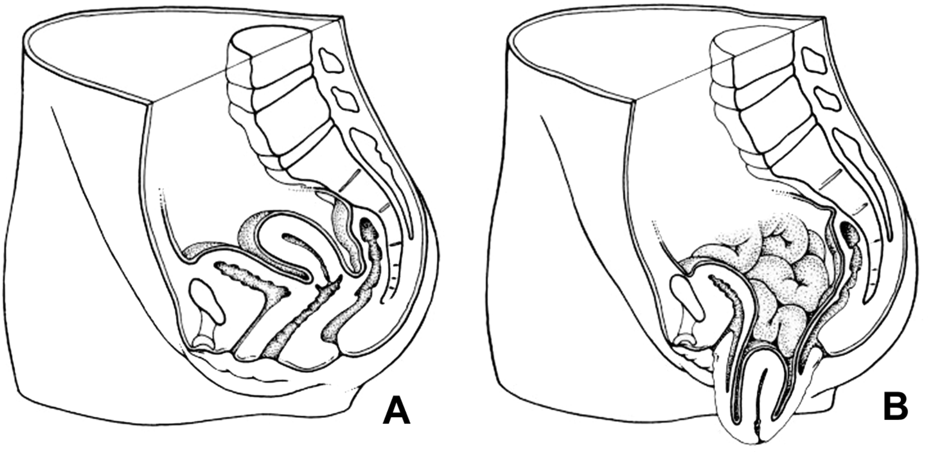

FIGURE 1.3: *Mechanism of the pelvic organ prolapse.* ***A*** *- Normal anatomical position.* ***B*** *- Total pelvic organ prolapse (adapted from Obstetrie en gynaecologie, Treffers et. al., 1995).*

Childbirth is the most common cause of damage to the pelvic floor, particularly where prolonged labour, large babies and instrumental deliveries are involved. Other factors include past surgery such as hysterectomy, lack of oestrogen due to the menopause, and conditions causing chronically raised intra-abdominal pressure such as chronic constipation, coughing, and heavy lifting.

1.3.1 Mechanisms of pelvic organ prolapse

M. levator ani is largely responsible for supporting both pelvic and abdominal organs and acts synergistically with the striated muscle of the anterior abdominal wall, also generating intra-abdominal pressure. Any increase in intra-abdominal pressure e.g. caused by coughing or sneezing, is applied equally to all sides of the pelvic and abdominal walls. If the levator ani is pathologically weakened or temporarily inactivated, the pressure on one side of a pelvic organ may become greater than that on the other, permitting the organ to descend (genital prolapse). If this movement carries the organ outside the pelvic cavity, pressure in the content of that organ will be directed unequally. For example, if the visco-urethral junction is displaced outside the pelvic cavity, an increase in intra-abdominal pressure normally distributed equally on the intraperitoneal or intra-abdominal portion of the urethra and the bladder, will affect the bladder alone. As a result, the intravesical pressure will increase more than the intra-urethral pressure, and urinary incontinence will occur.

1.3.2 Treatment of prolapse

Surgery for pelvic support problems attempts to restore the normal anatomic position of the prolapsed areas and to improve symptoms, which may be caused by the prolapse. The choice of surgical procedure is individualized. Factors that may influence this choice include examination findings, previous surgery, age, other medical illnesses and patient/physician preference. The surgery typically includes repair of tears in the muscle or suspension of the prolapsed tissues to stronger structures in the pelvis. In some cases, a piece of tissue may be taken from another area to help strengthen the area. The surgery may be performed through a vaginal or abdominal incision or a combination of both. One of the goals of surgery for pelvic organ prolapse is to repair all of the defects that are present in order to prevent the need for surgery in the future. Therefore, many women will require a combination of these procedures.

Vaginal Procedures

Vaginal procedures are done through an incision in the vagina. Some of the common vaginal procedures are described below.

- Anterior repairs help strengthen the front wall of the vagina overlying the bladder.
- Posterior repairs correct tears that may exist in the back wall of the vagina (the area directly above the rectum). This type of surgery may involve the use of a graft (taking a piece of tissue from another part of the body) to help strengthen the area.

- Vaginal Vault Suspension procedures use sutures (stitches) to attach the top of the vagina to stronger structures in the pelvic region.
- Perineorrhaphy involves reconstruction of the area between the vagina and rectum.
- Colpocleisis includes partial or complete closure of the vagina.

ABDOMINAL PROCEDURES

Abdominal procedures are done through an incision in the abdomen. Some of the common procedures are described below.

- Abdominal Sacrocolpopexy suspends the top of the vagina to a strong ligament on the front part of the sacrum (lower back bone) using a piece of tissue, muscle, or ligament from another part of the body.
- Paravaginal Defect Repair repairs places where the vagina has torn away from its attachment to the tissue that connects to the pelvic bone.

1.4 SKELETAL MUSCLE

Skeletal muscle represents the typical example of a structure-function relationship. At both the macro as well as microscopic levels, skeletal muscle is excellently adapted for force generation and movement. Because of this structure-function relationship, studies of muscle function are intimately tied to studies of muscle structure.

Skeletal muscle makes up most of the body's muscle and does not contract without nervous stimulation. It is under voluntary control and lacks anatomic cellular connections between fibres. The fibres (cells) are multinucleate and appear striated due to the arrangement of actin and myosin protein filaments. Each fibre is a single cell, long, cylindric and surrounded by a cell membrane. The muscle fibres contain many myofibrils that are made of myofilaments. These myofilaments are made of the contractile proteins. The key proteins in muscle contraction are myosin, actin, tropomyosin and troponin.

Skeletal muscle fibres have differences in metabolic and contractile properties. Changes in muscle function can be caused by alterations in activity (training), hormonal environment, or innervation. Skeletal muscle can undergo a limited regeneration in case of injury via satellite cells that are located on the periphery of the muscle fibre. These cells may be active in muscle hypertrophy as well.

Skeletal muscle comprises the largest single organ of the body. It is highly compartmentalized, and we often think of each compartment as a separate entity. Each of these individual muscles is composed of single cells or fibres embedded in a matrix of collagen. At either end of the muscle belly, this matrix becomes the tendon that connects the muscle to bone.

Muscle cells contain most of the structures common to all cells. Each cell is enclosed by a cell membrane or plasmalemma; they contain mitochondria for the oxidative metabolism of nutrients; and all the machinery necessary for protein synthesis. Skeletal muscle fibres are multinucleated and can be several centimeters long.

1.4.1 Morphology and physiology

There are two kinds of muscles in the pelvic diaphragma: skeletal and smooth muscles. Skeletal muscles make up a major part of the body; it is the prime means of locomotion. Voluntary nerves control them. When stimulated at a sufficiently high frequency, they can generate a maximal tension, which remains approximately constant over time. In this case, the muscle is tetanized: The activity of the contracting mechanism is thought to be maximal.

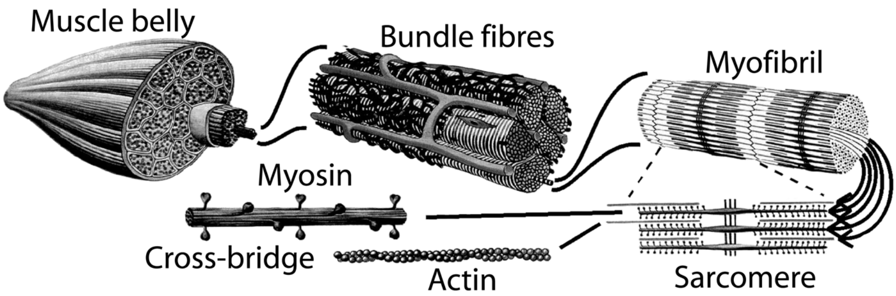

Figure 1.4: *Skeletal muscle anatomy adopted from Gray's anatomy (Warwick and Willems, 1973).*

Smooth muscles are not striated, and are not controlled by voluntary nerves. There are many kinds of smooth muscles, for example surrounding blood vessels.

Since a resting skeletal muscle has quite ordinary visco-elastic properties, the interesting part is the contraction. Muscles exert force when activated by stimuli from a nerve or artificially by an electrode. These stimuli start a chain reaction of chemical processes that initiate a connection between the actin filament and opposite myosin filament. Such a connection is addressed as a cross-bridge. The myo-filaments, actin and myosin, are together the smallest functional unit of a muscle, the sarcomere (Figure 1.4). In a muscle fibre a large number of sarcomeres are arranged in series. The alignment of sarcomeres in series, observed in parallel-arranged fibres, attributes to the name of striated muscle. Movement is initiated when the myo-filaments slide past one another. A large number of muscle fibres arranged in parallel form a muscle belly. Through aponeuroses (tendon-sheets) and tendons, the muscle fibres are attached to the bone structure at origin and insertion.

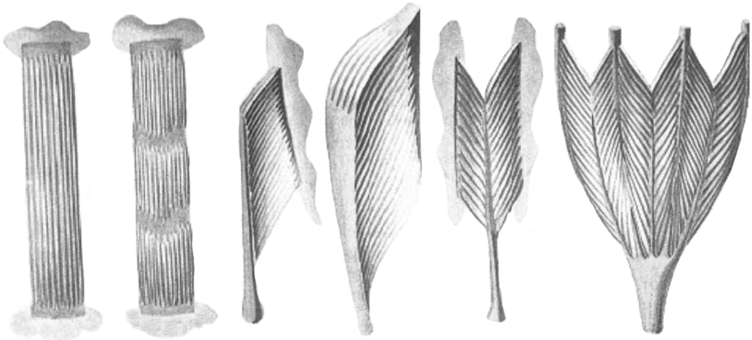

FIGURE 1.5: *Variety of muscle architectures, with from left to right: two parallel fibered, two uni-pennate and bi-pennate and multi-pennate muscle. Adopted from Gray's anatomy (Warwick and Willems, 1973).*

The arrangement of the fibres with respect to the line of pull in muscle defines muscle architecture. A schematic representation of a classification in architectural characteristics is given in Figure 1.5. The most common muscle architectures are the parallel fibered and the pennate muscles. In parallel fibered muscle (pelvic floor muscles) it is assumed that fibres are arranged along the line of pull of the muscle. The flat parallel architecture of the pelvic floor muscles suggests its function.

The active components of a muscle cannot function without the presence of passive mechanical structures. The fibres are arranged in a network of connective tissue, the endomysium (Figure 1.6). The muscle is organized in bundles of fibres, each bundle containing over a hundred fibres and surrounded by the perimysium. Finally, the outer surface of the muscle is shielded by the epimysium. Together with tendon and aponeurosis, the epimysium, perimysium and endomysium make up the passive, visco-elastic properties of the muscle. Other structures in the muscle, such as blood and lymph vessels, motor and sensor nerves, are not considered as contributing to the mechanical behaviour.

A muscle fibre is a single cell, ranging in length from a few millimeters to several centimeters, and in diameter from 10 to 100 μm. Unlike other cells, it has multiple nuclei, resulting from a fusion of myoblasts in the embryonic phase. The muscle fibres are organized in motor units with about 100 fibres not clustered but distributed over the muscle volume.

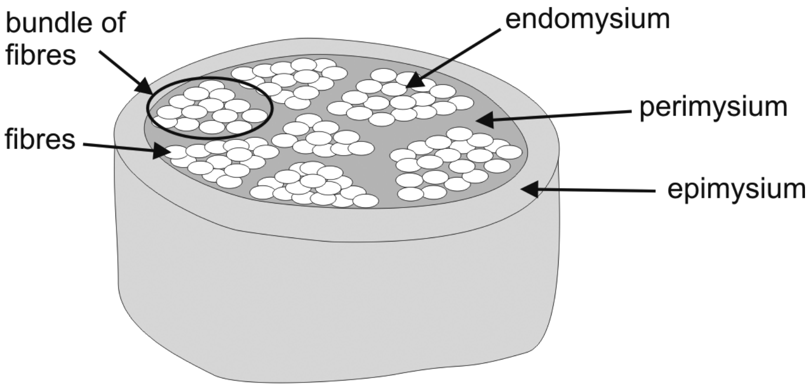

FIGURE 1.6: *Location of the connective tissues epimysium, perimysium and endomysium (adapted from Gielen, 1998).*

1.4.2 MECHANICS OF MUSCLE - MATERIAL AND STRUCTURAL PROPERTIES

Several aspects of muscle morphology and physiology have important consequences for the mechanics of muscle tissue. The main properties that define the amount of force exerted can be distinguished in material and structural properties.

Muscle is made of soft tissue, which allows large deformations. Like any other soft tissues, it has non-linear passive properties (Fung, 1981). From about the 18th century it is known, that the muscle volume is constant during contraction. In contrast with other biological soft tissues, muscle has the ability to exert force when activated. The level of activation determines the amount of force exerted. However, the level of activation depends on other properties such as firing rate of nerves, reaction rate of chemical process and other activation dynamic. The very important parameter for the amount of force exerted is muscle length, which is expressed in the force-length curve. According to the sliding filament theory (Huxley, 1957) sarcomere force depends on the amount of overlap of the myo-filaments. A characteristic point in this curve is the length at which maximal force is exerted, addressed as optimum length of sarcomere or fibre. Exerted force is reduced for lengths smaller than optimal length. Over optimum length, active force decreases. In addition, passive properties of the muscle tissue, however, contribute to the total force for lengths over passive slack length (the smallest length any force is exerted under passive condition).

Sarcomeres are arranged in series with each other in a muscle fibre. This suggests that force generated by these sarcomeres is equal. The fact that not all sarcomeres in series are identical, results in interaction that can lead to mechanical instable behaviour at lengths over optimum muscle fibre length (Sugi et. al., 1988). The number of sarcomeres in series determines the active length range of a muscle fibre. The amount of fibres arranged in parallel, the physiologic cross sectional area (PSCA) is a measure for the maximal active muscle force. The alignment of fibres in muscle indicates that muscle has anisotropic properties. Moreover, muscle architecture (e.g. pennation angle) is an important structural property as well.

1.5 MODELLING

In order to understand a complex system, it is often useful to extract most of its essential features and use them to create a simplified representation of the system or a model of the system. Such a model allows one to observe more closely the behaviour of the system and to make predictions regarding its performance under altered input conditions and different system parameters. Modelling is also widely used in biomechanics (Prendergast, 1997). The attractiveness of modelling is that many research questions can be tested (heuristic purpose of a model) and number of human experimental subjects can be limited. The great virtue of models is the heuristic purpose, besides predicting specific aspects of complex function. Another big advantage of a model is the freedom of the researcher to make the model as simple or as complex as his questions require, or as detailed as the outcome require.

1.5.1 CONTINUUM MODELLING BASED ON FE THEORY

Muscles in joint systems (e.g. in the upper or lower extremities) are activated to exert forces at the bones in line with their muscle line of action (Van der Helm, 1994). In contrast, the pelvic floor muscles are loaded perpendicular to the muscle line of action by the intra-abdominal pressure. A simple representation of the muscle action by a (one-dimensional) muscle line of action is not appropriate, but a more sophisticated approach using a finite element (FE) model of the muscle is necessary. In a FE model the relationship between the loading and muscle forces in three dimensions can be represented. FE models are numerical mathematical models - numerical because they rely on computers to find approximate solutions to large sets of equations. In order to create a FE representation of a structure, it is first conceptually divided into simple parts called elements. Consider a single element, the forces and displacements at the nodes are related by the stiffness matrix for the element. Each element has nodes, which join with the nodes on adjacent elements to re-create the total structure. The stiffness term for a node is then the addition of all the stiffness terms from the elements joined at that node. In this way, the stiffness matrix [**K**] for the whole structure can be obtained by re-assembly of the individual elements and it is called the global stiffness matrix. Equation 1.1 can be used to relate all nodal forces {F} and nodal displacements {δ}.

$$\{F\} = [\mathbf{K}] \cdot \{\delta\} \tag{1.1}$$

The forces on each node should be zero (equilibrium principle), except for the nodes to which an external load is applied. Knowing this, the entries can be inserted into {F}, and Equation 1.1 can then be solved for {δ} in order to obtain the complete set of nodal displacements. Strain and stress can be calculated from the nodal displacements if required.

1.5.2 Constitutive modelling

Continuum models based on FE theory are applied to study the mechanical behaviour and function of skeletal muscle. Biomechanical analysis of soft tissue requires quantification of their three-dimensional (3D) material properties, i.e. stress-strain behaviour. This necessitates accurate determination of stresses and strains under multiaxial loading, since uniaxial data do not uniquely characterize 3D. To present, such quantification has been partially successful for noncontracting tissue, including skin and blood vessels. Some studies have been performed on passive myocardium and passive and tetanised canine diaphragms (Strumpf et al, 1993). However, no multiaxial stress-strain data exist for the muscle tissue. The reasons for this include the complex geometry and composite nature of such tissue.

1.6 Definition of the problem

One in every nine women requires surgery for problems related to defective pelvic organ support. Among these women, one in every four needs a second operation (Olsen et al., 1997). Among women with documented prolapse, 76% had a defect in the support of the posterior compartment (rectocele) (Olsen et al., 1997). Despite the common occurrence of genital prolapse, the structural defects responsible for its formation remain poorly understood.

It is essential to understand these phenomena to improve surgical results. It is plausible that pelvic floor muscles have a fundamental influence in these disorders. Therefore, to study the complex biomechanical behaviour of the pelvic floor muscles and to investigate the effectiveness of reconstructive surgery, a computer model is necessary.

1.7 GOAL OF THE THESIS

The main research goal of this thesis is to study the complex biomechanical behaviour of the pelvic floor muscles and to investigate the effectiveness of reconstructive surgery.The goal is to study the pelvic organ prolapse mechanism (as described in Sections 1.2 and 1.5) and biomechanical behaviour of the pelvic floor muscles. The main loading of the pelvic floor muscles is due to intra-abdominal pressure. Muscles in joint systems (e.g. in the upper or lower extremities) are activated to exert forces at the bones in line with their muscle line of action. In contrast, the pelvic floor muscles are loaded perpendicular to the muscle line of action by the intra-abdominal pressure. A simple representation of the muscle action by a (one-dimensional) muscle line of action is not appropriate. A more sophisticated approach using a FE model of the muscle is necessary. In a FE model the relationship between the loading and muscle forces in three dimensions can be represented.

1.8 METHODOLOGY

Development of the FE model is presented in Figure 1.7. The experimental data concerning the pelvic floor morphology (geometrical data), muscle properties and loading data are necessary as well as boundary condition are necessary as an input for FE analysis. Thereafter, the displacement and the forces in diaphragma pelvis can be calculated.

The continuum model based on a FE theory is used for studying the mechanical behaviour of these muscles. The model is able to simulate several pathological situations such as temporary inactivation of the levator ani muscle or mechanism of the pelvic organ prolapse. Results of the analyses were validated using Magnetic Resonance Imaging (MRI) and electromyography EMG data obtained from experimental measurements performed on healthy volunteers as well as on patients. Moreover, the FE model should be able to predict the effect of surgical interventions and give insight into the function of pelvic floor muscles.

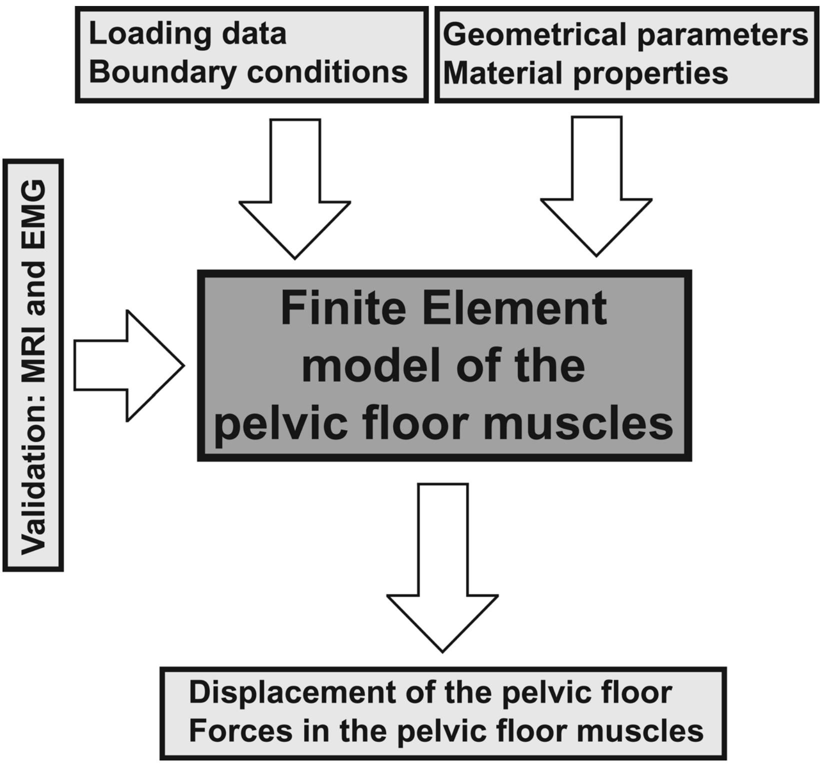

FIGURE 1.7: *Block diagram of the development of the FE model of the pelvic floor muscles*

1.9 CONTENTS OF THIS THESIS

The present thesis consists of chapters separately offered for publication, which can be studied independently of each other. The main goal of thesis is to study the complex biomechanical behaviour of the pelvic floor muscles. To this end the FE model of the pelvic floor muscles is developed (Chapter 6) and the pelvic floor muscles pathology is simulated (Chapter 7).

In ***Chapter 2***, the morphology of the pelvic floor is determined. Geometric parameters, as well as muscle parameters, of the pelvic floor muscles were measured on an embalmed female cadaver. A 3D geometric data set of the pelvic floor including muscle fibre directions has been obtained using a palpator device. A 3D surface model based on the experimental data, needed for mathematical modelling of the pelvic floor, has been created. For all parts of the diaphragma pelvis, the optimal muscle fibre length has been determined by laser diffraction measurements of the sarcomere length. In addition, other muscle parameters such as physiological cross-sectional area and total muscle fibre length were determined. Apart from these measurements we obtained a data set of the pelvic floor structures based on MRI of the same cadaver specimen.

In ***Chapter 3,*** a new constitutive model for the passive elastic behaviour of human pelvic floor muscles is developed. Since there was a lack of information concerning material properties of the pelvic floor muscles, we performed uniaxial and equibiaxial measurements. The data obtained are used to develop the Mooney-Rivlin (MR) constitutive model, which assumes the tissue to be isotropic and incompressible. The constants of the MR constitutive model are obtainable from experimental tests, which should be conducted with similar deformation modes to those appearing in vivo.

In ***Chapter 4***, the difference in the displacement of the pelvic floor muscles between 10 patients and 10 healthy volunteers is presented. The difference in EMG activity, the displacement, the intra-abdominal pressure (IAP) and the width of the levator hiatus are evaluated. In order to obtain the pelvic floor muscles response, the EMG measurements and the IAP measurements were performed simultaneously. Displacement was recorded separately using MRI.

In ***Chapter 5***, the effect of the loading of the pelvic floor by the weight of the internal organs in the erect and supine positions is investigated. The experimental measurements were performed using FONAR the Indomitable Stand-Up™ MRI machine. The effect of the loading of the pelvic floor (position, displacement and deformation of the diaphragma pelvis) was investigated in 12 female subjects (healthy volunteers) in the erect and supine positions.

In ***Chapter 6***, the biomechanical behaviour of the pelvic floor muscles is studied. The approach is to simulate the biomechanical behaviour of the pelvic floor muscles as a response to the loading by the IAP and muscle activation. We develop a FE model of the pelvic floor muscles based on cadaver morphology (Chapter 2) and a constitutive model for the passive elastic behaviour of human pelvic floor muscles (Chapter 3). The FE analysis of the pelvic floor muscles gives us the muscles' displacements in relation to the level of the IAP and muscle activation.

Chapter 7 continues the approach from Chapter 6. The FE model is used to understand the development of the genital prolapse as a result of the biomechanical loading of the pelvic floor musculature. Twelve specific load-cases are analysed using a biomechanical model based on FE theory. These load-cases describe the effect of the level of the muscle activation and IAP on the shape and displacement of the pelvic floor.

Finally, ***Chapter 8*** discusses results presented in this thesis and conclusions are drawn.

REFERENCES

Berglas, B., Rubin, I.C., 1953. Study of the supportive structures of the uterus by levator myography. Surg. Gyneocol Obstet, 97, pp 677-692.

Evers, J.L.H., Heineman, M.J., 1990. Gynaecology: A clinical atlas. St. Louis: Mosby.

Fung, Y.C., 1981. Biomechanics: mechanical properties of living tissue. Sprihger-Verlag, New York. ISBN 0-387-90472-7.

Gielen, S., 1998. A continuum approach to the mechanics of contracting skeletal muscle. PhD-thesis, Technical University of Eindhoven, Eindhoven.

Hadra, B.E., 1888. Lesions of the vagina and pelvic floor. Philadelphia: Records, McMullin.

Halban, J., Tandler, J., 1907. Anatomie und atiologie der genitalprolapse beim weibe. Vienna and Leipzig: Wilhelm Braumuller.

Hoyte, L., Schierlitz, L., Zou, K., Flesh, G., Fielding, J.R., 2001. Two- and 3-dimensional MRI comparison of levator ani structure, volume, and integrity in women with stress incontinence and prolapse. Am J Obstet Gynecol. 185, 11-19.

Hurt, W.G., 1997. Anterior colporrhaphy. In: Gershenson D, edior. Operative techniques in gynecologic surgery. Philadelphia: WB Saunders (Vol 2).

Huxley, A.F., 1957. Muscle contraction and theories of contraction. Prog Biophys Biochem, 7, 225-318.

Keele, C.A., Neil, E, 1971. Samson Wright's applied physiology, Twelfth edition, Oxford University press. ISBN 0-19-263316-3.

National Medical Registration of Dutch Hospitals. SIG Information, Utrecht, The Netherlands, 1996.

Nichols, D.H., Randall, O.L., 1996. Vaginal Surgery. Williams a Wilkins.

Olsen, A.L., Smith, V.J., Bergstorm, J.O., Colling, J.C., Clark, A.L., 1997. Epidemiology of surgically managed pelvic organ prolapse and urinary incontinence. Obstet Gynecol. 89, 501-506.

Power, R.M.H., 1948. Embryological development of the levator ani muscle. Am J Obstet Gynecol. 55, 367-381.

Prendergast, P.J., 1997. Finite element models in tissue mechanics and orthopaedic implants design. Clinical Biomechanics, Vol. 12, No. 5, 343-366.

Quinby, W.C., 1954. The anatomy and blood vessel of the pelvic floor. In: Meigs, J.V., ed. Surgical treatment of cancer of the cervix. New York: Grune & Stratton, 32.

Richardson, A.C., Lyon, J.B., Williams, N.E., 1976. A new look at pelvic relaxation. Am J Obstet Gynecol, 126, 568-573.

Shull, B.L., Benn, S.J., Kuehl, T.J., 1994. Surgical management of prolapse of the anterior vaginal segment: an analysis of support defects, operative morbidity, and anatomic outcome. Am J Obstet Gynecol. 171, 1429-1439.

Strumpf, R.K., Humphrey, J.D., Yin, F.C.P., 1993. Biaxial mechanical properties of passive and tetanized canine diaphragm. Am. J. Physiol. 365 (Heart Circ. Physiol. 34): H469-H475.

Sugi H., Tsuchiya T., 1988. Stiffness changes during enhancement and deficit of isometric force by slow length changes in frog skeletal muscle fibres. J Physiol, 407, 215-229.

Treffers, P.E., Heintze, A.P.M., Roland, K., 1995. Obstetrie en gynaecologie - De voortplanting van de mens. Utrecht 1995, Wetenschappelijke uitgeverij Bunge, ISBN 90-6348-049-0.

Van der Helm, F.C., 1994. A finite element muscoskeletal model of the shoulder mechanism. J Biomech, 27, 5, 551-569.

Warwic, R., Willems, P.L., 1973. Gray's Anatomy, 35th edition, Longman Group Ltd, Edinbourg, ISBN 0-443-01011-0.

Chapter 2

MEASURING MORPHOLOGICAL PARAMETERS OF THE PELVIC FLOOR FOR FE MODELLING PURPOSES

Abstract

The goal of this study was to obtain a complete data set needed for studying the complex biomechanical behaviour of the pelvic floor muscles using a computer model based on the finite element (FE) theory. The model should be able to predict the effect of surgical interventions and give insight into the function of pelvic floor muscles. Because there was a lack of any information concerning morphological parameters of the pelvic floor muscle structures, we performed an experimental measurement to uncover those morphological parameters. Geometric parameters as well as muscle parameters of the pelvic floor muscles were measured on an embalmed female cadaver. A three-dimensional (3D) geometric data set of the pelvic floor including muscle fibre directions was obtained using a palpator device. A 3D surface model based on the experimental data, needed for mathematical modelling of the pelvic floor, was created. For all parts of the diaphragma pelvis, the optimal muscle fibre length was determined by laser diffraction measurements of the sarcomere length. In addition, other muscle parameters such as physiological cross-sectional area and total muscle fibre length were determined. Apart from these measurements we obtained a data set of the pelvic floor structures based on nuclear magnetic resonance imaging (MRI) on the same cadaver specimen. The purpose of this experiment was to discover the relationship between the MRI morphology and geometrical parameters obtained from the previous measurements. The produced data set is not only important for biomechanical modelling of the pelvic floor muscles, but it also describes the geometry of muscle fibres and is useful for functional analysis of the pelvic floor in general. By the use of many reference landmarks all these morphologic data concerning fibre directions and optimal fibre length can be morphed to the geometrical data based on segmentation from MRI scans.

These data can be directly used as an input for building a mathematical model based on FE theory.

Keywords

Pelvic floor muscles; Sarcomere length; FE model; MRI

Published in ***J. Biomechanics 36(6) 2003, pp. 749-757.***

2.1 INTRODUCTION

The human pelvic floor is a very complex muscular structure (m. levator ani, m. coccygeus). The m. levator ani with its facial covering constitutes the pelvic diaphragm. In four-legged animals, its primary function is to wag the tail. When humans assumed an upright posture, they lost the tail as a functioning appendage, and the m. levator ani complex took on an entirely different purpose. The comparative anatomy of this evolution has functional significance and relevance to the physiology of the pelvis.

M. levator ani is largely responsible for supporting both pelvic and abdominal organs and acts synergistically with the striated muscle of the anterior abdominal wall, also generating intra-abdominal pressure (IAP). Any increase in IAP e.g. caused by coughing or sneezing, is applied equally to all sides of the pelvic and abdominal walls. If the levator ani is pathologically weakened or temporarily inactivated, the pressure on one side of a pelvic organ may become greater than that on the other, permitting the organ to descend (genital prolapse). If this movement carries the organ outside the pelvic cavity, pressure in the content of that organ will be directed unequally. For example, if the visco-urethral junction is displaced outside the pelvic cavity, an increase in IAP normally distributed equally on the intraperitoneal or intra-abdominal portion of the urethra and the bladder, will affect the bladder alone. As a result, the intravesical pressure will increase more than the intra-urethral pressure, and urinary incontinence will occur.

One in every nine women requires surgery for problems related to defective pelvic organ support. Among these women, one in every four needs a second operation (Olsen, 1997). Among women with documented prolapse, 76% had a defect in the support of the posterior compartment (rectocele) (Olsen, 1997). Despite the common occurrence of rectocele, the structural defects responsible for its formation remain poorly understood.

It is essential to understand these phenomena. It is plausible that pelvic floor muscles have a fundamental influence in these disorders. Therefore, to study the complex biomechanical behaviour of the pelvic floor muscles and to investigate the effectiveness of reconstructive surgery, a computer model based on the finite element (FE) theory is necessary. The main loading of the pelvic floor muscles is due to the IAP. In addition there will be the load due to the weight of the internal organs. Muscles in joint systems (e.g. in the upper or lower extremities) are activated to exert forces at the bones in line with their muscle line of action. In contrast, the pelvic floor muscles are loaded perpendicular to the muscle line of action by the IAP. A simple representation of the muscle action by a (one-dimensional) muscle line of action is not appropriate, but a more sophisticated approach using a FE model of the muscle is necessary. In a FE model the relationship between the loading and muscle forces in three dimensions can be represented.

For this model an experimental data set of both the geometric and the muscle parameters is required. In vivo, parameters based on nuclear magnetic resonance imaging (MRI) data for each individual patient are needed to obtain geometrical data of the pelvic floor. A palpator (a spatial linkage mechanism for 3D co-ordinate measurements) was used to obtain the necessary measurements of fibre directions and optimal fibre lengths of the pelvic floor muscles. These parameters cannot be obtained by use of MRI. The goal of this paper was to obtain all these parameters.

In this study we first measured the basic morphological data of the female pelvic floor needed for FE modelling. Secondly, we compared the MRI data set with the experimental measurements to determine what morphological information can possibly be obtained from the MRI measurements.

2.2 Materials and methods

All measurements were performed on one embalmed 72-year-old female cadaver specimen obtained for scientific research from the University Hospital AMC, Amsterdam. The specimen was selected for having no pathology to the pelvic floor. The cause of death was unknown and presumably not affecting the pelvic floor musculature. Length and weight of the cadaver could not be exactly determined, since the arms and legs of the body had been removed before the cadaver became available. Anatomical dimensions of the pelvis are given in Figure 2.1.

2.2.1 MRI measurements

Prior to dissection, specially prepared nylon screw markers for MRI measurements were manufactured. These markers produce no artifacts within MRI measurements. The markers were placed in the front part of the cadaver, two symmetrically to os pubis and to spina iliaca anterior superior on the left and right side, and in the distal side of cadaver, two symmetrically to os sacrum and one to L5 vertebral spina. It was possible to recover the position of the markers after MRI data processing. The markers also formed a reference coordinate system for the next experimental measurements. Finally, the markers were used for comparison and evaluation of both the experimental geometrical data and the data from MRI.

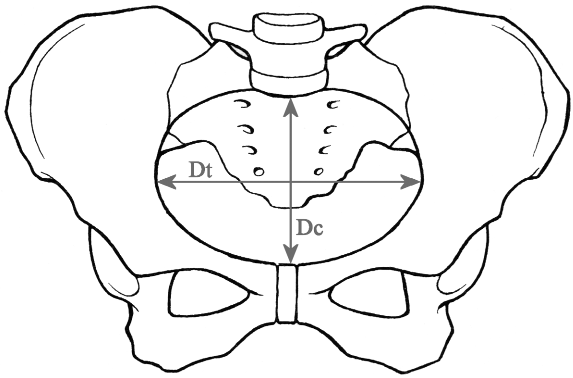

FIGURE 2.1: *Proportional anatomical dimensions of the cadaver specimen pelvis.* ***Dc*** *- Diameter conjugata:122 mm* ***Dt*** *- Diameter transversa :140 mm*

The MRI data set experiment was obtained using a GE Signa Horizon MRI scanner at the Radiology Department of the Academical Medical Center (AMC) in Amsterdam. The parameters of the measurement are summarized in Table 2.1. As the last step, three-dimensional (3D) reconstruction of the pelvic floor muscles was done (see Figure 2.4).

TABLE 2.1: *Measuring parameters and special settings for the cadaver measurements of the GE Signa Horizon MRI scanner during the MRI measurements.*

3D MR acquisition type
High resolution 512×512 pixels, 16bit
Pixel resolution 0.683×0.683 mm
Slice thickness 1.4 mm
Acquisition time 12:15 min
Spatial Resolution 1.5625 mm
Magnetic Field Strength 1.5 T
Repetition Time 11.7 s
Echo Time 4.2 s
Inversion Time 400 ms

2.2.2 Cadaver measurements - Geometrical parameters

First, the specimen was prepared for the geometrical measurements. To this end we removed the abdominal wall and all organs inside the pelvic floor to reveal the pelvic floor muscle structures. Secondly, the bony landmarks were identified by markers. Additional markers were placed, evenly and non-collinearly distributed in the pelvic bone (along the linea terminalis and crista iliaca), to be used as reference points to form a reference co-ordinate system for the experimental measurements. The following pelvic floor muscles were precisely prepared and cleared: m. levator ani complex, m. coccygeus, m. iliococcygeus and m. obturatorius internus - pars pelvis. After that, for each muscle element the visually estimated centroid of the origin and the insertion were marked with numbered labels, both on the bone and the muscle (if possible). Additional numbered labels were placed for each muscle fibre chosen to be measured. Bony landmarks were identified as well with numbered labels to mark significant bony contours in the pelvic floor. Palpable bony landmarks (e.g. spina iliaca anterior superior and symphysis pubica) were also marked. The position of palpable bony landmarks is needed for defining a local co-ordinate system of the pelvis for later comparison and evaluation of the geometrical model with data obtained from a living patient.

2.2.2.1 Palpator measurements

For measuring positions and geometry of the pelvic floor, we used a 3D-palpator (Pronk, Van der Helm, 1991), which is a special 3D device designed for this type of measurement. It has a standard deviation of 0.1 mm per co-ordinate. At the beginning of every measurement the co-ordinates of the reference marks were recorded. For the purposes of high accuracy measurements, special screw markers as reference markers were developed. These markers have a very accurate conical hole of 120º, which can be easily and precisely reached from a big radius. After repositioning of the cadaver specimen and measurement of a new data set, we were still able to recalculate this data set to the global co-ordinate system. This was done by use of the least-squares algorithm for equiform transformation from spatial marker co-ordinates (Veldpaus et al., 1988).

Prior to all geometrical measurements of the pelvic floor muscles, the positions of five reference points were measured. Subsequently, all palpable bony landmarks, bony contour landmarks, muscle markers and chosen significant muscle fibres were measured. The measurements were performed with the smallest force possible, in order to avoid any deformations of the muscle surface. The measurements resulted in a complete 3D geometrical data set of the pelvic floor muscles and structures.

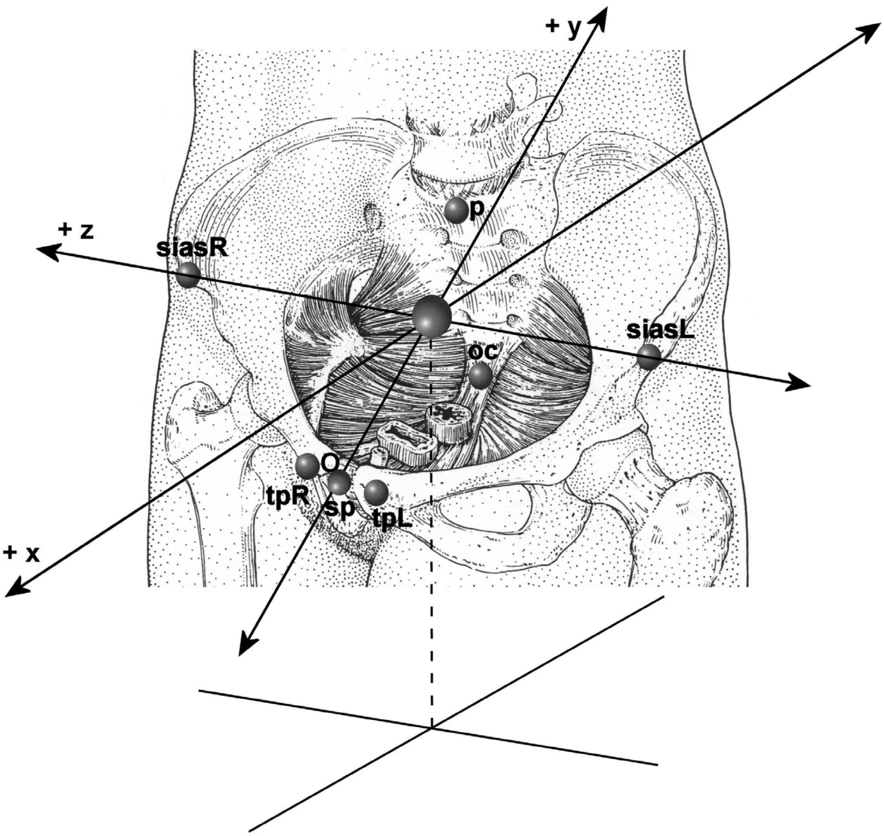

FIGURE 2.2: *Palpable bony landmarks and local orthogonal co-ordinate system of the pelvic floor. Direction of axes, origin of the co-ordinate system definitions, and pelvis orientation relative to a standing anatomical position. (Based on figure from Evers et al., 1990).* ***siasL*** *- spina iliaca anterior superior, left side,* ***siasR*** *- spina iliaca anterior superior, right side,* ***tpL*** *- tuberculum pubicum, left side,* ***tpR*** *- tuberculum pubicum, right side, p - promontorium,* ***oc*** *- os coccygeus,* ***sp*** *- symphysis pubica,* ***O*** *- origin of the co-ordinate system*

The data are expressed in a local orthogonal co-ordinate system of the pelvis, whose orientation is in agreement with the ISB co-ordinate system as shown in Figure 2.2. The axis system was defined by three landmarks: right and left spina iliaca anterior superior and symphysis pubica. These three points define the *y-z* plane in the following manner: construct a line passing from left to right anterior superior iliac spines to establish the +*z* axis. Next, establish a perpendicular to the *z* axis passing through symphysis pubica in a -*y* direction. A +*x* axis is defined normal to the *y-z* plane according to the right-hand rule. The origin of the co-ordinate system was established in the symphysis pubica. The *x-y* plane will be roughly aligned with the sagittal plane, the *y-z* plane with the frontal plane and *x-z* plane with transversal plane.

All data are then transferred into the new axis system.

2.2.2.2 Data processing

A 3D geometrical model (Figure 2.3) of the pelvic floor muscles based on the experimental data set from the palpator measurements was created. 3D NURBS splines were stretched through the data points measured using the palpator. Thereafter, NURBS surfaces lying through these spline curves were created. For the data processing the MATLAB^{TM} 6.0 software from The Mathworks Inc. was used. For visualization and surface modelling the Dscas1 (the Delft medical data visualization platform, Botha, 2001) was used.

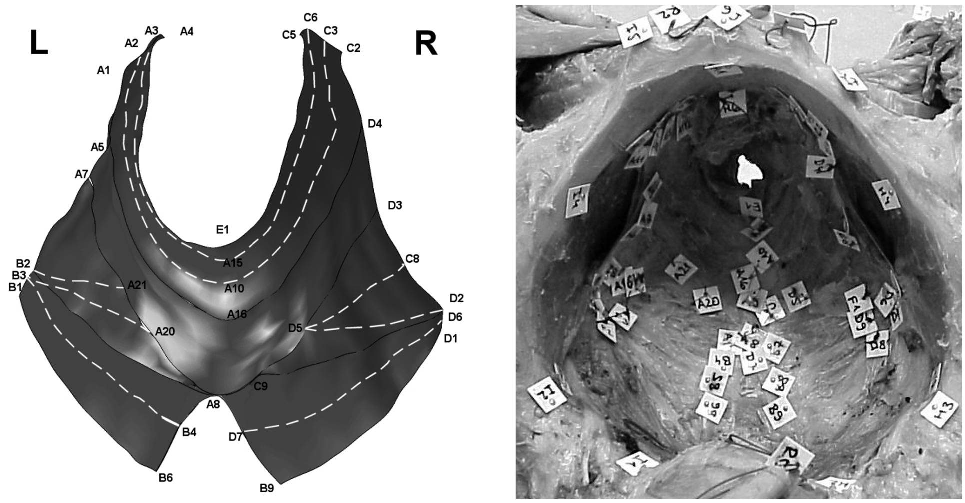

FIGURE 2.3: *Simplified description of particular muscle parts (significant muscle bundles) used also in Table 2.2. Labels are in accordance with data set available at the website (http://mms.tudelft.nl/morph_data/index.htm). Schema on the left side,* ***L*** *- left side,* ***R*** *- right side. Photo on the right side.*

2.2.3 CADAVER MEASUREMENTS - MUSCLE PARAMETERS

Prior to the measurements of the muscle parameters, the complete m. levator ani complex was removed. Each muscle was cleared from its surrounding tissue. For each muscle it was defined how many elements it should be divided into. The main criterion therefore was that the cleared pieces were representative for the chosen significant muscle bundles that were measured with the palpator. Therefore, the complete diaphragma pelvis was divided into eight muscle parts and these muscle parts were divided in total into 22 muscle elements representing the significant muscle bundles (see Figure 2.2 and Figure 2.3). The number of elements was chosen so that an equidistant distribution over the muscle covers most of its surface.

Optimal muscle fibre length was measured using a laser diffraction method (Klein Breteler et al., 1999). Pelvic floor muscles have no tendon, therefore the muscle fibre length is the same as the total muscle element length. Each muscle element was placed on a flat support and its origin and insertion labelled. The length between origin and insertion was then copied to a string and measured with a ruler. Each muscle element (representative fibre bundle) was weighed with the use of a high accuracy digital scale with a standard deviation of 0.05 g. Muscle elements were wiped with tissue to remove excess fluid before weighing. Pennation angles for these muscle elements were considered negligible. Because of the striated character of skeletal muscle, sarcomere length was measured by the diffraction of a He-Ne laser beam of about 1 mm in diameter (Young et al., 1990). Fibre bundle samples were positioned in the laser beam at a fixed distance (0.5 m) from a scale to allow direct reading of the sarcomere length. The samples were approximately 10 mm long and very thin, and were placed on a microscope glass. All samples were eased apart under an operation binocular microscope (used magnitude interval from 10× up to 24×). The resolution of the sarcomere length was 0.05 μm, depending on the quality of the embalming process. For each muscle fibre, three samples of sarcomere length at three representative locations along the bundle were recorded.

2.2.3.1 DATA PROCESSING

The optimum fibre length for each muscle was calculated as the fibre bundle length divided by mean sarcomere length in that fibre bundle, multiplied by the optimum sarcomere length of 2.7 μm (Walker and Schrodt, 1974). Optimum fibre length of a muscle element was the mean of its optimum fibre bundle lengths. The embalming process has no effect on the results, since the actual sarcomere length and muscle bundle length were measured and the optimum muscle length was calculated from the optimal sarcomere length in vivo (2.7 µm).

TABLE 2.2: *Summary of the muscle parameters for all muscles and all muscle elements of m. levator ani complex. Particular muscle parts are labelled in accordance with the data set available at the website (http:// mms.tudelft.nl/morph_data/index.htm) see also Figure 2.3.* ***PCSA*** *- physiologic cross-sectional area [cm^2]*

	weight [g]	volume [cm^3]	Mean fiber length *N=3*	Std. dev. [mm] *N=3*	Mean sarc. length [µm] *N=9*	Std. dev. [µm] *N=9*	No. of sarc. [1]	Optimal fibre length [mm]	PCSA [cm^2]
Left side									
m. levator ani - m. pubococcygeus	10.2	9.64	82.8	3.0	2.7	0.1	30932	83.5	1.17
A4-E1	4.1	0.43	82.0	0.0	2.7	0.2	30370	82.0	0.48
A3-A15	2.9	2.71	80.0	2.0	2.8	0.2	28829	77.8	0.35
A2-A10	2.3	2.17	82.3	2.5	2.7	0.1	30923	83.5	0.26
A1-A16	0.9	0.81	87.0	0.0	2.6	0.2	33605	90.7	0.09
m. iliococcygeus	2.1	1.99	80.0	1.9	2.7	0.1	30060	81.2	0.25
A7-A8	1.0	0.96	81.3	1.2	2.6	0.3	30984	83.7	0.12
A5-A16	1.1	1.03	87.7	1.2	2.7	0.3	29136	78.7	0.13
m. coccygeus (1)	0.8	0.74	41.8	4.5	2.5	0.0	16969	45.8	0.16
B2-A21	0.3	0.30	38.7	1.2	2.5	0.2	15570	42.0	0.07
B3-A20	0.5	0.44	45.0	0.0	2.5	0.1	18367	49.6	0.09
m. coccygeus (2)	4.8	4.50	51.6	2.8	2.5	0.2	20674	55.8	0.58
B2-A8	1.6	1.55	54.7	0.6	2.4	0.2	22466	60.7	0.26
B3-B4	1.8	1.68	50.7	2.3	2.7	0.2	19000	51.3	0.33
B1-B6	1.3	1.27	49.3	3.1	2.4	0.0	20556	55.5	0.23
Right side									
m. levator ani - m. pubococcygeus	10.0	9.47	82.7	4.1	2.9	0.0	28738	77.6	1.20
C2-A16	1.5	1.40	76.7	1.2	2.9	0.2	26620	71.9	0.20
C3-A10	1.5	1.41	85.0	1.0	2.9	0.2	29412	79.4	0.18
C6-A15	2.4	2.26	83.3	1.5	2.9	0.2	28860	77.9	0.29
C5-E1	4.7	4.41	85.7	0.6	2.9	0.2	30058	81.2	0.54
m. iliococcygeus	1.9	1.81	70.2	5.4	2.5	0.1	27768	75.0	0.24
D3-A8	1.0	0.97	74.0	1.0	2.5	0.1	29899	80.7	0.12
D4-A16	0.9	0.84	66.3	1.2	2.6	0.1	25636	69.2	0.12
m. coccygeus (1)	0.9	0.87	54.2	3.1	2.4	0.1	18520	50.0	0.18
D2-D5	0.6	0.56	43.0	2.7	2.4	0.2	18201	49.1	0.11
C8-D5	0.3	0.31	47.3	2.5	2.5	0.1	18839	50.9	0.06
m. coccygeus (2)	4.8	4.57	45.7	1.5	2.3	0.1	19726	53.3	0.86
D1-B9	1.8	1.73	47.3	2.5	2.4	0.2	19606	52.9	0.33
D6-D7	1.4	1.36	44.5	4.4	2.2	0.1	20075	54.2	0.25
D2-C9	1.6	1.47	45.3	0.6	2.3	0.2	19498	52.7	0.28

The physiological cross-sectional area (PCSA) of a muscle element at optimum length is a measure for the maximum force that a muscle can exert. PCSA was calculated as the mass divided by the density, resulting in muscle volume, and subsequently divided by the optimum fibre length of the relevant muscle element. The specific density of skeletal muscle tissue was taken to be 1.057 g/cm^3 since muscles were soaked during weighing (Lieber, 1992, Klein Breteler et al., 1999).

Results of these calculations are summarized in Table 2.2.

2.2.4 MODEL COMPARISON

A numerical comparison of two triangle model meshes, namely the 3D reconstruction based on the palpator measurements and the 3D reconstruction based on the MRI experiment, was performed. We used a Metro (a tool developed by Visual Computer Group, CNR-Pisa), to evaluate the difference between surfaces e.g. triangulated meshes. The measures were computed using an error defined as an approximation of the surface-to-surface distance between two corresponding sections of the meshes (Cignoni et al., 1998). The results of both the numerical and visual evaluations are summarised in Table 2.3 and Figure 2.6.

2.3 RESULTS

2.3.1 MRI MEASUREMENTS

Semi-automated gradient-oriented segmentation of the MRI scans was performed. Thereafter 3D reconstruction of the pelvic floor muscles was done (see Figure 2.4).

2.3.2 CADAVER MEASUREMENTS

Table 2.2 shows the summary of the muscle parameters for all muscles and all muscle elements of m. levator ani complex needed for building the FE model. The complete experimental data set concerning both the geometrical and the muscle parameters is available on the Internet (http://mms.tudelft.nl/morph_data/index.htm).

It was remarkable that all muscles were near the optimal muscle length as reflected in the small interval of sarcomere lengths between 2.2 and 2.9 μm (see Table 2.2). Mostly sarcomere lengths were at or just below the optimal muscle length. After simulated contraction, presumably all muscle bundles will be below optimal length on the ascending slope of the force-length curve.

2.3.3 Model comparison

Numerical comparison of two triangle model meshes was done and results of both the numerical and visual evaluations are summarised in Table 2.3 and Figure 2.6. This comparison was important in order to demonstrate the similarity between the present cadaver study and MRI studies. Mean surface-to-surface distance square error is 3.9 mm. The maximal error of 34.9 mm is due to a missing coccygeus muscle part in the 3D reconstruction of the pelvic floor muscles based on the MRI data set.

Table 2.3: *Summary of the numerical results as a mean and maximum surface-to-surface distances between meshes returned using absolute measures.*

	Value [mm]
Maximal Error	34.9
Mean Error	2.2
Mean Square Error	3.9

2.4 Discussion

This study was performed to uncover the morphological parameters of the pelvic floor muscle complex for FE modelling purposes. When a FE model is developed for a living patient or healthy subject, the only way to obtain morphological parameters is using MRI scans. Important parameters like the optimum muscle length and fiber orientation cannot be obtained from MRI scans, and must be imported from a cadaver study. Therefore, it is important to enable a link between the present cadaver study and MRI studies. The bony landmarks enable the construction of a local co-ordinate system of the pelvis. MRI data were described with respect to this local co-ordinate system, as well as the muscle data in this cadaver study. The similarity between the data sets was good.

The experimental measurement of the pelvic floor structures was performed in a specimen fixed by injection embalming. These specimens are known to exhibit distorted spatial relationships (Richter, 1966) and these topographic relationships do not correspond to the data available from living women. After embalming, the m. levator ani, as well as the sphincter muscles (e.g. m. sphincter ani externus and m. sphincter ani internus) lose their tone. All internal organs and structures moved downwards, because they lack support by diaphragma pelvis.

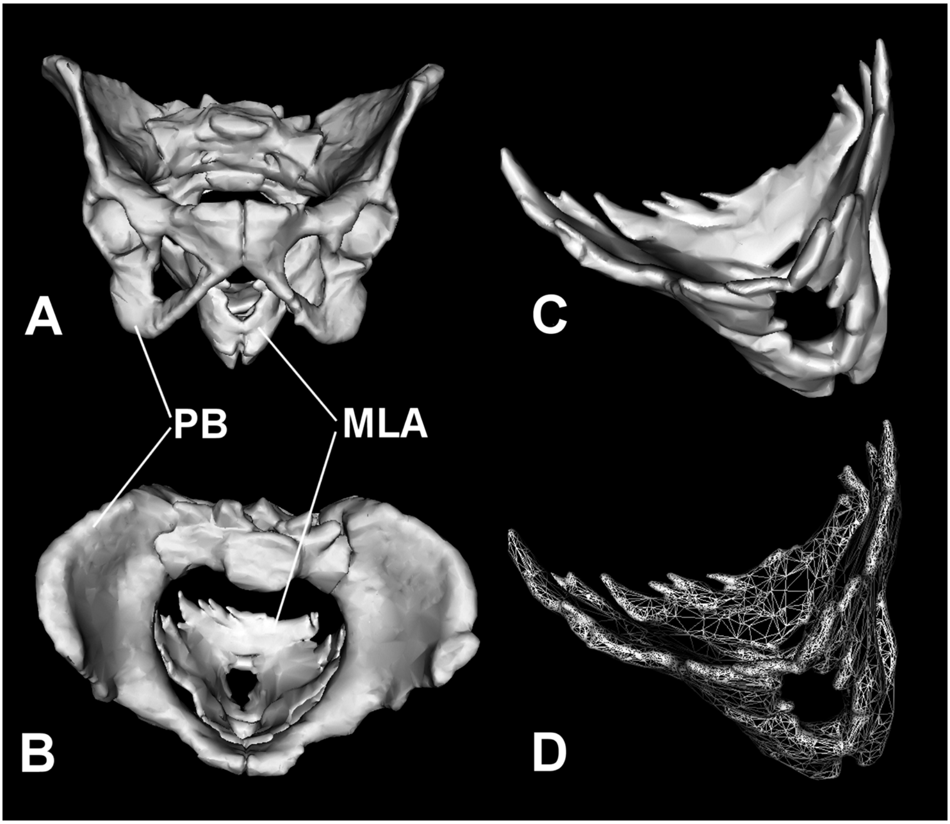

Figure 2.4: *The 3D geometrical model of the pelvic floor muscles based on the experimental data set from the MRI measurements. The 3D reconstruction of the pelvic bone (PB) and m. levator ani complex (MLA) on the left side: **A** - frontal view, **B** - top view. Detail of the 3D reconstruction of the m. levator ani complex on the right side: **C** - levator ani muscle complex, volume model, **D** - levator ani muscle complex, triangle model.*

Loss of the muscle tone after death has been addressed by studying some cadavers during the phase of rigor mortis (DeLancey, 1999). Therefore, there is a difference in the pelvic floor topology between the cadaver and the living patient. However, this does not affect the muscle parameters, such as optimal sarcomere length. In the biomechanical model based on the FE theory, the muscle position can be reconstructed by imposing the appropriate muscle tone. In the FE model the loading forces and muscle forces are simulated, and the muscle finds a new position depending on the load condition and simulated muscle activation. That solves the problem of the loss of the muscle tone in the cadaver experiment.

For the purposes of mathematical modelling of the pelvic floor based on the FE theory, one has to take into account all these morphological changes, especially in the pre-processing phase of the model development (e.g. loading of the pelvic floor muscles). Furthermore, the comparison of the cadaver MRI scans with the MRI of living women returned relatively large differences in the pelvic floor topography.

Geometrical data on the gross anatomy of pelvic floor muscles can be obtained by the use of high resolution MRI scanning. Unfortunately, additional morphologic data concerning foremost muscle fibre directions cannot be obtained from MRI. These morphological data as well as additional muscle parameters can be obtained from cadaver experiment. By the use of many reference landmarks (e.g. spina iliaca anterior superior, symphysis pubica, promontorium, os coccygeus etc., see also Figure 2.2) all these morphological data can be morphed onto the geometrical data based on segmentation from MRI scans. Thereafter all these data can be used as input for building a mathematical model based on FE theory.

The purpose of this experiment was to discover the relationship between the MRI morphology and geometrical parameters obtained from the previous measurements. The produced data set is not only important for biomechanical modelling of the pelvic floor muscles and to investigate the effectiveness of the reconstructive surgery, but it also describes the geometry of muscle fibres that can be used for functional analysis of the pelvic floor in general.

2.4.1 MRI MEASUREMENTS

The parameters of the MRI measurements are given in Table 2.1. The semi-automated gradient-oriented segmentation of the MRI scans was performed because there is no proprietary automatic image processing segmentation tool for segmenting muscle tissue within MRI scans yet. Even in relatively high resolution MRI scans (512 × 512 pixels, pixel resolution of 0.68 mm), segmentation of levator ani muscle was very difficult. These difficulties arose primarily because of the small thickness of levator ani muscle (approximately 2 mm) and there was almost no difference in contrast between levator ani muscle and surrounding soft tissues. Difficulties in in-vivo MRI data set segmentation are expected. Presently, no solution has been found for this problem.

2.4.2 GEOMETRICAL PARAMETERS MEASUREMENTS

Because of the relatively flat muscle shape of the m. levator ani complex, the geometry and topology was scanned relatively easy. In this study only the surface geometry of the diaphragma pelvis was determined. Concerning the relatively constant thickness of the muscle element for FE modelling purposes, the pelvic floor muscles can be simulated by the use of shell elements. A single shell element layer or multi-layer shell element mesh with constant thickness is obviously the best solution to this problem.

This study was performed on only one cadaver specimen, which is relevant for purposes of FE modelling. A previous anatomical study (De Blok, 1982) showed that there is no significant inter-individual and intra-individual difference in pelvic floor morphology. Additional cadaver studies focusing on pelvic floor morphology can evaluate the relevance of morphologic parameters obtained from this study.

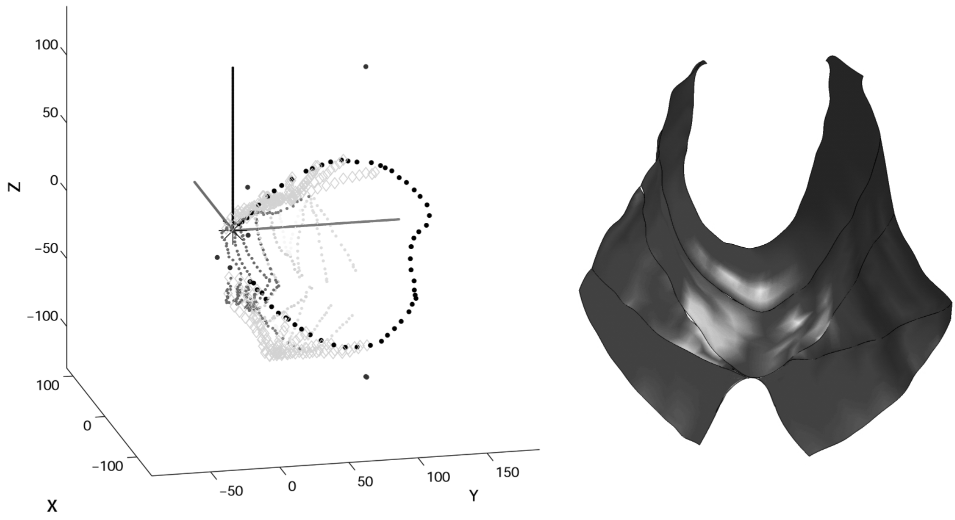

FIGURE 2.5: *The 3D geometrical model of the pelvic floor muscles based on the experimental data set from the palpator measurements. Points measured by the use of the palpator on the left side. Pelvic floor muscles surface rendered on the right side.*

2.4.3 Muscle parameters - Sarcomere length measurements

Recording the muscle sarcomere length for each bundle of the pelvic floor muscles enables the reconstruction of the muscle optimum length. From the muscle optimum length, the force-length curve can be reconstructed using data from muscle physiology (Klein Breteler et al., 1999). The force-length curve is important because it determines the maximal force in a certain position. In addition, the muscle stiffness is higher at the ascending slope of the force-length curve than at the descending slope (Sugi and Tsuchiya, 1988). Muscle stiffness is an important factor for the stability of the system, and will determine the necessity of additional proprioceptive feedback control of the pelvic floor muscles.

The muscle fibre length was measured directly as the distance between the beginning and end of the straightened muscle bundle. Measured muscle bundle length varied a little within certain muscles, because of the trapezoidal muscle shape (see Figure 2.5 and Figure 2.3). Within a muscle, the element length differences were correlated with spatial position. The mean muscle fibre length and the standard deviation were calculated (see Figure 2.2).

Laser diffraction is a very accurate method for measuring sarcomere lengths, especially if the muscle tissue is perfectly embalmed (if not, sarcomere unit damage can be observed). Sarcomere lengths between 2.0 and 3.2 μm were measured, which is within the range that Walker and Schrodt (1974) argued to be consistent with the sliding filament theory. This makes it plausible that filament lengths have not changed during the embalming process. Sample preparation did not permanently alter the sarcomere length. In a few muscle elements, it was not possible to measure the sarcomere length. Those were considered as artifacts and were further ignored. We assumed, that the muscle fibres were broken during rigor mortis or during the embalming process.

Sarcomere length measurements in m. coccygeus were very difficult, because of the relatively large atrophy of the skeletal muscle tissue. Presumably, it was caused by the age of the cadaver specimen.

2.4.4 Model comparison

We consider that the relatively high maximal error (see Table 2.3 and Figure 2.6) is due to geometric difference in the coccygeus muscle between the surface model from the palpator measurements and the MRI experiment. Thickness of this muscle was determined up to one mm. Therefore segmentation of the posterior part of this muscle is almost impossible due to low resolution within MRI scans. On the other hand the mean surface-to-surface distance error seems to be low (mean square error of 3.9 mm) given the number of manipulations and tasks performed (e.g. removing internal organs, clearing pelvic floor muscles from its surrounding tissue) within this large experiment. The maximal error of 34.9 mm is due to a missing coccygeus muscle part in the 3D reconstruction of the pelvic floor muscles based on MRI data set. The segmentation of this muscle part was not possible because of resolution difficulties described above.

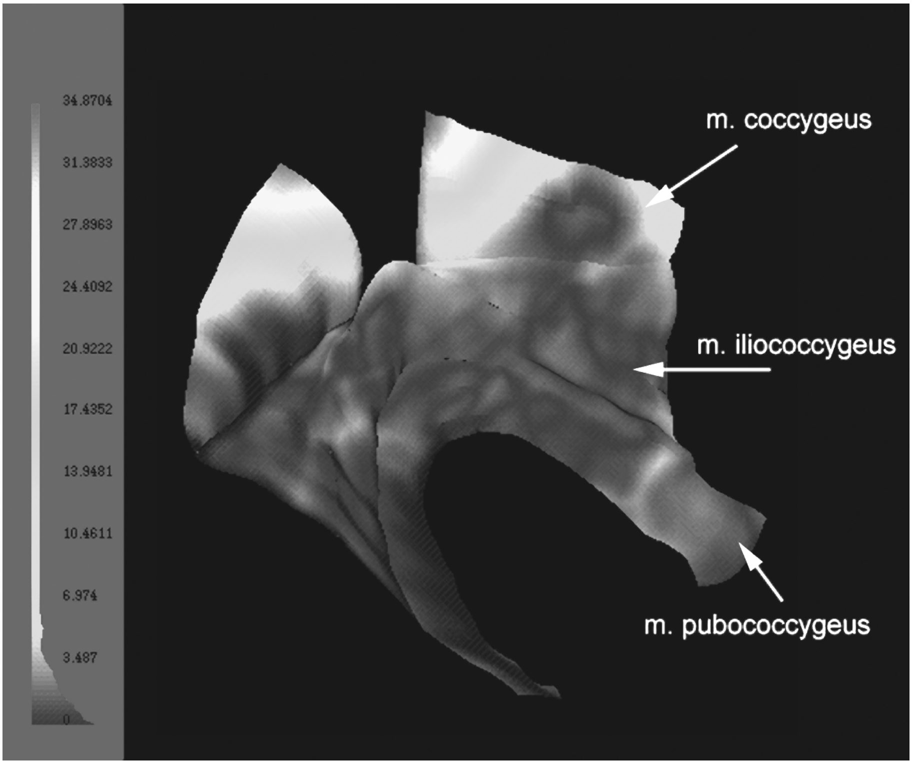

FIGURE 2.6: *The graphical results output from the Metro tool software (Cignoni, 1998). Surface distance-to-distance maximum error colour bar on the left side, the graphical visualisation of the error distribution in the 3D reconstruction of the pelvic floor muscles based on the palpator measurements on the right side. Mean surface-to-surface distance square error is 3.9 mm (see also Table 2.3). The maximal error of 34.9 mm is due to a missing coccygeus muscle part in the 3D reconstruction of the pelvic floor muscles based on MRI data set.*

MRI scans will be used in future. These results show that it is feasible to transfer cadaver data (muscle fibre direction, optimum muscle length) to the MRI data set.

2.5 Conclusions

The produced data set is not only important for biomechanical modelling of the pelvic floor muscles and to investigate the effectiveness of the reconstructive surgery, but it also describes the geometry of muscle fibres that is useful for functional analysis of the pelvic floor in general.

By the use of many reference landmarks (e.g. spina iliaca anterior superior, symphysis pubica, promontorium, os coccygeus etc.) all these morphological data concerning fibre directions and optimal fibre length can be morphed onto the geometrical data based on segmentation from MRI scans.

These data can be directly used as an input for building a mathematical model based on FE theory.

Acknowledgements

The study was realized thanks to co-operation between the facilities of the co-authors and the Academical Medical Center in Amsterdam. The authors wish to thank the Department of Anatomy and Embryology of the AMC Amsterdam (Head of department: Prof. Dr. W.H. Lamers; Head of dissection rooms: Drs. Kees de Jong) for offering the facilities to perform the specimen preparation and Dr. J. Stoker from Department of Radiology of the AMC Amsterdam for co-operation and performing the MRI measurements.

References

Botha, C.P., Post, F.H., 2001. A visualization platform for shoulder replacement surgery, in IMIVA - Satellite Workshop of MICCAI 2001, 61-64.

Cignoni, P., Rocchini, C., Scopigno, R., 1998. Metro: measuring error on simplified surfaces. Computer Graphics Forum, Blackwell Publishers, vol. 17(2), 167-174.

De Blok, S., 1982. The connective tissue of the adult female pelvic region. A dissectional analysis. Acta Morphol Neerl Scand. 20(2), 191-212.

DeLancey, J.O.L., 1999. Structural anatomy of the posterior pelvic compartment as it relates to rectocele. Am J Obstet Gynecol. Vol 180, No.4, 815-823.

Evers, J.L.H., Heineman, M.J., 1990. Gynaecology: A clinical atlas. St. Louis: Mosby.

Klein Breteler, M.D., Spoor, C.W., Van der Helm, F.C.T. 1999. Measuring muscle and joint geometry parameters of a shoulder for modeling purposes. J. Biomech. 32(11), 1191-1197.

Lieber R.L., 1992. Skeletal muscle structure and function. Williams a Wilkins.

Nichols, D.H., Randall, O.L., 1996. Vaginal Surgery. Williams a Wilkins.

Olsen, A.L., Smith, V.J., Bergstorm, J.O., Colling, J.C., Clark, A.L., 1997. Epidemiology of surgically managed pelvic organ prolapse and urinary incontinence. Obstet Gynecol. 89, 501-506.

Pronk, G.M., Van der Helm, F.C.T., 1991. The palpator, an instrument developed for measuring the 3D-positions of bony landmarks in a fast and easy way. J. Med. Eng. Tech. 15, 15-20.

Richter, K., 1966. Lebendige anatomie der vagina. Geburtshilfe frauenheilkd 26, 1213-1223.

Sugi, H., Tsuchiya, T., 1988. Stiffness changes during enhancement and deficit of isometric force by slow length changes in frog skeletal muscle fibers. J. Physiol. 407, 215-229.

Veldpaus, F.E., Woltring, H.J., Dortmans, L.J.M.G., 1988. A least-square algorithm for the equiform transformation from spatial marker co-ordinates. J. Biomech. 21(1), 45-54.

Walker, S.M., Schrodt, G.R., 1974. I segment lengths and thin filament periods in skeletal muscle fibres of the rhesus monkey and the human. Anatomical Record 178, 63-82.

Young, L.L., Papa, C.M., Lyon, C.E., George, S.M., Miller, M.F., 1990. Comparison of microscopic and laser diffraction methods for measuring sarcomere lengths of contracted muscle fibres of chicken pectoralis major muscle. Poultry Science 69, 1800-1802.

Chapter 3

A CONSTITUTIVE MODEL FOR THE PASSIVE ELASTIC BEHAVIOUR OF HUMAN PELVIC FLOOR MUSCLES

Abstract

Objective: *The goal of this study is to derive passive material parameters of the pelvic floor muscles. A constitutive model needed for studying the complex biomechanical behaviour of these muscles is developed. This model can be used for computer modelling of the pelvic floor.*

Methods: *Since there was a lack of any information concerning passive material properties of the pelvic floor muscles, uniaxial and equibiaxial measurements were performed. The data obtained were used to estimate parameters of the Mooney-Rivlin (MR) constitutive model, which assumes the tissue to be isotropic and incompressible.*

Results: *The constants of the MR constitutive model are obtained from experimental tests, which have been conducted with similar deformation modes to those appearing in vivo.*

Conclusions: *The produced data set describes the passive elastic material properties of the pelvic diaphragm. The constitutive model based on these data can be directly used as an input for building a mathematical model based on finite element theory. This can be used for the investigation of the effectiveness of reconstructive surgery. The presented elastic constants describing the non-linear passive elastic behaviour of the pelvic floor muscles represents a good fit of the experimental data.*

Relevance: *The present study helps to understand the biomechanical behaviour and material properties of the pelvic floor muscles, which should be beneficial to clinicians and engineers developing new biomaterial prosthesis or surgical techniques for prolapse repair.*

Keywords

Pelvic floor muscles; Material parameters; Elasticity; Finite element model

In review ***Clinical Biomechanics***

3.1 INTRODUCTION

The pelvic diaphragm in human is a very complex muscular structure. Levator ani muscle with its fascial covering constitutes the pelvic diaphragm. It is largely responsible for supporting both pelvic and abdominal organs and acts synergistically with the striated muscle of the anterior abdominal wall, also generating intra-abdominal pressure (IAP). Any increase in IAP e.g. caused by coughing or sneezing, is applied equally to all sides of the pelvic and abdominal walls. If the levator ani is pathologically weakened or temporarily inactivated, the pressure on one side of a pelvic organ may become greater than that on the other, permitting the organ to descend (genital prolapse). One in every nine women requires surgery for problems related to defective pelvic organ support. Among these women, one in every four needs a second operation (Olsen et al., 1997). Despite the common occurrence of genital prolapse, the structural defects responsible for its formation remain poorly understood.

It is essential to understand prolapse phenomena to improve surgical results. Obviously, the pelvic floor muscles have a fundamental influence in these disorders. To study the complex biomechanical behaviour of the pelvic floor muscles, and to investigate the effectiveness of reconstructive surgery, a computer model is necessary. The main loading of the pelvic floor muscles is due to IAP. Additionally, there will be loading due to the weight of the internal organs. Muscles in joint systems (e.g. in the upper or lower extremities) are activated to exert forces at the bones in line with their muscle line of action. In contrast, the pelvic floor muscles are loaded perpendicular to the muscle line of action by IAP. A simple representation of the muscle action by a (one-dimensional) muscle line of action is not appropriate. A more sophisticated approach using a finite element (FE) model of the muscle is necessary. In a FE model the relationship between the loading and muscle forces in three dimensions (3D) can be represented. For this model an experimental data set of both the geometric and muscle material properties is required.

Continuum models have been applied to study the mechanical behaviour and function of skeletal muscle. Biomechanical analysis of soft tissue requires quantification of their 3D material properties, i.e. stress-strain behaviour. This necessitates accurate determination of stresses and strains under multiaxial loading, since uniaxial data do not fully characterize behaviour in 3D. To present, such quantification has been partially successful for non-contracting tissue, including skin and blood vessels. Some studies were performed on passive myocardium and passive and tetanised canine diaphragm (Strumpf et al., 1993). However, no multiaxial stress-strain data exist for human pelvic floor muscles. The reasons for this include the complex geometry and composite nature of such tissue.

The passive material properties of the pelvic floor muscles are unknown. The active material properties are due to muscle dynamics and cannot be obtained from cadaver measurements. The passive material properties can be derived from stress-strain data based on the tissue testing. In addition, a good material model describing the non-linear material behaviour of muscle tissue must be developed.

The goal of this study is to derive passive material parameters of the pelvic floor muscles needed as an input for a FE model of the pelvic floor. The uniaxial and equibiaxial data were obtained for human pelvic floor muscles. The non-linear elasticity data obtained were used to develop the Mooney-Rivlin (MR) constitutive model for the pelvic floor muscle tissue. This isotropic incompressible constitutive model is included in several widely available FE software. The constants of the MR constitutive model are obtainable from experimental tests, which should be conducted with similar deformation modes to those appearing in vivo.

3.2 Material and methods

3.2.1 Tissue testing

All measurements were performed on three female pelvic floor fresh cadaver specimens (82, 66 and 38 years old). Samples were frozen directly after becoming available within an interval of 4-16 hours after death. Before testing, the samples were defrosted and stored in saline solution at 4°C. All samples were prepared under sterile conditions. Fat and other connective tissues were removed from the surface of the muscle tissue. Thereafter, the samples were pressed flat and sectioned. For uniaxial test 15 × 3 mm strips of muscle tissue were prepared. For bi-axial testing square areas of 20 × 20 mm were prepared. Pelvic floor muscle are thin and flat structure with constant thickness along the specimen. The thickness of each sample was measured at several locations using the preparation microscope and an average was taken. Accuracy of thickness measurement was 0.01 mm. In both tests, strain rates of 30% per minute were used. Samples were preconditioned and irrigated with 0.9% saline solution during the test. All tests were performed at a temperature of 25°C.

3.2.1.1 Uniaxial testing

Specimens were gripped in pneumatically activated stainless steel grips with coatings of emery paper to prevent slippage during the test. The gauge length was determined after clipping the specimen. The grips were mounted on a Zwick displacement controlled tensile testing machine. The load data were recorded using a data acquisition card on a local PC. Extension of the specimen was taken to be the crosshead displacement. The samples were preloaded up to 0.05 N and thereafter preconditioned up to upper reversal point of 0.2 N in three cycles. Strain rate of 30% per minute was used in both the preconditioning and testing phase. The tests were stopped when tearing began at either the grips or along the length of the specimen.

3.2.1.2 BI-AXIAL TESTING

A specially designed equibiaxial rig device (Prendergast et al., 2003) was used on a standard uniaxial Zwick testing machine. This device ensures equal forces in both testing directions. It comprises a number of working assemblies as shown in Figure 3.1. The suspension assembly consists of four horizontal arms of equal length stemming from a central block secured to the crosshead of the testing machine. The four arms supports four identical balance beams. Each beam is free to pivot on a polished stainless steel shoulder screw. The base plate is secured to the base of the testing machine. The base plate consists of four brackets containing pairs of stainless steel pulleys. The main function of the bracket-pulley assemblies is to turn the vertical cable network through 90° and guide them toward the square specimen of pelvic floor muscle tissue positioned centrally to the base plate. High strength thread lines are used for the cable network. Four lines of equal length are attached to the rig at various positions. The route of a line can be seen from Figure 3.1. Each line originates from a position on a balance beam. Each line is guided along a curved groove at the end of the beam. This is to ensure that each line is in constant tension during rotations as well as ensuring it remained perpendicular to the base plate assembly. Each line is suspended from the balance beam and passes through the pulley-bracket fixture on the base plate and is turned through 90° towards the central area of the base plate. Each line passes through a loading bracket before returning via a similar route to the end of the adjacent balance beam. The loading bracket transfers the loads from the line to the specimen. The jaw end of each crocodile clip is used to grip the specimen and the other end is linked to a vertical dowel pin on the Perspex bracket.

The rig was validated using a square piece of isotropic silicone and it produced equal stretch in both directions (Lally et al., 2004). The load was measured using the load cell attached to the overhead lever assembly system. The load required to overcome the friction in the pulleys without sample was determined to be 0.5 N (Lally et al., 2004). This was subtracted from the total load on the specimen.

FIGURE 3.1: *Equibiaxial rig device setup mounted on a standard uniaxial Zwick testing machine. The specimen is placed in the centre of the rig base. A digital CCD camera is used for monitoring the displacement of the specimen.*

The thickness of the specimens was 2.96 ± 0.61 mm. The square specimen (20 × 20 mm) was visually oriented (muscle fibre direction and transverse direction as a principal directions) and gripped using the jaw ends of crocodile clips, equally distributed along each side of the specimen. The muscle fibre direction is clearly recognisable on the surface of the specimen since the fibres are arranged parallel. The clips were adjusted to ensure that each jaw remained firmly locked during the test. After gripping, a 3 × 3 orthogonal array of dots was printed on the surface of the specimen using water-resistant, oil-based, quick drying ink. Schema of the set-up is shown in Figure 3.2.

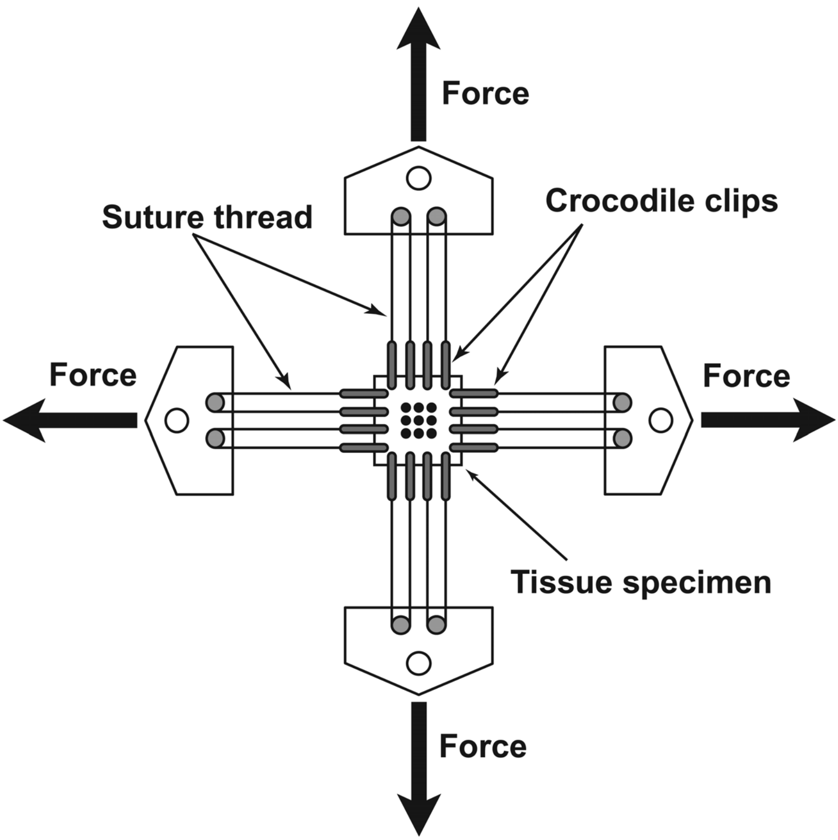

FIGURE 3.2: *Schematic diagram of the equibiaxial testing setup. The square (20 × 20 mm) tissue specimen is gripped using the jaw ends of crocodile clips, equally distributed along each side of the specimen. In order to measure tissue strain, a 3 × 3 orthogonal array of dots was printed on the surface of the specimen using water-resistant, oil-based, quick drying ink. The specimen is thereafter loaded with equal force in both testing directions.*

The gauge length was determined using markers by CCD camera. The specimen was placed in the centre of the rig and the crosshead of the Zwick machine was advanced until any slack was eliminated from the specimen. The specimen was irrigated with 0.9% saline solution during testing. The samples were preloaded up to 0.05 N and thereafter preconditioned up to upper reversal point of 0.2 N in three cycles. The same test protocol was used as during the uniaxial testing. The tests were stopped when tissue tearing or slippage began at the jaws of the crocodile clips.

The stretch was measured by monitoring the displacement of dots printed on the surface of the specimen. A digital CCD camera was used to take images of the tissue at a predetermined frequency of 1Hz. All images were processed using an image-processing package built-in MATLAB^{TM} 6.0 software from The Mathworks Inc. As a result, the centroids of at least four of the dots on the tissue were recorded. The strain of the tissue in both principal directions was determined from the movement of the centroids of these four dots on the specimen from picture to picture as the load increased. The engineering stress was calculated by dividing the load in each principal direction by the initial effective cross-sectional area of the specimen. This produced the stress-strain data in the two principal directions (muscle fibre and transverse direction).

3.2.2 Histological analysis

After the last stretching protocol, each specimen was fixed in 10% Formalin solution. Histological analysis was performed in all specimens to evaluate the percentage of striated and smooth muscle type in the specimens. Samples were taken from the remaining tissue in a random manner. Sections of 4 mm of thickness from the paraffin-embedded, formalin-fixed blocks were stained with hematoxylin and eosin. Thereafter, the percentage of the striated and smooth muscle type was determined in all specimens.

The number, and the individual diameter, of type I (slow twitch) and type II (fast twitch) fibres was not possible to determine due to the embalming process.

3.2.3 Sarcomere length measurements

Because of the striated character of skeletal muscle, sarcomere length was measured by the diffraction of a He-Ne laser beam of about 1 mm in diameter (Young et al., 1990). Fibre bundle samples were positioned in the laser beam at a fixed distance (0.5 m) from a scale to allow direct reading of the sarcomere length. The samples were approximately 10 mm long and very thin, and were placed on a microscope glass. All samples were eased apart under an operation binocular microscope (used magnitude interval from 10× up to 24×). Details of laser diffraction technique measurements are described in Janda et al. (2003). The resolution of the sarcomere length was 0.05 μm. For each muscle specimen, ten samples of sarcomere length at several representative locations were recorded.

3.2.4 CONSTITUTIVE MODELLING

A MR strain energy density function (Mooney, 1940) was used to develop a constitutive model of the non-linear elastic behaviour of the pelvic floor muscles. This elastic material model assumes that material response is isotropic and materials are also assumed to be incompressible. General MR form of the strain energy function can be written as:

$$W = \sum_{i=1}^{N} \sum_{j=1}^{N} a_{ij}(I_1 - 3)^i (I_2 - 3)^j \tag{3.1}$$

where W is the strain energy density function and I_1 and I_2 are the first and second invariants of Cauchy-Green tensor (Green et al., 1968, Lai et al., 1993). The strain energy density function W (Equation 3.1) can be expanded in order to obtain the particular forms of the generalized MR model, namely the two, three, five and nine parameter strain energy density functions:

$$W = a_{10}(I_1 - 3) + a_{01}(I_2 - 3) \tag{3.2}$$

$$W = a_{10}(I_1 - 3) + a_{01}(I_2 - 3) + a_{11}(I_1 - 3)(I_2 - 3) \tag{3.3}$$

$$W = a_{10}(I_1 - 3) + a_{01}(I_2 - 3) + a_{20}(I_1 - 3)^2 + a_{11}(I_1 - 3)(I_2 - 3) + a_{02}(I_2 - 3)^2 \tag{3.4}$$

$$\begin{aligned} W = {} & a_{10}(I_1 - 3) + a_{01}(I_2 - 3) + a_{20}(I_1 - 3)^2 + a_{11}(I_1 - 3)(I_2 - 3) + a_{02}(I_2 - 3)^2 \\ & + a_{30}(I_1 - 3)^3 + a_{21}(I_1 - 3)^2(I_2 - 3) + a_{12}(I_1 - 3)(I_2 - 3)^2 + a_{03}(I_2 - 3)^3 \end{aligned} \tag{3.5}$$

The equations above represent first, second and third order models. The increase in complexity of the expression of the strain energy function density W should, in principle, correspond to an increase in accuracy of modelling the deformation modes. In general, there is no limitation on model order, N. A higher N may provide a better fit to the exact solution; however, it may, on the other hand, cause numerical difficulty in fitting the material constants and requires enough data to cover the entire range of interest of deformation. Therefore, a very high N value is not usually recommended (MSC.Marc, reference manual). When a suitable form of the strain energy density function W is chosen, the parameters a_{ij} (elastic constants) are found by non-linear regression. In some cases it may be found that the predicted non-linear elasticity is unaffected by a particular parameter and therefore the parameter is redundant and may be set to zero. However, the final set of parameters must satisfy the requirement for positive definiteness of the elastic behaviour. These conditions can be violated if insufficient data are used in the regression (Holzapfel et al., 2000).

3.3 Results

The complete data set describing the non-linear elastic passive material properties of the pelvic floor muscles was obtained. This data set includes both uniaxial and the equibiaxial properties of the pelvic floor muscle tissue.

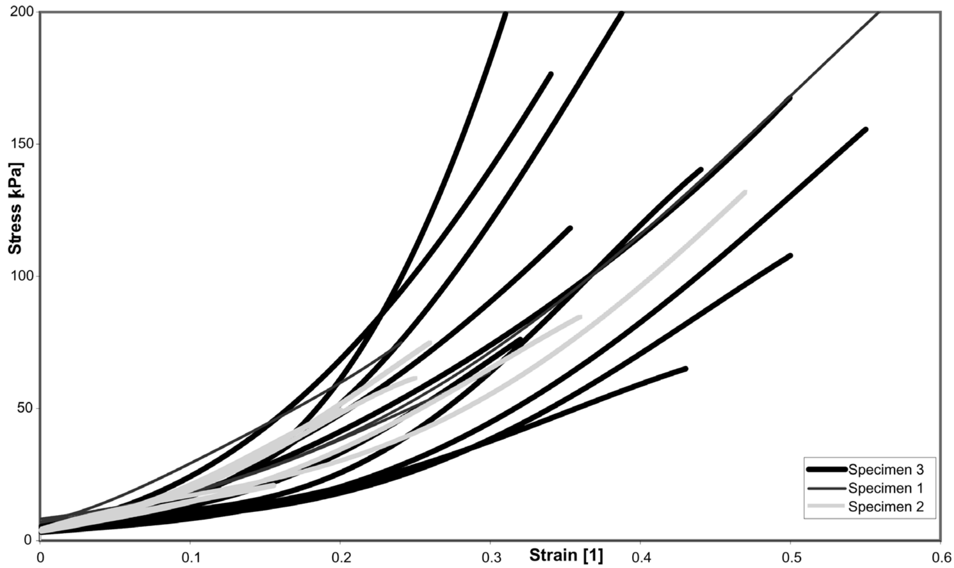

Figure 3.3: *The representative uniaxial stress-strain response for passive material properties of the pelvic floor muscles (raw data fits). All uniaxial stress-strain curves lie in the same interval. No significant difference was found within each particular specimen. Moreover, the non-linear and elastic behaviour of the pelvic floor muscle tissue is obvious.*

3.3.1 TISSUE TESTING

Representative uniaxial and equibiaxial stress-strain responses for passive pelvic floor muscles are shown in Figure 3.3 and Figure 3.4.

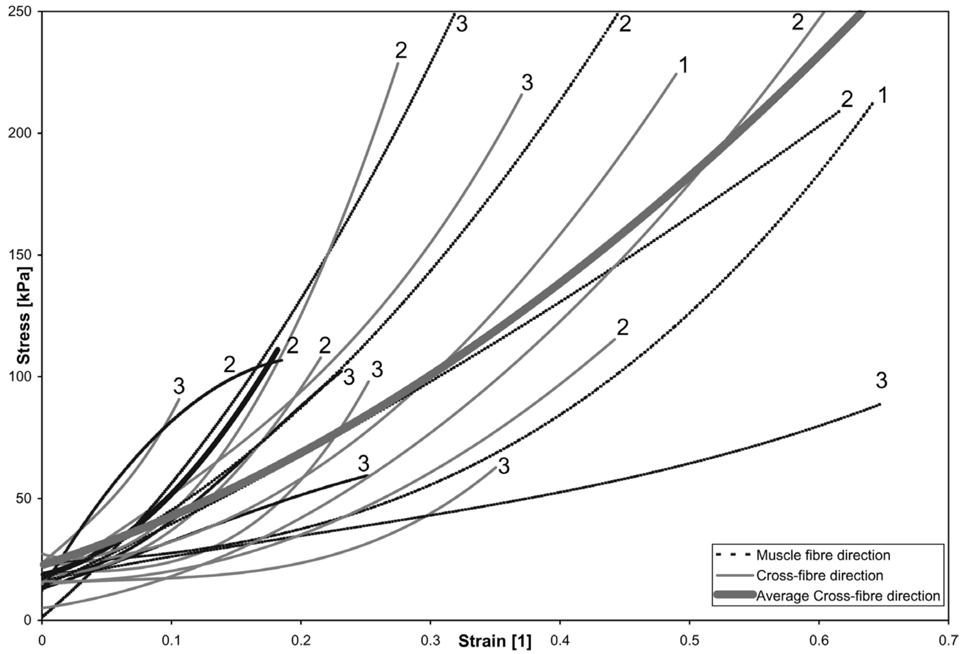

FIGURE 3.4: *The representative equibiaxial stress-strain response for passive material properties of the pelvic floor muscles (raw data fits). Particular specimens are labelled with numbers. In equibiaxial test, the behaviour in both fibre and transverse direction is non-linear with increasing stresses at higher stretches, indicating a limited maximum degree of extensibility. Visual inspection of the stress-strain plot suggests that the tissue is stiffer in the muscle fibre direction. In six of nine equibiaxial tests performed on three specimens, six samples were stiffer in muscle fibre direction while only three were stiffer in transverse direction. Moreover, the non-linear and elastic behaviour of the pelvic floor muscle tissue is obvious. The average transverse direction (thick curve) was used for fitting third order deformation Mooney-Rivlin material model (Table 3.3).*

Relatively high hysteresis (from 5 to 20% in strain) was observed in all tested samples (see example in Figure 3.5). This was observed only in the first preconditioning cycle. In second and third preconditioning cycle, the hysteresis was insignificant.

All uniaxial stress-strain curves lie in the same interval. No significant difference was found within each particular specimen (see Figure 3.3).

As in many other soft tissues, the behaviour of the pelvic floor muscle tissue is non-linear and elastic (Figure 3.3 and Figure 3.4). In equibiaxial tests, the behaviour in both fibre and transverse direction is non-linear with increasing stresses at higher strains, indicating a limited maximum degree of extensibility. Visual inspection of the stress-strain plot suggests that the tissue is stiffer in the muscle fibre direction. In six of nine equibiaxial tests performed on three specimens, six samples were stiffer in muscle fibre direction while only three were stiffer in transverse direction.

3.3.2 Histological analysis

Percentage of particular muscle type for all specimens are summarised in Table 3.1. The results show that the pelvic floor muscles are composed from both muscle fibre types with almost the same ratio.

Table 3.1: *Results from histological analysis of the embalmed pelvic floor muscles. Percentage of striated and smooth muscle type in the specimen. Samples were taken from the tissue in a random manner.*

	Striated muscle fibres percentage	Smooth muscle fibres percentage
Specimen 1	50	50
Specimen 2	60	40
Specimen 3	60	40

3.3.3 Sarcomere length measurements

The results of the sarcomere length measurements in all specimens are shown in Table 3.2. It was remarkable that all muscles were near the optimal muscle length as reflected in the small interval of sarcomere lengths between 2.0 and 3.3 μm. Mostly sarcomere lengths were at or just below the optimal muscle length. Obvious differences in sarcomere length in particular specimens were found. The standard deviation within specimen was very small (see Table 3.2).

TABLE 3.2: *Results from the sarcomere length measurements using a laser diffraction technique. Obvious difference in sarcomere length in particular specimens were found. Sarcomere lengths between 2.0 and 3.3 µm were measured, which is within the range that Walker and Schrodt (1974) argued to be consistent with the sliding filament theory.*

	Mean sarcomere length [µm] *N=10*	Standard deviation [µm] *N=10*
Specimen 1	3.05	0.16
Specimen 2	2.17	0.23
Specimen 3	2.84	0.13

3.3.4 CONSTITUTIVE MODELLING

Since the MR constitutive model assumes the material to be isotropic, it was necessary to establish only one equibiaxial stress-strain curve to define the material properties of the pelvic floor muscle tissue. Therefore, an average stress-strain curve was determined from the stress-strain curve in transverse directions. The stress-strain curves in the muscle fibre direction were not considered, since they were presumably affected by rigor mortis (Van Ee et al., 2000).

The strain energy density function for the nine-parameter model (Equation 3.5) was fitted to the equibiaxial data. A particular form of the generalized MR model, namely the Third Order Deformation (TOD) model (Equation 3.6), was used to obtain the elastic constants using a non-linear regression routine.

$$W = a_{10}(I_1 - 3) + a_{01}(I_2 - 3) + a_{20}(I_1 - 3)^2 + a_{11}(I_1 - 3)(I_2 - 3) + a_{03}(I_2 - 3)^3 \qquad (3.6)$$

This non-linear regression routine is available in the MSC.Marc (Palo Alto, CA) FE package and was used to determine the five material constants of Equation 3.6 (see Table 3.3). Since the strain energy density function of both constitutive models (the nine parameters model Equation 3.5 and TOD model Equation 3.6) is uniform, the remaining constants in the nine parameter MR constitutive model (Equation 3.5) are set to zero. Material constants of the human pelvic floor muscles for a particular order deformation model are summarised in Table 3.3. The TOD model provided the best fit of the experimental data. The least square error for a particular fit is given in Table 3.3.

TABLE 3.3: *Elastic constants describing the non-linear passive elastic behaviour of the pelvic floor muscles. The non-linear regression routines in MSC.Marc (Palo Alto, CA) were used (Equation 3.2, Equation 3.3, Equation 3.4, Equation 3.5 and Equation 3.6) in order to determine material constants for Mooney-Rivlin deformation model. Third order deformation (TOD) model provided the best fit of the experimental data. The least square error for particular fit is also given.*

	Mooney-Rivlin (Equation 3.2)		Mooney-Rivlin (Equation 3.3)		Mooney-Rivlin (Equation 3.4)		Mooney-Rivlin TOD (Equation 3.5 and 3.6)	
	Best-fit values [MPa]	Pos. const. [MPa]	Best-fit values [MPa]	Posi. const. [MPa]	Best-fit values [MPa]	Pos. const. [MPa]	Best-fit values [MPa]	Pos. const. [MPa]
a_{10}	-0.022084	0	-0.023218	0.001397	-0.012717	0	-0.015510	0
a_{01}	0.035584	0.023799	0.036456	0.018107	0.027997	0.019530	0.029881	0.022005
a_{11}	0	0	-0.000091	0.001669	-0.000489	0.001212	0.002003	0.000181
a_{20}	0	0	0	0	0.003795	0.000778	-0.000420	0.000234
a_{30}	0	0	0	0	0	0	-0.000634	0.000385
Error	0.000458	0.326449	0.000334	0.051404	0.000001	0.039565	0	0.102702

3.4 DISCUSSION

This study was performed to determine the passive material properties of the pelvic floor muscle tissue for FE modelling purposes. The study was performed on fresh cadaver specimens. This material is very difficult to obtain. The goal of our study was not to describe population specific properties of the pelvic floor muscle. Therefore we consider, that for developing the constitutive model of these muscles at first three specimens should be sufficient. In the future work, more specimens will be tested and the inter-individual comparison will also be provided.

3.4.1 TISSUE TESTING

The testing was carried out at room temperature and not body temperature. This is not expected to have a significant effect on tests of only several minutes duration. The samples were preloaded and thereafter preconditioned in three cycles (see Figure 3.5). The hysteresis was insignificant in second and third cycle. We suggested that the three preconditioning cycles are sufficient for purposes of material testing. Strain rates of 30% per minute were used in both the preconditioning and testing phases. These values were based on a pilot experiment with the pelvic floor muscle tissue and the strain rate was chosen to avoid any dynamic effects of the tissue loading. The specimens used for tissue testing contained a muscle fascia, which is a part of diaphragma pelvis. This muscle fascia varies in thickness within the location in the pelvic floor and can influence the stress-strain response of the tissue. However, influence of the muscle fascia cannot be determined in our measurements. We measured the complex stress-strain response of the diaphragma pelvis composite, which will be used, and is sufficient, for FE modelling of the pelvic floor.

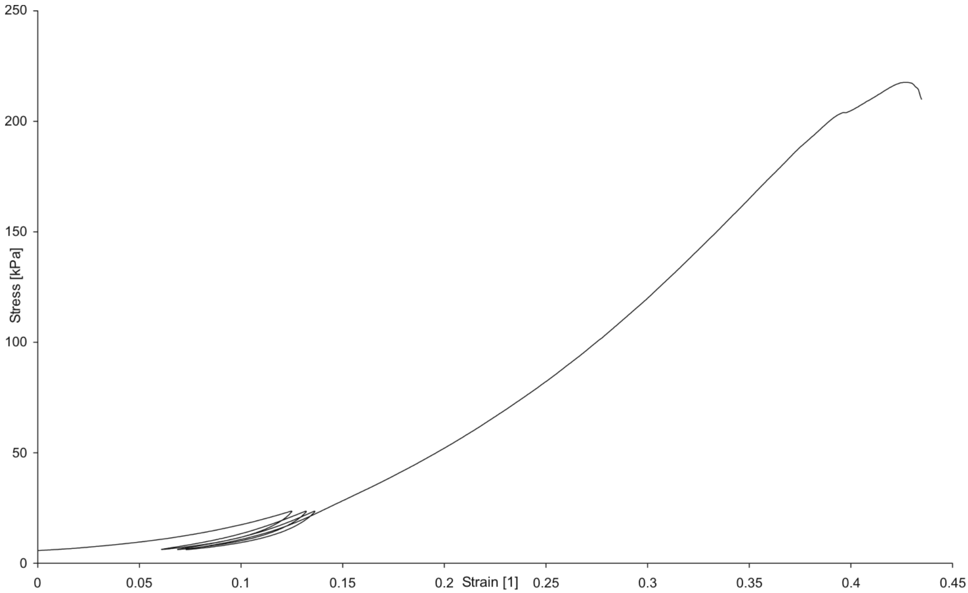

FIGURE 3.5: *Example of typical stress-strain response of the passive material properties of the pelvic floor muscles (raw data). Relatively high hysteresis was observed in the first preconditioning cycle. In the second and third preconditioning cycles, the hysteresis was insignificant.*

No inter-specimen or intra-specimen differences in stress-strain mechanical behaviour were found in the uniaxial tests. All uniaxial stress-strain curves lie in the same interval within all specimens as shown in Figure 3.3. Rigor mortis effects within uniaxial tests are unknown. The uniaxial data were not used for constitutive modelling.

We suggest to use only the muscle transverse direction stress-strain data from the equibiaxial test as a measure of the passive properties of the muscle tissue, since the fibre direction data are presumably strongly affected due to rigor mortis. Rigor mortis is the result of an increasing number of cross-bridges connecting the actin and myosin filaments after death. Rigor mortis affects the stiffness in fibre direction, but not the stiffness perpendicular to fibre direction (transverse direction). The transverse direction can be used for modelling the passive elastic non-linear behaviour of the muscle using the MR material model. The passive component results mainly from the extra-cellular matrix (i.e. connective tissue), and it can be assumed that it is similar in the muscle fibre direction and transverse direction, resulting in an isotropic MR model. The active component of the muscle cannot be obtained in a cadaver study. It only can be reconstructed implementing active muscle properties in a FE model.

Previous studies revealed that the living muscle was significantly stronger and absorbed more energy to failure than any of the postmortem post-rigor specimens, regardless of their handling (Van Ee et al., 2000). While the tissue of bone, ligament, tendon, and skin undergo small changes in mechanical properties post-mortem, skeletal muscle stiffness and failure load have been reported to vary significantly (Gottsauner-Wolf et al., 1995, Leitschuh et al., 1996). Results from Van Ee et al. (2000) demonstrated that post-rigor handling of cadaveric tissue prior to testing greatly affects muscle properties. Post-rigor skeletal muscle is significantly less stiff than perimortem and live passive tissue. These results, however, are not influenced by freezing (Van Ee et al., 2000).

3.4.2 Histological Analysis

The pelvic floor muscles are composed from both muscle fibre types with almost the same ratio, which is in agreement with results from de Blok, (1982). Unfortunately, the function (muscle and reflexive properties) of the smooth muscle remains unknown. The composition from both muscle fibre types is presumably important for function of the diaphragma pelvis.

3.4.3 Sarcomere length measurements

Recording the muscle sarcomere length (in relaxed condition) within the pelvic floor muscles enables the reconstruction of the muscle optimum length. From the muscle optimum length, the force-length curve can be reconstructed using data from muscle physiology (Klein Breteler et al., 1999). The force-length curve is important because it determines the maximal force in a certain position. In addition, the muscle stiffness is higher at the ascending slope of the force-length curve than at the descending slope (Sugi and Tsuchiya, 1988).

Muscle stiffness is an important factor for the stability of the system, and will determine the necessity of additional proprioceptive feedback control of the pelvic floor muscles.

Laser diffraction is a very accurate method for measuring sarcomere lengths (Klein Breteler et al., 1999). Sarcomere lengths between 2.0 and 3.3 μm were measured, which is within the range that Walker and Schrodt (1974) argued to be consistent with the sliding filament theory. Sample preparation did not permanently alter the sarcomere length. Some differences in sarcomere length in particular specimens were found. However, no relation to the specimen or particular location was found. The differences in sarcomere length could not explain the differences in stress-strain behaviour in the muscle fibre direction. Therefore, rigor mortis affects muscle properties and passive material properties cannot be measured in vitro.

3.4.4 DETERMINING THE MOONEY-RIVLIN CONSTANTS

Muscle consists of more than 70% water and behaves as nearly incompressible. Nearly incompressible material behaviour can lead to so-called locking of element in a numerical procedure. This becomes visible as oscillations in the displacement fields (Oomens et al., 2003). For this reason it is better to consider the material fully incompressible. The MR isotropic constitutive model was used for modelling the passive properties of the muscle.

The MR elastic model was chosen because of the wide availability in commercially available FE software. In this way, our solution may be widely used. Other constitutive models for the passive properties of the pelvic floor muscles could be determined, and indeed be superior to the MR model used here. The variability of the elastic behaviour observed in tested tissues suggests that the model proposed here is useful for the biomechanical purposes.

For constitutive model (Equation 3.6) and associated constants given in Table 3.3, the second derivate W with respect to the invariants B_{ij} (Cauchy-Green tensor) must be positive definite (Truesdell, 1952). I.e. the slope of the stress-strain curve must not be less than zero. This imposes the following conditions:.

$$\frac{\partial W}{\partial I_1} + (1 + \lambda_i) \cdot \frac{\partial W}{\partial I_2} > 0 \tag{3.7}$$

where λ_i is a stretch ($\lambda_i = 1 + \varepsilon_i$). All sets of constants presented in Table 3.3 satisfy this condition. The "best fit" constants have negative parameters and therefore do not satisfy the stricter condition that:

$$\frac{\partial W}{\partial I_1} > 0 \qquad \frac{\partial W}{\partial I_2} > 0 \tag{3.8}$$

Although the algorithm accepts up to six different deformation states, it can be shown that apparently different loading conditions have identical deformations, and are thus equivalent. After eliminating the several equivalent modes of testing, there are only three independent deformation states for which experimental data are needed: (1) Uniaxial tension, (2) Equibiaxial tension and (3) Pure shear. Pure shear deformation experiments are very difficult to perform. Besides, the shear properties are only relevant if the muscle is thick. The pelvic floor muscles are very thin (average of 3 mm). We assumed that the shear stress can be considered negligible. Data fitting can be done for uniaxial tension, equibiaxial tension or both modes simultaneously. In general, using both modes simultaneously results in the most accurate experimental data fit needed for constitutive modelling, especially in biomechanical analyses. However, we suggest the use of only the passive (transverse direction) component from the equibiaxial testing, since stiffness in the muscle fibre direction is presumably affected by rigor mortis. This applies to uniaxial as well as bi-axial measurements in the muscle fibre direction. This process does not affect the transverse direction.

3.5 Conclusions

The produced data set describes the passive elastic material properties of the pelvic diaphragm. The constitutive model based on these data can be directly used as an input for building a mathematical model based on FE theory, which can be used for the investigation of the effectiveness of reconstructive surgery.

Material properties of the muscle in the fibre direction are greatly affected by rigor mortis. Therefore, passive muscle properties can only be determined in transverse direction. The passive material properties in the muscle fibre direction can be derived from transverse direction data. Active muscle properties must be derived using a muscle model relating activation and muscle length.

The presented elastic constants in a Mooney-Rivlin Third Order Deformation Model, describing the non-linear passive elastic behaviour of the pelvic floor muscles, represent a good fit of the experimental data. A bi-axial material model is necessary for a thin layer like the pelvic floor.

ACKNOWLEDGEMENTS

The study was realized thanks to co-operation with the OLVG Hospital in Amsterdam. The authors wish to thank the Department of Pathology, (Head of department: Dr. J.L.G. Blaauwgeers) for offering the facilities and for performing the histological analysis of the pelvic floor muscles.

REFERENCES

De Blok, S., 1982. The connective tissue of the adult female pelvic region. A dissectional analysis. Acta Morphol Neerl Scand. 20(2), 191-212.

Gottsauner-Wolf, F., Grabowski, J. J., Chao, E. Y. S., and An, K. N., 1995. Effects of freeze/thaw conditioning on the tensile properties and failure mode of bone-muscle-bone units: a biomechanical and histological study in dogs. J. Orthop. Res., 13, No. 1, pp. 90-95.

Green, A.E., Zerna, W., 1968. Theoretical Elasticity, Clarendon Press, Oxford.

Holzapfel, G.A., Gasser, T.C., Ogden, R.W., 2000. A new constitutive framework for arterial wall mechanics and a comparative study of material models. Journal of Elasticity 61, 1-48.

Janda, S., Van der Helm, F.C.T., de Blok, S.B, 2003: Measuring morphological parameters of the pelvic floor for FE modelling purposes. Journal of Biomechanics, 36/6, 749-757.

Klein Breteler, M.D., Spoor, C.W., Van der Helm, F.C.T. 1999. Measuring muscle and joint geometry parameters of a shoulder for modeling purposes. J. Biomech. 32(11), 1191-1197.

Lai, W.M., Rubin, D., Krempl, E., 1993. Introduction to Continuum Mechanics, Pergamon Press.

Lally, C., Reid, A.J., Prendergast, P.J., 2004: Elastic Behaviour Of Porcine Coronary Artery Tissue Under Uniaxial And Equibiaxial Tension. Annals of Biomedical Engineering.

Leitschuh, P. H., Doherty, T. J., Taylor, D. C., Brooks, D. E., and Ryan, J. B., 1996. Effects of postmortem freezing on the tensile properties of the rabbit extensor digitorum longus muscle tendon complex. J. Orthop. Res., 14, pp. 830-833.

Mooney, M., 1940. A theory of large elastic deformation. Journal of Applied Physics 11, 582-591.

Oomens, C.W.J., Maenhout, M, van Oijen, C.H., Dorst, M.R., Baaijens, F.P., 2003. Finite element modelling of contracting skeletal muscle. Phil. Trans. R. Soc. Lond. B 358, 1453-1460.

Olsen, A.L., Smith, V.J., Bergstorm, J.O., Colling, J.C., Clark, A.L., 1997. Epidemiology of surgically managed pelvic organ prolapse and urinary incontinence. Obstet Gynecol. 89, 501-506.

Prendergast, P.J., Lally, C., Daly, S., Reid, A.J., Lee, T.C., Quinn, D., Dolan, F., 2003. Analysis of prolapse in cardiovascular stents: a constitutive equation for vascular tissue and finite element modelling. J. of Biomech. Eng. 125, 692-699.

Strumpf, R.K., Humphrey, J.D., Yin, F.C.P., 1993. Biaxial mechanical properties of passive and tetanized canine diaphragm. Am. J. Physiol. 365 (Heart Circ. Physiol. 34): H469-H475.

Sugi, H., Tsuchiya, T., 1988. Stiffness changes during enhancement and deficit of isometric force by slow length changes in frog skeletal muscle fibers. J. Physiol. 407, 215-229.

Truesdell, C.A., 1952. The mechanical foundations of elasticity and fluid dynamics. Journal of Rational Mechanics and Analysis, 1, 182.

Van Ee, C.A., Chasse, A.L., Myers, B.S., 2000. Quantifying skeletal muscle properties in cadaveric test specimens: Effect of mechanical loading, postmortem time and freezer storage. Journal of Biomechanical Engineering, Vol. 122, pp. 9-14.

Walker, S.M., Schrodt, G.R., 1974. I segment lengths and thin filament periods in skeletal muscle fibres of the rhesus monkey and the human. Anatomical Record 178, 63-82.

Young, L.L., Papa, C.M., Lyon, C.E., George, S.M., Miller, M.F., 1990. Comparison of microscopic and laser diffraction methods for measuring sarcomere lengths of contracted muscle fibres of chicken pectoralis major muscle. Poultry Science 69, 1800-1802.

Chapter 4

PELVIC FLOOR MUSCLE DISPLACEMENT IN RELATION TO THE LEVEL OF THE INTRA-ABDOMINAL PRESSURE AND MUSCLE ACTIVATION

Abstract

Objective: *The main goal of this experiment is to analyse the behaviour of the pelvic floor in patients and healthy volunteers.*

Study design: *The EMG activity, the displacement, the intra-abdominal pressure (IAP) and the width of the levator hiatus are evaluated. The EMG and IAP measurements are performed simultaneously. Displacement is recorded separately using MRI. All measurements are performed in three conditions: Rest, holding of the max level of the IAP and max contraction of the pelvic floor muscles (Conditions a, b, and c respectively).*

Results: *The effects of several within subject factors are evaluated using a general linear model of repeated measurements procedure (ANOVA). The EMG activity in the healthy volunteers is significantly higher (P=0.041) than in the patients. No significant difference in IAP was found (P=0.542) between healthy volunteers and the patients. No significant difference in the mean displacement of the diaphragma pelvis (P=0.671) was found between healthy volunteers and the patients. The displacement in the posterior part of the levator ani muscle is significantly larger (P=0.024) in the patient group. The width W of levator hiatus is significantly larger (P=0.002) in the group of selected patients with cystocele than in the healthy volunteers.*

Conclusions: *The presented results demonstrate: 1) significantly lower muscle activation (EMG activity) in the patient group; 2) no difference in the displacement in relation to the level of IAP; 3) larger width W of the levator hiatus in group of patients with cystocele but no difference in the depth D of the levator hiatus. No significant difference was found in the level of the IAP between groups. Performing MRI scanning in the rest and during holding the maximal level of the IAP provides the best information about the position and the displacement of the pelvic floor muscles. The combination of EMG, IAP and the width W of levator hiatus in these two conditions can be used for diagnostic purposes.*

Keywords

Pelvic floor muscles; intra-abdominal pressure; MRI; EMG

4.1 INTRODUCTION

The human pelvic floor is a very complex muscular structure. The m. levator ani with its fascial covering constitutes the pelvic diaphragm. M. levator ani is largely responsible for supporting both pelvic and abdominal organs and acts synergistically with the striated muscle of the anterior abdominal wall generating intra-abdominal pressure (IAP). Any increase in IAP caused for example by coughing or sneezing, is applied equally to all sides of the pelvic and abdominal wall. If the levator ani is pathologically weakened or temporarily inactivated a genital prolapse can occur. Genital prolapse is a major cause of morbidity in women. Genital prolapse is a condition in which pelvic organs (vagina, uterus, bladder, etc.), normally supported by the pelvic floor muscles, protrude outside the pelvic floor.

One in every nine women requires surgery for problems related to defective pelvic organ support (Olsen et al., 1997). Among these women, one in every four needs a second operation. Among women with documented prolapse, 76% had a defect in the support of the posterior compartment (Olsen et al., 1997). Despite the common occurrence of those diseases, the structural defects responsible for its formation remain poorly understood.

The pelvic floor muscles have a fundamental influence in the pelvic disorders. To study the complex biomechanical behaviour of the pelvic floor muscles and to investigate the effectiveness of reconstructive surgery, a computer model based on the finite-element (FE) theory is developed (Chapter 6). The model is able to predict the position of the pelvic floor depending on the load (e.g. IAP) and activation of the muscles. The model has to be validated with experimental data about the position of the pelvic floor (measured with Magnetic Resonance Imaging - MRI), muscle activation (EMG measurements) and IAP.

No studies are found describing the difference in the position of the pelvic floor between healthy subjects and patients with the pelvic organ prolapse. There is also a lack of any knowledge about the relationship between the position and activation of the pelvic floor muscles and the level of the IAP. Since the IAP is the main loading of the pelvic floor, it will affect the displacement of the pelvic floor. Activation of the pelvic floor muscles is necessary to increase the IAP (except during activities like coughing, sneezing etc.). Whether the muscles are lengthened or shortened, which will result in respectively downward or upward movement of the pelvic floor, depends on the level of the IAP and the level of muscle activation. There is a direct relation between the pressure in the compartment, the tensile stress in the wall of the compartment and the curvature of the wall of the compartment (Equation 4.1) van Leeuwen and Spoor (1992):

$$dp = -\sigma_f \cdot c_f \cdot dr \tag{4.1}$$

where dp is the pressure difference, σ_f is the stress in the muscle fibre, $c_f = 1/R_f$ is the local curvature (R_f = local radius of curvature) and dr represents the muscle thickness. If the muscles are activated, the tensile stress will increase and the curvature will decrease for the same IAP (which also depends on the activation of the abdominal muscles). Presumably, there is a difference in muscle activation between healthy persons and patients. This difference is presumably caused due to the pathology in the pelvic floor and must be studied in order to understand the behaviour of the diaphragma pelvis. Furthermore, the data can also be used for validation of the biomechanical model of the pelvic floor muscles.

The main goal of this experiment is to analyse the behaviour of the pelvic floor in patients and healthy volunteers. This behaviour is a result of muscle activation and loading by IAP and the displacement of the diaphragma pelvis. The difference in EMG activity, the displacement, the IAP and the width of the levator hiatus are evaluated during rest, maximal IAP and maximal pelvic contraction.

4.2 MATERIAL AND METHODS

All measurements are performed on 20 female subjects - ten healthy volunteers and ten patients (Table 4.1). All subjects were solicited in co-operation with the Department of Gynaecology of the OLVG Hospital in Amsterdam. Inclusion criteria for volunteers are: older than 18 years, comprehension of the aim and the conditions of the experiment. The exclusion criteria for volunteers are: identifiable acute or chronic diseases or urologic or gynaecologic dysfunction, pregnancy, previous or planned surgery in the pelvic floor compartment, contraindication for MRI (e.g. pacemaker, vascular clip in brain, claustrophobia) and not understanding aim and conditions of the experiment. Inclusion criteria for patients are: older than 18 years, primary genital prolapse without previous surgery in the pelvic floor compartment, comprehension of the aim and the conditions of the experiment. The exclusion criteria for patients are: pregnancy, previous surgery in the pelvic floor compartment, contraindication for the MRI (e.g. pacemaker, vascular clip in brain, claustrophobia), not understanding aim and conditions of the experiment.

After explaining the rationale of the study complemented by printed information, written informed consent was obtained and a health questionnaire ad-ministered to each participant. Permission for this study was obtained from the Medical Ethical Committee in OLVG Hospital, Amsterdam.

TABLE 4.1: *Characteristics of the subjects - individual and group information. BMI = body mass index.*

Group	Subject No.	Age (years)	Height (cm)	Weight (kg)	BMI (kg/m^2)	No. of vaginal deliveries	Diagnosis
Healthy volunteers *N=10*	1	29	170	63	21.8	0	
	2	50	161	62	23.9	0	
	3	24	167	80	28.7	0	
	4	43	169	65	22.8	2	
	6	55	172	77	26.0	3	
	7	43	178	63	19.9	2	
	10	48	178	67	21.1	1	
	12	48	178	77	24.3	0	
	14	33	172	60	20.3	1	
	15	26	171	61	20.9	0	
	Mean	39.9	171.6	67.5	23.0		
	Std	11.0	5.4	7.5	2.8		
Patients *N=10*	5	52	165	77	28.3	1	Stress urinary incontinence
	8	62	175	90	29.4	2	Cystocele gr III + Rectocele gr I
	9	59	169	79	27.7	1	Cystocele gr III
	11	55	165	70	25.7	2	Cystocele gr II
	13	75	168	85	30.1	1	Cystocele gr II + Rectocele gr I
	16	56	178	73	23.0	2	Rectocele gr II/III
	17	67	175	108	35.3	1	Rectocele gr III + descensus uteri
	18	71	178	70	22.1	2	Cystocele gr II
	19	40	160	58	22.7	2	Cystocele gr II
	20	34	178	70	22.1	1	Cystocele gr III + Rectocele gr I
	Mean	57.1	171.1	78.0	26.6		
	Std	12.9	6.5	13.8	4.3		

4.2.1 EMG AND IAP MEASUREMENTS

A two-channel perineal surface EMG is measured using the Medical Measurement Systems modular Solar Gold 4T urodynamics system. The NORAXON^{TM} dual electrodes composed of two circular electrodes (outer diameter of 2 cm, electrode diameter of 0.5 cm) placed on one supporting fabric strip are used during the experiment. The distance between the electrodes is 2 cm. These electrodes are placed lengthwise along the sagittal plane approximately 1 cm anterior to the anus. Electrodes are placed on both left and right side of the perineum. Electrodes are moistened with a conductive gel medium and connected to the Solar Gold 4T unit. The Kendall^{TM} Meditrace 133 electrodes placed on the spina iliaca anterior superior on each side (left and right) are used as a ground and connected to the Solar Gold 4T unit. The EMG signal goes through two channels differential amplifier with: noise less than 1 mVrms, input impedance of 1GΩ, CMRR > 120dB@50Hz and IMRR > 160dB. Subsequently, the signal is filtered with a high pass filter (-3dB) of 10Hz; slope is 6dB/oct and low pass filter (-3dB) of 5kHz with very steep anti-aliasing filter. The data are recorded at 11.025 kHz sample frequency with a 16-bit AD converter. Thereafter, the EMG signal is rectified (full-wave rectification). After rectification, the signal is filtered using a moving average FIR filter. The data are resampled to a sampling rate of 50Hz having the effect of a digital low-pass filter. The data are measured in microvolts (μV).

Simultaneously, the IAP is measured using an intra-rectal catheter connected on the same urodynamics system. The intra-rectal unisensor microtipcatheter with a diameter of 2 mm is placed in the rectum (approximately 4 cm). Before insertion, the pressure is set to zero, in order to calibrate the level of the IAP in relation to the atmospheric pressure. This catheter is a standard intra-rectal pressure device and is often used during routine urodynamics examinations. The pressure is recorded in cm of water column at a sampling rate of 50Hz.

4.2.1.1 Procedures

Each subject was asked to disrobe and to assume a supine position on the physiotherapy bed with legs straightened. With the assistance of a physiotherapist, each subject tried all the conditions several times with the help of feedback using the EMG and IAP data on a LCD display. Thereafter, each subject was asked to perform one of the three measurement conditions as explained below:

a) Rest - Condition a: In this condition, the subject is asked to maintain rest while lying, to avoid any movements and to breathe normally. EMG activity and the level of IAP are recorded.

b) Max IAP - Condition b: In this condition, the subject is asked to maintain the maximal level of the IAP by both breath holding and abdominal muscle contraction. The subject is asked to maintain this condition for at least 20 s. During this time the EMG activity and the level of IAP are recorded.

c) Max ACT - Condition c: During this condition subject is asked to perform maximal contraction of the pelvic floor muscles for at least 20 s. She is also asked to breathe normally and to minimize abdominal muscle wall contraction during this condition (i.e. no build-up IAP). EMG activity and the level of IAP are recorded during the pelvic floor contraction phase.

All these conditions are performed in this sequence: a, b, c, a, b, c, a, b and c. No movement is allowed between these conditions. The time for performing these measurements is approximately 30 minutes per subject.

4.2.1.2 DATA PROCESSING

The EMG data are filtered and processed by use of the MATLAB^{TM} 6.1 software from The Mathworks Inc. The EMG data are split up for each condition (a, b, and c) into segments of about 15 s. In this study, muscle activation is modelled as a second order system. Thus, data are filtered using a second order Butterworth filter. The quantified cut off frequency (natural frequency) is 2.5 Hz. These values are similar to those found in the literature. Potvin et al., (1996) found a rather wide range for trunk extensor muscles (2.0-3.3 Hz) while Bobet and Norman (1990) identified the elbow flexor and extensor muscles and found values of 1.9-2.8 Hz. Olney and Winter (1985) estimated values of 1.0-2.8 Hz for lower limb muscles during walking. For each condition, a mean value of the EMG signal is calculated.

The mean value of the IAP is calculated over the same period of 15s.

Analysis of variance (ANOVA) is performed in order to quantify the effect of conditions a, b and c, the EMG activity, the IAP and the displacement. A general linear model (GLM) for repeated measurements is analysed separately for EMG and IAP. The dependent variables are EMG and IAP. The independent variables are: Condition b vs. c and left and right side of the pelvic floor. The group (patients vs. healthy volunteers) is used as a between subject factor. The SPSS 12.0.1 software is used for this statistical analysis in all cases during this study.

4.2.2 MRI MEASUREMENTS

Directly after the EMG measurements, the subjects had MRI measurements. Several T1-weighted gradient echo or T2-weighted turbo spin-echo MRI sequences are performed in order to obtain the displacement of the pelvic floor muscles. The measurements are performed using a 1.5T Philips MRI Gyroscan Intera scanner at the Department of Radiology of the OLVG Hospital in Amsterdam. The MRI volume is chosen in order to cover the diaphragma pelvis (m. levator ani and m. coccygeus) between symphysis pubica and os coccygeus. The same cubic MRI volume is used for all scan conditions. The first scan session (Condition a as described in Section 4.2.2.1 on page 70) is performed in the rest position with the highest resolution possible. This session formed a reference image data set. Thereafter, sequences of fast sessions are taken during holding of the maximal level of the IAP (for about 21 s) and during the maximal contraction of the pelvic floor muscles without increasing the level of IAP. Fast sessions are repeated three times. The MRI settings for all conditions are summarised in Table 4.2. A syn-cardiac coil is used during all sessions.

TABLE 4.2: *Measuring parameters and settings of the Philips MRI Gyroscan Intera scanner during the MRI measurements in all conditions. Condition a - rest, Condition b - max IAP, Condition c - max ACT.*

MRI settings	Condition a	Conditions b, c
Session type	Cor TT2 SE	Cor T1 GR
Slice thickness [mm]	4	4
Spatial Resolution [mm]	5	7
Field of view (FOV)	300	375
RFOV	80	70
Matrix resolution [pixels] 16bit	512x512	256x256
Pixel resolution [mm/pixel]	0.58	1.46
Number of slices	25	11
MR acqusition type	2D	2D
Acquisition time	1min 59s	21s
TR [ms]	4547	3.58
TE [ms]	90	1.79
Magnetic field strength [T]	1.5	1.5
Coil type	Syn-cardiac	Syn-cardiac
Fast imaging mode	TSE	FFE

4.2.2.1 PROCEDURES

Subjects were requested not to eat for four hours before the measurements. This condition is necessary to ensure good MRI image quality. Each subject was asked to assume a supine position within the MRI scanner. Each subject was instructed to perform one of the three conditions of measurement as explained below:

a) Rest - Condition a: The subject is asked to maintain rest, to avoid any movements and to breathe normally. A Coronal T2 weighted turbo spin-echo MRI sequence is performed for approximately 2 minutes.

b) Max IAP - Condition b: In this condition, the subject is asked to maintain the maximal level of the IAP by both breath holding and abdominal muscle contraction. The subject is asked to maintain this condition for at least 21 s. During this time, a Coronal T1 weighted gradient-echo MRI sequence is performed.

c) Max ACT - Condition c: During this condition, the subject is asked to perform maximal contraction of the pelvic floor muscles for at least 21 s. She is asked to breathe normally and to minimize the abdominal muscle wall contraction during this condition. A Coronal T1 weighted gradient-echo MRI sequence is performed during the pelvic floor muscle contraction phase.

The sessions are performed in this sequence: a, b, c, b, c, b, and c. No movement is allowed between these conditions. A 30 s rest period followed each condition to minimize fatigue.

These three conditions are chosen as the only repeatable conditions in both parts of experiment (EMG + IAP and MRI part). Without measuring IAP and muscle activity inside the MRI scanner, the subjects are able to repeat only these three conditions (a, b and c). The measurements lasted approximately 20 minutes per subject.

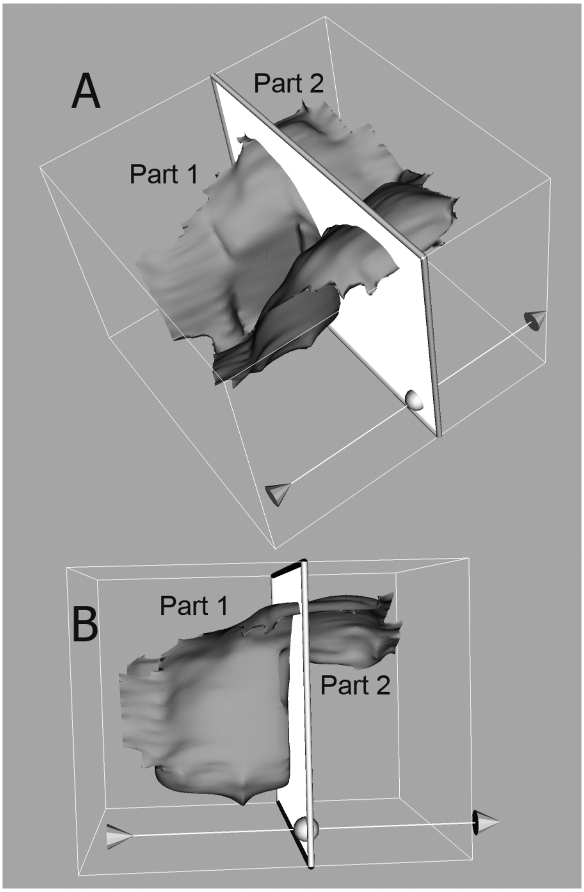

FIGURE 4.1: *The 3D reconstruction of the pelvic floor muscles based on semi-automated gradient-oriented single line segmentation of the MRI data. An implicit (cutting plane) is displayed. This is based on an anatomical division of the diaphragma pelvis as follows: Part 1 consists all organs structures such as the vagina and the rectum and Part 2 consists the posterior part (m. coccygeus) of the diaphragma pelvis. The arrow is pointing posteriorly in both views.* ***A*** *- perspective view from top left side.* ***B*** *- left side view.*

4.2.2.2 Data processing

Semi-automated gradient-oriented segmentation of the MRI scans is performed. A single line is generated as a representation of an inner surface border of pelvic floor muscles. 3D reconstructions of the pelvic floor muscles are made in all measured conditions (see Figure 4.1 for an example).

For use in numerical comparison, the 3D surfaces are divided into two parts. This is based on an anatomical division of the diaphragma pelvis as follows: Part 1 (anterior part) consists of all organ structures such as the vagina and the rectum and Part 2 consists of the posterior part (m. coccygeus) of the diaphragma pelvis (see Figure 4.1). This division is necessary for determining the local effects between all conditions. A comparison for both parts (Part 1 and 2) is done in Condition b with respect to a, and Condition c with respect to a. The MESH software developed by Aspert et al., (2002) is used to evaluate the difference between iso-surfaces (triangulated meshes). It uses symmetric Hausdorff distance to compute a mean error between two given surfaces (Aspert et al., 2002). For visualization and surface modelling of the data, the DeVIDE (the Delft Visualisation and Image processing Development Environment, Botha, 2004) software is used.

The mean distance between the given surfaces is used as a dependent variable for ANOVA. GLM for repeated measurements is analysed. The independent variables are Condition b vs. c, and Part 1 vs. Part 2 of the diaphragma pelvis. Patients vs. healthy volunteers are analysed as a between subject factor.

The diagnosis of most of the patients (seven of ten) is a cystocele (see Table 4.1) in the anterior part of Part 1. Cystocele is primarily a consequence of damage to the vagina - either its support or the vaginal wall itself (Nichols and Randall, 1996). Therefore, one slice is selected in order to determine local changes in the shape and position of the levator ani muscle. The position of this slice is determined using the landmarks (levator hiatus at the level of vagina). Thereafter, the closest neighbourhood slice is selected in this compartment. In this slice, the distance between centroids of the femur heads (HD) is determined. Thereafter, the distance (depth D) is determined from the centre of the line connecting both femur centroids to the lowest border of the levator ani muscle. The width W of the levator hiatus is determined as a distance of the left and right borders of the levator ani muscle perpendicular to D at 50% of the length of D (see Figure 4.2). The hip distance HD, maximal depth D and width W are determined in all conditions (rest, max IAP, max ACT).

The depth D and width W of the levator hiatus in all three conditions are used as dependent variables for ANOVA. GLM for repeated measurements is analysed for these independent variables: Condition a, b, and c. The selected group of patients ($N=7$) vs. healthy volunteers ($N=10$) is used as between subject factor.

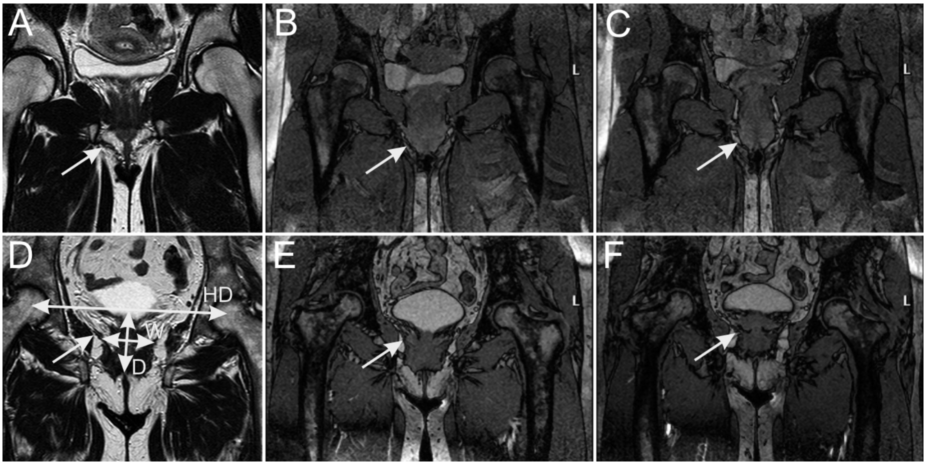

FIGURE 4.2: *Example of coronal MRI images of the female pelvis in supine position for a healthy subject (Images A, B and C) and patient with cystocele (Images D, E, and F). The distance between centroids of the femur heads (HD) was determined (see example in the Image D). Thereafter, the distance (depth) of the lowest border of the levator ani muscle (D) was determined from the centre of the line connecting both femur centroids. The width W of the levator hiatus was determined as a distance of the outer border of the levator ani muscle perpendicular to the D in the 50% of the length of D. The hip distance HD, maximal depth D and 50% width W were determined in all conditions (rest, max IAP, max ACT) and are summarised in Table 4.6.* ***A*** *- coronal slice of the levator ani muscle in rest (Condition a) - healthy subject.* ***B*** *- coronal slice of the levator ani muscle during max IAP (Condition b) - healthy subject.* ***C*** *- coronal slice of the levator ani muscle during max ACT (Condition c) - healthy subject.* ***D*** *- coronal slice of the levator ani muscle in rest (Condition a) - patient.* ***E*** *- coronal slice of the levator ani muscle during max IAP (Condition b) - patient.* ***F*** *- coronal slice of the levator ani muscle during max ACT (Condition c) - patient.*

4.3 RESULTS

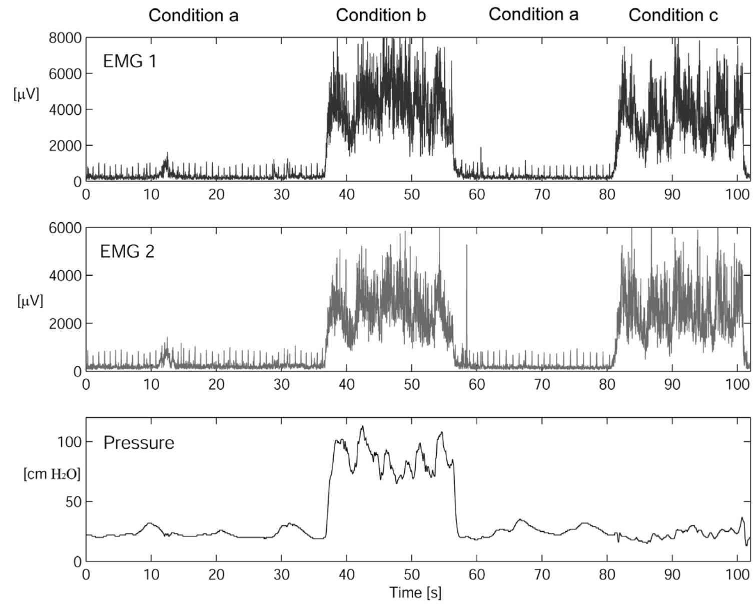

FIGURE 4.3: *An example of the EMG and IAP recordings (raw data) obtained for a healthy subject (subject no.: 4, see Table 4.1) by MMS Solar Gold 4T urodynamics system. The perineal surface EMG is shown in microvolts for both sides (EMG 1 - right side, EMG 2 - left side). The IAP was determined in cm of water column. The measurements were performed during rest (Condition a), during holding max level of IAP (Condition b) and during performing max contraction of the muscles (Condition c). The heartbeat can be observed as a noise.*

4.3.1 EMG AND IAP MEASUREMENTS

The EMG and IAP data for each subject are summarised in Table 4.3 and Table 4.4. Examples of EMG and IAP recordings are displayed in Figure 4.3, Figure 4.4 and Figure 4.5. Figure 4.3, Figure 4.4 and Figure 4.5 illustrate that, a high level of IAP is observed in Condition b, while a constant level of IAP is observed in conditions a and c. An example of recordings for a healthy subject is given in Figure 4.3. There is a high EMG activity in Condition b and c, while very low activity can be observed in Condition a. A high level of IAP is observed in Condition b, while a constant level of IAP is observed in conditions a and c. Examples of recordings of two different patients with cystocele are given in Figure 4.4 and Figure 4.5. In Figure 4.4, there is a high EMG activity only in Condition c, while hardly any activity can be observed in conditions a and b. In Figure 4.5, there is a low EMG activity in conditions b and c with respect to Condition a.

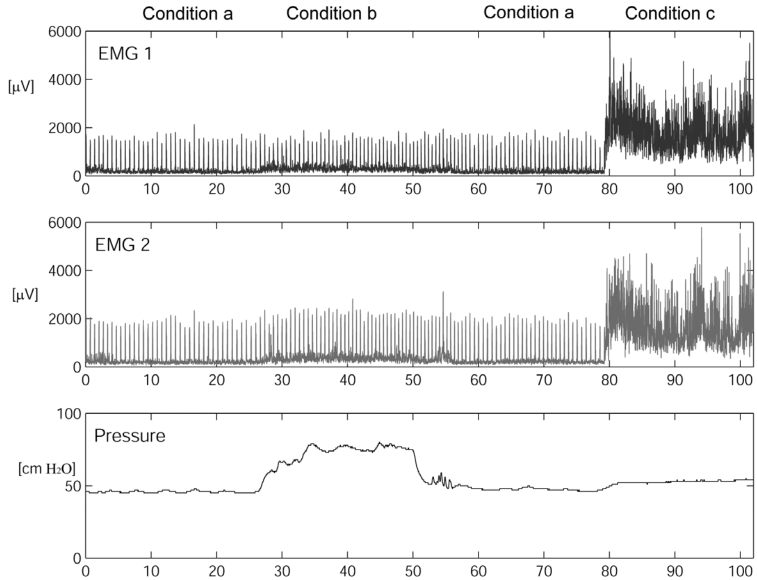

FIGURE 4.4: *An example of the EMG and IAP recordings (raw data) obtained for a patient (subject no.: 9, see Table 4.1) from MMS Solar Gold 4T urodynamics system. The perineal surface EMG is shown in microvolts for both sides (EMG 1 - right side, EMG 2 - left side). The IAP was determined in cm of water column. The measurements were performed during rest (Condition a), during holding max level of IAP (Condition b) and during performing max contraction of the muscles (Condition c). The heartbeat can be observed as a noise.*

A significantly higher mean EMG activity (p=0.029) was found during max contraction of the muscles (Condition c) than during holding max level of the IAP (Condition b). There is no significant effect in EMG activity between left and right side (P=0.774). Test of between-subject factors revealed a significantly higher EMG activity (P=0.041) in the group of healthy volunteers than in the patients.

A significantly higher level of mean IAP (p<0.001) was found during holding max level of IAP (Condition b) than during max contraction of the muscles

(Condition c). Test of between-subject factors revealed no significant difference in the level of IAP (P=0.542) between the healthy volunteers and patients.

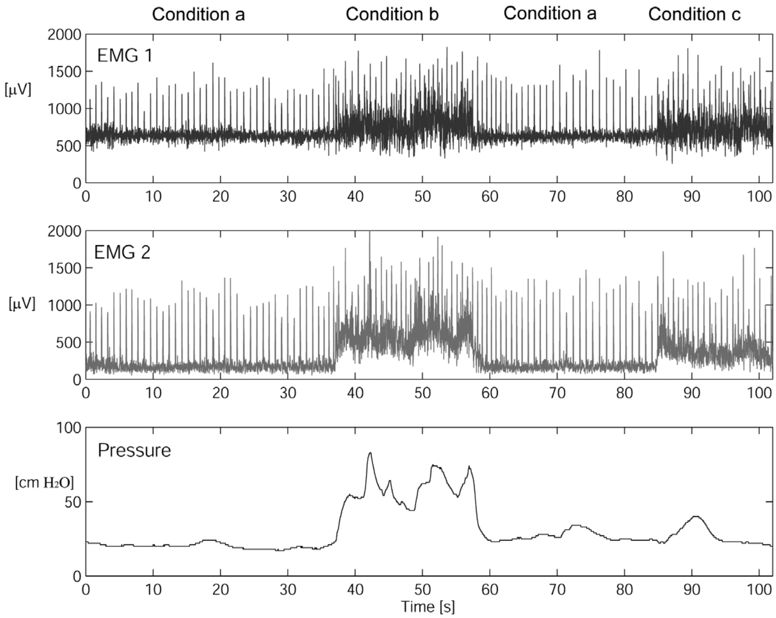

FIGURE 4.5: *An example of the EMG and IAP recordings (raw data) obtained for a patient (subject no.: 20, see Table 4.1) from MMS Solar Gold 4T urodynamics system. The perineal surface EMG is shown in microvolts for both sides (EMG 1 - right side, EMG 2 - left side). The IAP was determined in cm of water column. The measurements were performed during rest (Condition a), during holding max level of IAP (Condition b) and during performing max contraction of the muscles (Condition c). The heartbeat can be observed as a noise.*

4.3.2 MRI MEASUREMENTS

The results of the mean distance are summarised in Table 4.5. A significantly larger displacement (p=0.006) is found in Condition b than in Condition c. Moreover, there is a significantly larger (P<0.001) displacement in Part 1 than in Part 2 of the diaphragma pelvis. A test of between-subject factors revealed no significant difference in the mean displacement of the diaphragma pelvis (P=0.671) between the healthy volunteers and patients. A significant group difference (P=0.024) is found in the displacement between Part 1 and Part 2.

The position of the levator ani muscle in Condition b is always below the position observed in Condition a (see Figure 4.7). The position of the levator ani muscle in Condition c intersects with the muscle in Condition a (see Figure 4.7).

Results of the depth D and width W of the levator ani muscle in the anterior part of Part 1 are summarised in Table 4.6. A highly significant effect (P<0.001) is found in the depth D between all conditions (a, b and c). Test of between-subject factors revealed no significant difference in the depth D (P=0.861) between the healthy volunteers and selected patients with cystocele (*N=7*).

TABLE 4.3: *Summary of the perineal surface EMG measurements. All measurements represent the mean values of the EMG signal in microvolts. EMG activity is measured on both sides of the diaphragma pelvis. IAP is measured simultaneously (see Table 4.4). IAP = intra-abdominal pressure.*

Group	Subject No.	EMG [µV] Right side - EMG 1 Rest	Max IAP Mean (*N=3*)	Max IAP Std (*N=3*)	Max ACT Mean (*N=3*)	Max ACT Std (*N=3*)	Left side - EMG 2 Rest	Max IAP Mean (*N=3*)	Max IAP Std (*N=3*)	Max ACT Mean (*N=3*)	Max ACT Std (*N=3*)
Healthy volunteers *N=10*	1	410	2497	285	3854	699	777	2052	202	2784	448
	2	229	539	23	975	497	2351	2195	90	2324	150
	3	286	1443	205	1879	13	275	1288	130	1607	85
	4	212	3638	857	3419	223	163	2224	404	2493	155
	6	381	1007	84	1152	94	662	1114	44	1141	149
	7	1418	2451	126	2365	148	714	1378	13	1634	30
	10	213	615	47	890	298	646	999	244	994	69
	12	1259	1400	69	2385	31	938	1082	114	2507	191
	14	367	1401	337	904	207	349	1618	563	777	170
	15	420	1191	270	1015	375	212	864	167	576	277
	Mean	*519*	*1618*		*1884*		*709*	*1481*		*1684*	
	Std	*440*		*966*		*1095*	*634*		*512*		*801*
Patients *N=10*	5	286	811	83	785	72	239	753	77	686	36
	8	538	804	31	979	73	462	772	32	956	50
	9	282	377	45	1574	261	320	476	57	1402	300
	11	343	1309	130	1646	110	248	1259	61	1500	56
	13	391	1469	131	1560	387	296	1438	170	1231	52
	16	277	1231	231	2073	268	188	915	65	2211	335
	17	366	1033	179	1256	139	378	1183	101	1309	156
	18	541	977	106	1739	285	634	1248	110	1535	175
	19	343	581	45	535	36	184	754	161	813	142
	20	656	933	118	888	141	216	773	114	424	13
	Mean	*402*	*952*		*1303*		*316*	*957*		*1206*	
	Std	*131*		*332*		*492*	*142*		*306*		*511*

A highly significant effect (P<0.001) is found in the width W between all conditions (a, b and c). Test of between-subject factors revealed a significantly larger width W (P=0.002) in the group of selected patients (*N=7*) than in healthy volunteers (*N=10*).

The results show that there is a significant difference in the width (P<0.001) of the levator hiatus while performing all conditions between patients and healthy volunteers. This phenomenon can also be observed from raw MRI scans (see Figure 4.2 and Figure 4.7). In contrary, the maximal depth of the levator ani muscle does not significantly differ during all conditions between both groups (Figure 4.2 and Table 4.6).

TABLE 4.4: *Summary of the level of IAP measurements. All measurements represent the mean values of the pressure in Pascals. Perineal surface EMG was measured simultaneously (see Table 4.3). IAP = intra-abdominal pressure.*

Group	Subject No.	Intra-abdominal pressure [kPa]				
		Rest	Max IAP		Max ACT	
			Mean (*N=3*)	Std (*N=3*)	Mean (*N=3*)	Std (*N=3*)
Healthy volunteers *N=10*	1	1.75	9.48	1.00	2.33	0.67
	2	3.30	13.21	1.23	3.83	0.30
	3	2.53	10.43	1.32	5.77	0.63
	4	2.12	7.87	1.79	2.27	0.43
	6	2.30	5.12	0.57	4.83	0.41
	7	2.27	7.74	0.34	3.86	0.23
	10	1.50	7.54	1.23	2.27	0.34
	12	6.11	7.72	0.08	7.54	0.70
	14	3.37	6.76	0.40	4.07	1.14
	15	3.82	6.66	0.48	5.05	0.56
	Mean	*2.9*	*8.3*		*4.2*	
	Std	*1.3*		*2.3*		*1.7*
Patients *N=10*	5	3.94	9.94	0.55	4.95	0.21
	8	1.58	3.18	0.06	2.51	0.14
	9	4.56	6.67	1.30	4.82	0.31
	11	0.18	1.62	0.53	0.76	0.07
	13	7.16	14.02	0.41	11.01	1.34
	16	2.00	6.47	0.53	3.01	0.22
	17	5.72	12.19	4.69	6.55	1.51
	18	3.52	6.29	0.81	4.38	0.11
	19	1.10	2.13	0.31	1.31	0.13
	20	1.96	5.60	0.27	2.16	0.36
	Mean	*3.2*	*6.8*		*4.1*	
	Std	*2.2*		*4.1*		*3.0*

4.4 DISCUSSION

The main goal of this experiment was to analyse the behaviour of the pelvic floor in patients and healthy volunteers. To this end, experimental measurements were performed in order to obtain a complete data set of the position, the displacement and the activation of the pelvic floor muscles in 20 female subjects (10 patients and 10 healthy volunteers).

The results show the differences between patients and healthy volunteers: 1) difference in EMG activity, 2) no difference in the mean displacement in relation to the level of IAP, 3) difference in width W but no difference in depth D of the levator hiatus between healthy subjects and patients with cystocele.

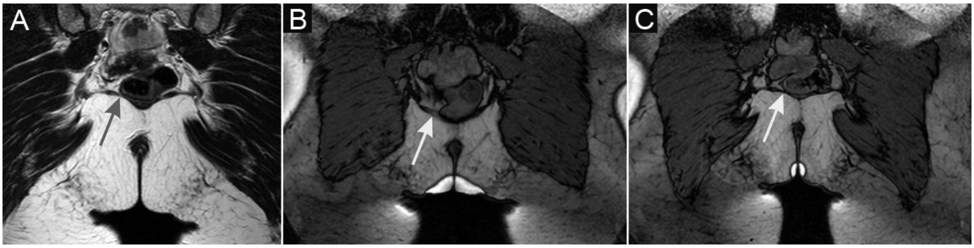

FIGURE 4.6: *Typical example of coronal MRI images of the healthy female pelvis, where the shape and position of the pelvic floor muscle (small arrows) is demonstrated.* ***A*** *- coronal slice in Part 2 of the diaphragma pelvis during rest (Condition a).* ***B*** *- coronal slice in Part 2 of the diaphragma pelvis during max IAP (Condition b).* ***C*** *- coronal slice in Part 2 of the diaphragma pelvis during max ACT (Condition c). The most obvious difference is observed in the posterior part (m. coccygeus) of the diaphragma pelvis (Part 2) where the muscle assumes a dome shape in supine position (Image A) during conditions a and c (Images A and C) while a basin shape can be found in Condition b (Image B).*

The lower EMG activity in the patient group suggest lower muscle activation and therefore lower muscle force generated by muscle assuming that the same EMG force relationship exists for each subject. No significant difference was found in the level of IAP between both groups. The lower muscle force generation in the patient group can be presumably caused either due to lower muscle activity (low EMG) or due to muscle atrophy. The width of levator hiatus in the selected patient group ($N=7$) was significantly larger (P=0.002) than in the healthy volunteer group.

<u>In considering the presented results following main questions arise:</u>

1) What is the effect on the width of the levator hiatus if the muscle is insufficiently activated?

2) What is the effect on width of the levator hiatus if the connective tissue in the levator hiatus is more compliant than normal?

And finally clinical questions arise:

3) Is muscle training effective if there is a problem in connective tissue of the levator hiatus?

4) On what spot in the diaphragma pelvis the surgeon has to focus on during reconstructive surgery if: a) the muscle activation is insufficient (the muscle is not able to generate enough force) and the connective tissue has a normal compliancy; b) the muscle activation is normal (muscle is able to generate enough force) but the connective tissue of the levator hiatus is more compliant?

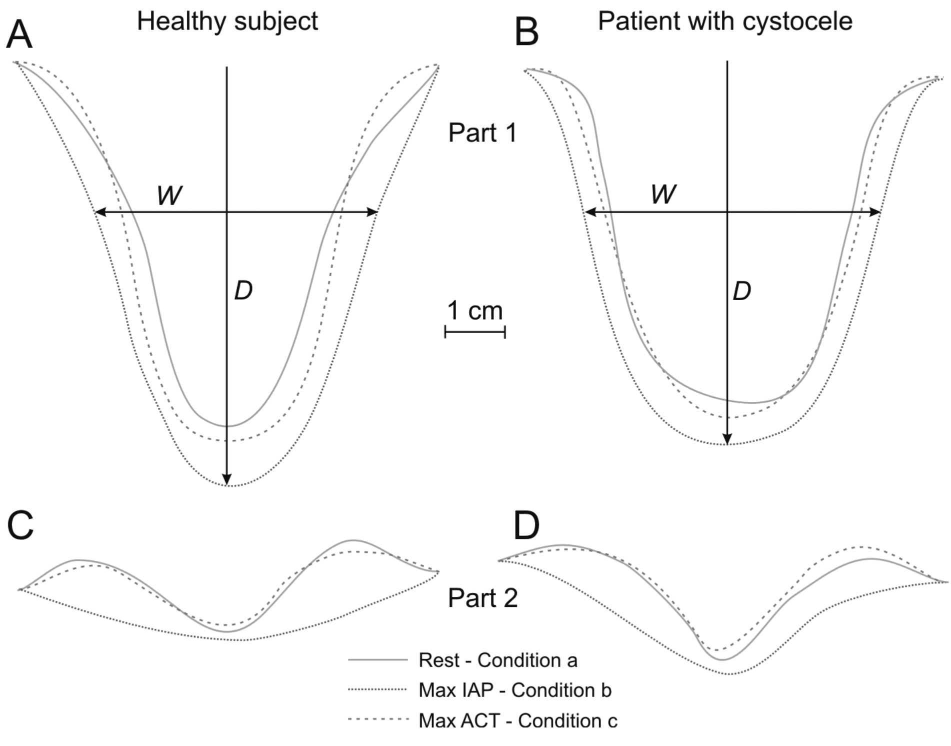

FIGURE 4.7: *Schema of the position of the pelvic floor muscles in healthy subject and patient with cystocele. The level where the depth (D) and width (W) of the levator hiatus is determined is also displayed. The mean displacement of the muscles is summarised in Table 4.5. The depth (D) and width (W) of the levator hiatus in all conditions is given in Table 4.6.* ***A*** *- position of the muscle in all conditions in Part 1 - healthy subject.* ***B*** *- position of the muscle in all conditions in Part 1 - patient.* ***C*** *- position of the muscle in all conditions in Part 2 - healthy subject.* ***D*** *- position of the muscle in all conditions in Part 2 - patient.*

In order to answer all these questions a biomechanical model of the pelvic floor based on FE theory is developed (Chapter 6). The model is able to predict the position of the pelvic floor depending on the loading (e.g. IAP) and activation of the muscles.

4.4.1 EXPERIMENTAL DESIGN

Since it is not possible to measure EMG and IAP within the MRI scanner the experiment is split into two parts. In the first part, the EMG and IAP are performed simultaneously. MRI recordings are performed in the second part in the same conditions.

All procedures used during this experiment are standard clinical procedures with low associated risks. Some difficulties were expected during breath holding and holding of the maximal level of the IAP in the supine position. Some subjects did not find it comfortable in the MRI scanner because of the level of noise during scanning. Nevertheless, all subjects dealed well with this.

4.4.2 EMG AND IAP MEASUREMENTS

Surface EMG was found to be one of the best ways to measure activity of the levator ani muscle (Voorham-van der Zalm et al., 2004). The use of vaginal or rectal electrodes is not accurate enough since these electrodes measure sphincter activity and the activity of structures other than the levator ani muscle (Voorham-van der Zalm et al., 2004). The EMG data in microvolts are used for further analysis, since it is not possible to normalise the EMG signal within this study. No proper maximal EMG could be obtained as reference. There is not any absolute reference in the muscle strength. Max level of IAP cannot be used to determine the muscle activity and force.

4.4.3 MRI MEASUREMENTS

Coronal slices are chosen since all muscle parts of the pelvic floor diaphragma are easily recognizable in this section, which is necessary for segmentation of the muscles. Pelvic floor organs are much better recognizable in sagittal sections, but these slices cannot be used for muscle segmentation. In each condition, one mid-sagittal slice and several coronal slices are acquired, since the main goal of our study was to evaluate the position of the pelvic floor muscles and not the organs.

TABLE 4.5: *Summary of the mean displacement (in millimeters) with respect to the rest position of the pelvic floor muscles for individual subjects and the mean values for both groups. The mean symmetric Hausdorff distance was calculated for comparison of the two corresponding 3D reconstruction for both parts of the diaphragma pelvis (see Figure 4.1), for all three conditions (Rest, Max IAP, Max ACT) in the supine position of subject. IAP = intra-abdominal pressure.*

Group	Subject No.	Mean Displacement [mm]			
		Max IAP		Max ACT	
		Part 1	Part 2	Part 1	Part 2
Healthy volunteers *N=10*	1	3.1	1.6	3.4	2.2
	2	3.1	1.4	2.2	2.0
	3	3.3	1.7	3.0	2.2
	4	3.9	1.5	3.1	1.3
	6	3.8	2.0	3.4	1.5
	7	3.6	1.8	3.4	1.5
	10	3.2	1.9	2.2	1.9
	12	3.1	2.0	2.5	2.3
	14	2.5	1.8	1.8	1.8
	15	2.8	1.4	2.8	1.3
	Mean	*3.2*	*1.7*	*2.8*	*1.8*
	Std	*0.4*	*0.2*	*0.5*	*0.4*
Patients *N=10*	5	3.0	2.5	3.1	2.7
	8	3.3	2.2	2.9	2.2
	9	2.9	1.5	2.4	1.4
	11	3.9	1.9	3.8	2.3
	13	2.4	3.1	2.2	2.5
	16	3.1	1.9	2.2	2.2
	17	2.2	1.7	1.9	1.4
	18	3.8	2.6	2.8	2.3
	19	2.1	2.2	2.1	2.2
	20	2.2	2.4	2.4	1.9
	Mean	*2.9*	*2.2*	*2.6*	*2.1*
	Std	*0.6*	*0.4*	*0.5*	*0.4*

Each subject was already instructed how to perform all conditions in the first part (EMG + IAP) of the experiment. However, the performance of these conditions during the MRI measurements cannot be checked. It is not possible to measure EMG within an MRI scanner because of the strong magnetic field affecting all electronic and metallic devices. IAP can be accurately measured using optical pressure sensors connected by optical cables with the measuring device, which must be positioned outside the MRI scanner. Unfortunately, we did not have such a device during this experiment. Therefore, these three conditions were selected as the only repeatable conditions (a, b, and c) in the two measurement sessions.

3D reconstruction based on semi-automated gradient-oriented single line segmentation of the MRI scans is performed. Segmentation of the thin layer muscle tissue such as m. levator ani and m. coccygeus is very difficult and no automatic segmentation tool is available. An inner surface border of muscle was chosen since the diaphragma pelvis is a flat structure and the inner surface of the muscle is well recognisable and representative for the displacement.

Each surface representing the diaphragma pelvis is divided into two compartments. This is performed based on an anatomical division. The purpose of this division is to quantify the differences in the organ compartment (Part 1) and posterior compartment (Part 2). Since a numerical comparison is performed for the whole compartment, such a division can suppress local differences within the compartment. Presumably, this played a role in the fact that no significant difference was found between groups, since the diagnosis suggests local differences in the anterior compartment of Part 1.

The mean symmetric Hausdorff distance between the surfaces is used for quantifying the difference between particular conditions. Using the mean distance value can suppress local effects, however, it is a reproducible method for calculating the difference between two corresponding surfaces. The position of the levator ani muscle in all conditions is shown in Figure 4.7. It is obvious, that the muscle in Condition b is always below the position observed in Condition a. The position of the levator ani muscle in Condition c intersects with the muscle in Condition a (see Figure 4.7). Therefore, it is difficult to make conclusions about the position of the muscle using the mean distance in Condition c. This also applies to the mean displacement of the muscle, which does not give a proper value in Condition c because of the intersection. This applies for both parts (Part 1 and Part 2). A relatively high standard deviation for average displacement (see Table 4.5) was found in all conditions (a, b and c). This is presumably caused due to the inter-individual differences. For diagnostic purposes, conditions a and b seem to be the most proper, since they can give us all necessary information about the position and displacement of the muscle.

In order to examine the effect of local differences in pelvic floor, the patient diagnosis data was inspected. The patient group is not a homogenous group; therefore, a group of seven patients with cystocele (prolapse in anterior compartment of Part 1) was selected. In this group, the morphological measurements of the depth of the levator hiatus and width were determined. Selection of the slice is based on close neighbourhood corresponding slice in the same position. This method is selected in order to avoid errors caused due to interpolation between slices, since the data set consists only of 11 images during Conditions b and c. This method, with an accuracy of about 7 mm (maximal error is equal to the slice spacing), is able do determine the differences in the position and shape of the levator ani muscle. Since the cystocele is not a local phenomenon, in terms of the accuracy of this method, this can be successfully used for clinical evaluation.

TABLE 4.6: *Summary of the depth D and width W of the levator hiatus in all conditions (Rest, Max IAP, Max ACT). The distance between centroids of the femur heads (HD) was determined (Figure 4.2). Thereafter, the distance D of the lowest border of the levator ani muscle was determined from the centre of the line connecting both femur centroids. The width W of the levator hiatus was determined as a distance of the outer border of the levator ani muscle perpendicular to the D in the 50% of the length of D (see Figure 4.2). IAP = intra-abdominal pressure.*

Group	Subject No.	Hip diameter [mm]	Condition: Rest		Max IAP		Max ACT	
			Depth D [mm]	Width W [mm]	Depth D [mm]	Width W [mm]	Depth D [mm]	Width W [mm]
Healthy volunteer *N=10*	1	183	60	34	70	35	65	36
	2	174	53	38	76	56	56	45
	3	173	63	31	88	45	81	41
	4	183	66	32	92	54	79	53
	6	183	66	29	79	41	78	41
	7	182	70	39	79	41	79	41
	10	175	67	32	82	47	73	36
	12	198	70	38	91	42	81	42
	14	181	68	38	91	62	78	50
	15	168	61	31	75	41	66	34
	Mean	*180.0*	*64.4*	*34.0*	*82.3*	*46.4*	*73.4*	*41.9*
	Std	*8.3*	*5.4*	*3.6*	*7.7*	*8.2*	*8.5*	*6.1*
Patien with cystocele *N=7*	8	183	64	42	70	51	64	44
	9	176	67	41	76	60	66	51
	11	179	82	41	92	48	89	44
	13	175	74	47	94	66	91	60
	18	180	58	45	73	51	59	41
	19	180	60	60	73	60	69	59
	20	185	72	42	88	66	76	62
	Mean	*179.8*	*68.3*	*45.3*	*81.0*	*57.6*	*73.5*	*51.5*
	Std	*3.5*	*8.4*	*6.7*	*10.0*	*7.3*	*12.5*	*8.6*
Patients without cystocele *N=3*	5	179	68	37	70	54	72	48
	16	178	66	33	80	48	74	48
	17	182	70	40	83	52	78	52
	Mean	*179.7*	*68.0*	*36.7*	*77.7*	*51.3*	*74.7*	*49.3*
	Std	*2.1*	*2.0*	*3.5*	*6.8*	*3.1*	*3.1*	*2.3*

Performing MRI scanning in the rest and during holding the maximal level of the IAP provides the best information about the position and the displacement of the pelvic floor muscles. The combination of EMG, IAP and the width W of levator hiatus in these two conditions can be used for diagnostic purposes. It seems, that muscle, which is not able to generate enough force, is not able to hold the diaphragma pelvic in equilibrium during the high level of IAP. Presumably, there is also the effect of the connective tissue in pelvic floor region. If the muscle is fully activated but the connective tissue in levator hiatus is weakened, there is always a risk of not reaching equilibrium with the IAP. These hypotheses will be tested using a biomechanical model of the pelvic floor.

The most obvious difference in the position and shape of the diaphragma pelvis between all conditions is observed in the posterior part (m. coccygeus) of the diaphragma pelvis (Part 2). The muscle assumes a dome shape in Condition a and c, while a basin shape can be observed in Condition b (see Figure 4.6). This difference is also present in Part 1 of the diaphragma pelvis, however, it is less visually obvious. This shape difference is caused due to the loading of the diaphragma pelvis (IAP and weight of internal organs). The weight of internal organs in the pelvic floor compartment pushes the diaphragma pelvis downwards in erect position, while during the supine condition the gravity force vector is directing to the back (Chapter 5). The IAP has a major role in the loading and therefore to the displacement of the pelvic floor muscles, since the maximal displacement is observed during performing max IAP (see Table 4.4). This effect can be observed in the Figure 4.2 and Figure 4.6.

The shape difference in particular parts of diaphragma pelvis (Figure 4.2 and Figure 4.6) is obviously caused due to the weight of the internal organs (Chapter 5). A dome shape during rest in supine position was already observed (Hjartardottir et. al., 1997). They also measured movement of the levator ani muscle and the width of the levator hiatus in 12 healthy subjects. However, their definition of the levator hiatus width is not clear and they did not look at the difference between healthy subjects and patients.

4.5 CONCLUSIONS

The presented results demonstrate: 1) significantly lower muscle activation (EMG activity) in the patient group; 2) no difference in the mean displacement in relation to the level of IAP; 3) larger width W of the levator hiatus in group of patients with cystocele but no difference in the depth D of the levator hiatus. No significant difference was found in the level of the IAP between both groups.

The level of IAP is also determined by the abdominal muscles, and is equal for patients and healthy subjects. The increased width of the levator hiatus might be the result of the reduced muscle activation, or of more compliant connective tissue.

Performing MRI scanning in the rest and during holding the maximal level of the IAP provides the best information about the position and the displacement of the pelvic floor muscles. The combination of EMG, IAP and the width W of levator hiatus in these two conditions can be used for diagnostic purposes.

ACKNOWLEDGEMENTS

The authors wish to give special thanks to all volunteers and patients participating during this study.

The study was realized thanks to co-operation between the facilities of the co-authors of the Onze Lieve Vrouwe Gasthuis Hospital in Amsterdam. The authors wish to thank the Department of Physiotherapy (Marijke Cieremans and Ineke Ruyter-Liem) for co-operating during the EMG measurements and instructing subjects with tasks and the Department of Radiology for offering the facilities to perform the MRI measurements (particularly to Nelly de Jong and MRI scanner operators for performing the MRI scanning). The authors wish to thank to Medical Measurement Systems (particularly Robert Gort, Jos Hanraads, Sake Kroondijk and Ico Jongman) for offering the modular Solar Gold 4T urodynamics system and providing excellent support during our measurements.

REFERENCES

Aspert, N., Santa-Cruz, D., Ebrahimi, T., 2002. MESH: Measruing errors between surfaces using the Hausdorff distance. In proc. of the IEEE ICME 2002, vol. 1, 705-708.

Bobet, J., Norman, R.W., 1990. Least-squares identification of the dynamic relation between the electromyogram and joint moment. J. Biomech. 23(12), 1275-1276.

Botha, C.P., 2004. DeVIDE: The Delft Visualisation and Image processing Development Environment, tech. rep., Delft Technical University.

Hjartardottir, S., Nilsson, J., Petersen, C., Lingman, G., 1997. The female pelvic floor: A dome - not basin. Acta Obstet Gynecol Scand 76, 567-571.

Nichols, D.H., Randall, O.L., 1996. Vaginal Surgery. Williams a Wilkins.

Olney, S.J., Winter, D.A., 1985. Predictions of knee and ankle moments of force in walking from EMG and kinematic data. J. Biomech. 18(1), 9-20.

Olsen, A.L., Smith, V.J., Bergstorm, J.O., Colling, J.C., Clark, A.L., 1997. Epidemiology of surgically managed pelvic organ prolapse and urinary incontinence. Obstet Gynecol. 89, 501-506.

Potvin, J.R., Norman, R.W., McGill, S.M., 1996. Mechanically corrected EMG for the continuous estimation of erector spinae muscle loading during repetitive lifting. Eur J Appl Physiol. 74, 119-132.

Van Leeuwen, J.L., Spoor, C.W., 1992. Modelling mechanically stable muscle architecture. Phil. Trans. R. Soc. Lond. B 336, 275-292.

Voorham-Van der Zalm, P.J., Pelger, R.C.M., Van Heeswijk-Faase, I.C., Wasser, M.N.J.M., Ouwerkerk, T.J., Verhoef, J., Delemarre, H.B.V.M., Lycklama a Nijeholt, G.A.B., 2004. Placement of probes in electro stimulation and biofeedback training. Accepted by the International urogynecology journal and pelvic floor dysfunction.

Chapter 5

LOADING EFFECT OF THE WEIGHT OF THE INTERNAL ORGANS ON THE PELVIC FLOOR IN ERECT AND SUPINE POSITIONS

Abstract

Objective: *All MRI scanners currently used in hospitals are designed for acquiring images of patients in the supine position. In the supine position, the weight of the internal organs is not loading the pelvic floor. The main goal of this study was to investigate the effect of the loading of the pelvic floor due to the weight of the internal organs in the erect and supine positions.*

Study design: *MRI measurements are performed using a FONAR Stand-Up™ MRI scanner (which can be used in both a vertical or horizontal position) on 12 healthy subjects under three conditions (during rest, holding maximal level of intra-abdominal pressure (IAP) and during maximal contraction of the pelvic floor muscles without IAP). A numerical comparison of the pelvic floor in all conditions is performed using the mean symmetrical Hausdorff distance between corresponding surfaces. The mean distance between the surfaces is used as dependent variable for ANOVA.*

Results: *A highly significant effect ($p<0.001$) was found in the displacement between the erect and supine positions. In addition, there is a significant effect in the displacement between rest, maximal IAP and maximal contraction and the anterior and posterior parts of the diaphragma pelvis.*

Conclusion: *A highly significant effect in the position of the diaphragma pelvis was found between the erect and supine position. It is obviously caused due to the weight of internal organs. Present clinical MRI evaluation of the pelvic floor muscles performed on patients in the supine position cannot provide the correct information about the functional behaviour of the pelvic floor, since it is not loaded. Performing MRI scanning in supine position during holding the maximal level of the IAP provides diagnostic information about the position and the displacement of the pelvic floor muscles. Loading due to IAP and the weight of internal organs is related to the displacement and shape of the pelvic floor muscles.*

Keywords

Pelvic floor muscles; intra-abdominal pressure; MRI; weight of the pelvic organs, shape of the pelvic floor

5.1 INTRODUCTION

The human pelvic floor is a very complex muscular structure. The m. levator ani with its fascial covering constitutes the pelvic diaphragm. M. levator ani is largely responsible for supporting both pelvic and abdominal organs and acts synergistically with the striated muscle of the anterior abdominal wall in generating intra-abdominal pressure (IAP). Any increase in IAP e.g. caused by coughing or sneezing, is applied equally to all sides of the pelvic and abdominal walls. If the levator ani is pathologically weakened or temporarily inactivated a genital prolapse can occur. Genital prolapse is a major cause of morbidity in women. Genital prolapse is a condition in which pelvic organs (vagina, uterus, bladder, etc.), normally supported by the pelvic floor muscles, protrude outside the pelvic floor.

One in every nine women requires surgery for problems related to defective pelvic organ support (Olsen, 1997). Among these women, one in every four needs a second operation. Among women with documented prolapse, 76% had a defect in the support of the posterior compartment (Olsen, 1997). Despite the common occurrence of those diseases, the structural defects responsible for its formation remain poorly understood.

It is plausible that pelvic floor muscles have a fundamental influence in these disorders. To study the complex biomechanical behaviour of the pelvic floor muscles and to investigate the effectiveness of reconstructive surgery, a computer model based on the finite-element (FE) theory was developed (Chapter 6). The model is able to predict the position of the pelvic floor depending on the load (e.g. IAP, weight of the organs) and activation of the muscles. The model must be validated with experimental data about the position of the pelvic floor (measured with magnetic resonance imaging MRI), muscle activation (EMG measurements) and IAP.

No studies were found describing the position of the pelvic floor structures, such as organs inside the pelvic region and the diaphragma pelvis in the erect position. There is also a lack of any knowledge about the relationship between the position of the pelvic floor muscles and the level of the IAP. Since the IAP and the weight of the internal organs are the main loading factors of the pelvic floor, they will affect the displacement of the pelvic floor in the erect and supine positions. Activation of the pelvic floor muscles is necessary to increase the IAP (except during activities like coughing, sneezing etc.). Whether the muscles are lengthened or shortened, which will result in respective downward or upward movement of the pelvic floor, depends on the level of the IAP and the level of muscle activation. There is a direct relation between the pressure in the compartment, the tensile stress in the wall of the compartment, and the curvature of the wall of the compartment (Equation 5.1) van Leeuwen and Spoor (1992):

$$dp = -\sigma_f \cdot c_f \cdot dr \tag{5.1}$$

where dp is the pressure difference, σ_f is the stress in the muscle fibre, $c_f = 1/R_f$ is the local curvature (R_f = local radius of curvature) and dr represents the muscle thickness. If the muscles are activated, the tensile stress will increase and the curvature will decrease for the same IAP (which also depends on the activation of the abdominal muscles). The loading is different depending on whether the subject assumes an erect or supine position. Since all clinical MRI scanners are used in supine position, the evaluation of the loading effect of the internal organs is crucial for diagnostic purposes. The data can also be used for validation of the biomechanical model of the pelvic floor muscles.

The main goal of this experiment was to investigate the effect of the loading of the pelvic floor by the weight of the internal organs in the erect and supine positions. The experimental measurements were performed using FONAR the Indomitable Stand-Up™ MRI machine. The effect of the loading of the pelvic floor (position, displacement and deformation of the diaphragma pelvis) was investigated in 12 female subjects (healthy volunteers) in the erect and supine positions. This part of the experiment was performed in co-operation with the Centre for Biomedical Functional Imaging (CBFI), Aberdeen University, Scotland.

5.2 Material and methods

All measurements were performed on 12 female healthy subjects. The subjects were solicited in co-operation with the CBFI, Aberdeen University. Mean age ([range] ± SD) was 38.4 years ([28 - 53] ± 7.8 years); body mass index was 23.7 ([19.7 - 28.6] ± 2.6). Five subjects were nulliparous, seven subjects had one up to three vaginal deliveries. Inclusion criteria for volunteers were: older than 18 years, comprehension of the aim and the conditions of the experiment. The exclusion criteria for volunteers were: identifiable acute or chronic diseases or urologic or gynaecologic dysfunction, pregnancy, previous or planned surgery in the pelvic floor compartment, contraindication for MRI (e.g. pacemaker, vascular clip in brain, claustrophobia), and not understanding aim and conditions of the experiment.

After explaining the rationale of the study, complemented by printed information, written informed consent was obtained and a health questionnaire ad-ministered to each participant. Permission for this study was obtained from the Medical Ethical Committee in Aberdeen University, Scotland.

5.2.1 MRI MEASUREMENTS

Several T1 and T2-weighted gradient-echo or fast spin-echo MRI sequences were performed in order to obtain the position of the pelvic floor muscles. The measurements were performed using the FONAR the Indomitable Stand-Up™ MRI scanner at the Positional MRI Centre, Woodend Hospital, Aberdeen. The MRI volume is chosen in order to cover the diaphragma pelvis (m. levator ani and m. coccygeus) between symphysis pubica and os coccygeus. The same cubic MRI volume is used for all scan conditions. The first scan session (Condition a as described in Section 5.2.1.1 on page 94) is performed in the rest with the highest resolution possible. The MRI settings for all conditions are summarised in Table 5.1. This session formed the reference image data set. Thereafter, fast sequences are taken during holding of the maximal level of the IAP (for about 31 s) and during the maximal contraction of the pelvic floor muscles without increasing the level of the IAP. Fast sequences are repeated three times.

TABLE 5.1: *Measuring parameters and the settings of the FONAR the Indomitable Stand-Up™ MRI scanner during the MRI measurements in all conditions. The same settings were used in both erect and supine positions of the subject. Condition a - rest, Condition b - max IAP, Condition c - max ACT.*

MRI settings	Condition a	Conditions b, c
Session type	Cor T2 FSE	Cor T1 GE
Slice thickness [mm]	5	10
Spatial Resolution [mm]	5.5	10.75
Field of view (FOV)	40	40
RFOV	1.5	1
Matrix resolution [pixels] 16bit	256x160	256x160
Pixel resolution [mm/pixel]	1.56	1.56
Number of slices	20	7
Acquisition time	3min 30s	31s
TR [ms]	6240	196
TE [ms]	160	11
Magnetic field strength [T]	0.6	0.6
Coil type	Torso	Torso

This protocol is performed with the subject in the erect and supine positions. The measurements lasts approximately 45 minutes per subject.

5.2.1.1 Procedures

Subjects were requested not to eat for four hours before the measurements. This condition is necessary to ensure good MRI image quality. Each subject is asked to assume an erect position within the MRI scanner. Each subject was instructed to perform each of the three conditions as explained below:

a) Rest - Condition a: The subject is asked to maintain rest, avoid any movements and breathe normally. The position of the subject is fixed using a belt around the chest. Coronal T2 weighted fast spin-echo MRI sequence is performed for approximately 3.5 minutes.

b) Max IAP - Condition b: In this condition, the subject is asked to maintain the maximal level of IAP by both breath holding and abdominal muscle contraction. The subject is asked to maintain this condition for at least 31 s. During this time, a Coronal T1 weighted gradient-echo MRI sequence is performed.

c) Max ACT - Condition c: During this condition, the subject is asked to perform maximal contraction of the pelvic floor muscles for at least 31 s. She is asked to breathe normally and to minimize the abdominal muscle wall contraction during this condition. A coronal T1 weighted gradient-echo MRI sequence is performed during the pelvic floor muscles contraction phase.

The sessions are performed in this sequence: a, b, c, b, c, b and c. No movement was allowed between these conditions. A 30 s rest period followed each condition to minimize fatigue.

Directly thereafter, the MRI examination bed is moved to the supine position. The subject is not allowed to move while the bed is moving. Each subject is instructed to perform the same three conditions of measurement as explained above (Conditions a, b, and c).

These three conditions are chosen as the only repeatable conditions. This assumption is based on previous experimental measurements on the pelvic floor (Chapter 4). Without measuring IAP and muscle activity, the subjects are able to repeat only these three conditions (a, b, c).

5.2.1.2 Data processing

Semi-automated gradient-oriented segmentation of the MRI scans is performed. A single line is generated as a representation of the inner surface border of the pelvic floor muscles.

3D reconstructions of the pelvic floor muscles are made in all measured conditions (see Figure 5.1 for example). Since the position of the pelvic compartment changes slightly between the erect and supine position in the MRI scanner (see Figure 5.3A and B), all data from the measurements in the erect position are transformed into the local co-ordinate system of the supine position using corresponding bony landmarks.

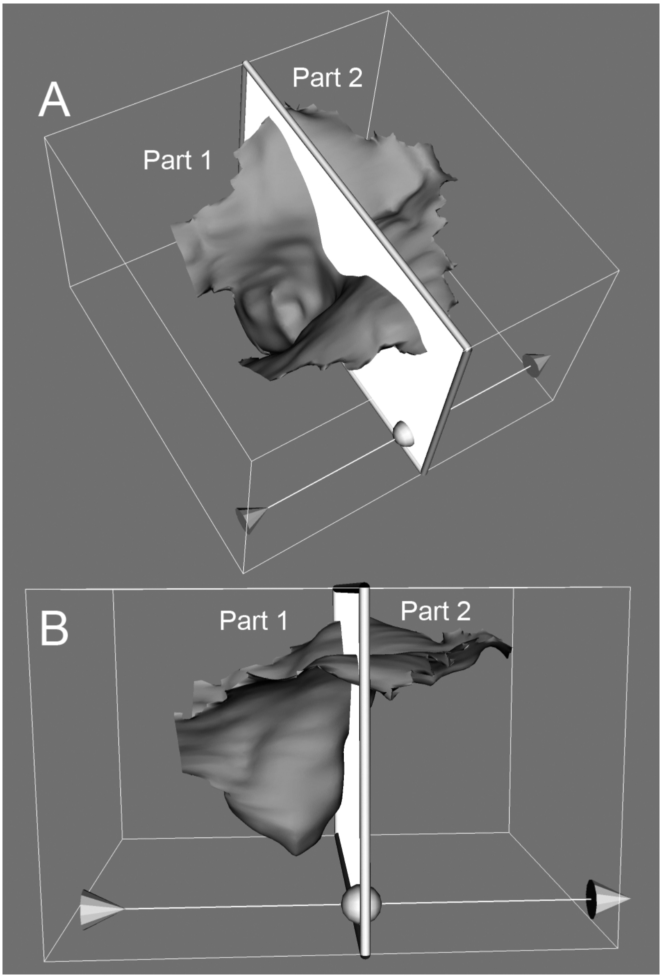

FIGURE 5.1: *The 3D reconstruction of the pelvic floor muscles based on semi-automated gradient-oriented single line segmentation of the MRI data. An implicit (cutting plane) is displayed. This is based on an anatomical division of the diaphragma pelvis as follows: Part 1 consists of all organs structures as the vagina and the rectum and Part 2 consists of the posterior part (m. coccygeus) of the diaphragma pelvis. The arrow is pointing posteriorly in both views.* ***A*** *- perspective view from top left side.* ***B*** *- left side view*

At least four corresponding bony landmarks are chosen on each 3D reconstruction of the pelvic bone (for instance: symphysis pubica, fossa acetabuli, spina iliaca anterior inferior, spina ischiadica). Given two sets of corresponding points, a transformation is computed that yields the best fit mapping of the first set onto the second set, in a least squares sense. A closed-form solution for this least-square problem (Horn, 1987) was implemented in the DeVIDE software by Botha, (2004). Only seven slices were recorded in conditions b and c. This is insufficient for reconstruction of the local co-ordinate system. It is assumed that the subject did not move between conditions a, b and c.

For use in numerical comparison, the 3D surfaces are divided into two parts. This is performed based on an anatomical division of the diaphragma pelvis as follows: Part 1 (anterior part) consists of all organ structures such as the vagina and the rectum and Part 2 consists of the posterior part (m. coccygeus) of the diaphragma pelvis (see Figure 5.1). This division is necessary for determining the local effects between conditions. It is also used for calculating the displacement field between corresponding parts. A comparison between the erect and supine position for both parts is performed in the rest condition (Condition a) in order to obtain a distance field and therefore to quantify the difference between these conditions within a subject. Furthermore, comparison of both parts are performed in Condition b, and Condition c (with respect to the rest position) for erect and supine conditions for each subject (see Figure 5.2). The MESH software developed by Aspert et al. (2002) is used to evaluate the difference between iso-surfaces (triangulated meshes). It uses symmetric Hausdorff distance to compute a mean error between two given surfaces (Aspert et al., 2002). During rest (Condition a), the levator ani muscle was always lower in the erect than supine position. For visualization, surface modelling and transformation of the data the DeVIDE (the Delft Visualisation and Image processing Development Environment, Botha, 2004) software is used.

The mean distance between the given surfaces is used for analysis of variance. A general linear model (GLM) for repeated measurements is analysed for these factors: within subject factors - erect and supine position, Condition b vs. Condition c, and Part 1 vs. Part 2 of the diaphragma pelvis. In this design, the independent variables are represented by erect and supine position, Condition b and c, and Part 1 and 2 of the diaphragma pelvis. The dependent variable is represented by the mean symmetrical Hausdorff distance between two triangulated meshes. SPSS 12.0.1 software was used for this statistical analysis.

5.3 RESULTS

The results of the numerical evaluations are summarised in Table 5.2. An example of the graphical result (numerical comparison of whole diaphragma pelvis in the rest condition between the erect and supine position) as generated by the MESH tool is given in Figure 5.2.

The effects of within subject factors are evaluated using the GLM repeated measures procedure. A highly significant relation ($p<0.001$) is found between the displacement in the erect and supine positions. Moreover, there is a significant relation between the displacement during Conditions b and c ($P=0.015$), and in Part 1 and Part 2 ($P=0.001$) of the diaphragma pelvis. These effects are also obvious from visual inspection of the corresponding MRI slices in these conditions as shown in Figure 5.3 and Figure 5.4.

TABLE 5.2: *Summary of the mean displacement in millimetres of the pelvic floor muscles for individual subjects and the mean values for the whole group. The mean symmetric Hausdorff distance was calculated for comparison of the two corresponding 3D reconstruction for both parts of the diaphragma pelvis (see Figure 5.1), for all three conditions (rest, maximal IAP, maximal ACT) and for both erect and supine positions of the subject. Max IAP and max ACT is determined with respect to the rest condition in supine position. IAP = intra-abdominal pressure.*

Subject No.	Mean Displacement [mm]									
	Erect x Supine		Erect				Supine			
	Rest		Max ACT		Max IAP		Max ACT		Max IAP	
	Part 1	Part 2	Part 1	Part 2	Part 1	Part 2	Part 1	Part 2	Part 1	Part 2
1	1.5	1.9	3.8	4.4	4.2	3.9	3.1	1.9	3.6	2.3
2	0.9	0.9	2.8	3.2	3.2	2.9	3.2	2.3	2.7	2.2
3	1.0	1.0	4.0	2.5	5.0	2.2	2.1	1.7	3.2	1.8
4	1.1	1.3	2.5	2.5	3.4	3.1	1.4	1.5	2.5	1.6
5	1.2	1.0	3.0	2.9	2.9	2.5	2.6	1.6	2.5	2.0
6	1.4	1.5	3.4	3.1	3.3	2.8	1.4	0.8	1.7	0.8
7	1.5	1.3	3.0	2.4	3.5	2.9	2.0	1.9	2.5	1.5
8	1.5	1.5	3.6	3.3	3.8	3.1	2.8	2.4	2.8	2.3
9	1.0	1.0	4.2	2.8	4.1	3.3	1.4	1.2	1.8	1.6
10	0.6	0.4	2.5	1.6	2.9	2.2	2.4	0.9	1.4	1.0
11	1.3	2.0	3.2	4.4	3.8	4.6	1.9	1.9	2.8	2.2
12	1.1	1.2	3.3	2.8	3.4	2.9	1.7	1.7	2.9	1.6
Mean	*1.2*	*1.3*	*3.3*	*3.0*	*3.6*	*3.0*	*2.2*	*1.7*	*2.5*	*1.7*
Std	*0.3*	*0.4*	*0.6*	*0.8*	*0.6*	*0.7*	*0.7*	*0.5*	*0.6*	*0.5*

In Figure 5.3, the shape and position of the pelvic floor muscle (small arrows) is demonstrated in the rest condition in the erect position, for both erect and supine positions. A slightly different shape of the pelvic floor compartment can be observed between the erect and supine positions (Image A and B). The most obvious difference in the position and shape of the diaphragma pelvis between the erect and supine position is observed in the posterior part (m. coccygeus) of the diaphragma pelvis (Part 2) where the muscle assumes a dome shape in the supine position (Image F) while a basin shape can be found in the erect position (Image E). A similar shape difference is also present in Part 1 (Image C and D). This shape difference is caused by the weight of the internal organs. The mass of internal organs in the pelvic floor compartment pushes the diaphragma pelvis downwards during the erect position (gravity force g in Image A), while during the supine position the mass force is pointing to the back (gravity force g in Image B). This effect is present in both parts of the diaphragma pelvis (Images C, D, E, F).

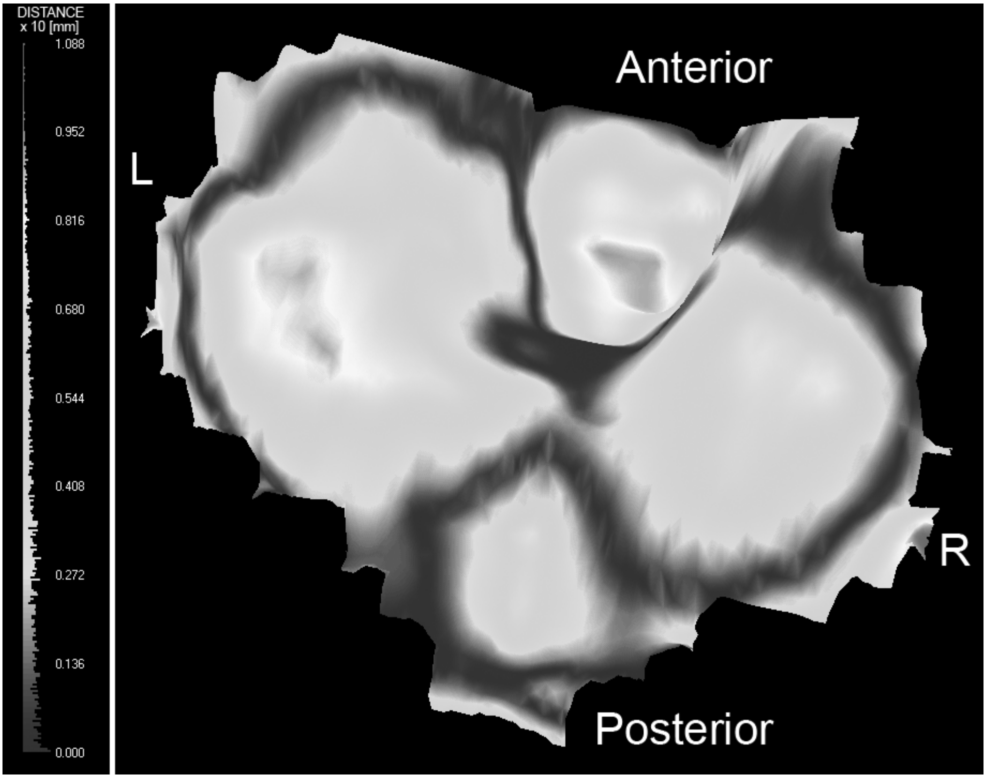

FIGURE 5.2: *An example of the graphical results output from the MESH tool software (Aspert et al., 2002). Surface symmetric Hausdorff distance maximum error colour bar on the left side, the graphical visualisation of the error distribution in the 3D reconstruction of the pelvic floor muscles based on the single line segmentation of the MRI data on the right side. In this particular example the surface model of the whole diaphragma pelvis is compared between the erect and supine positions.*

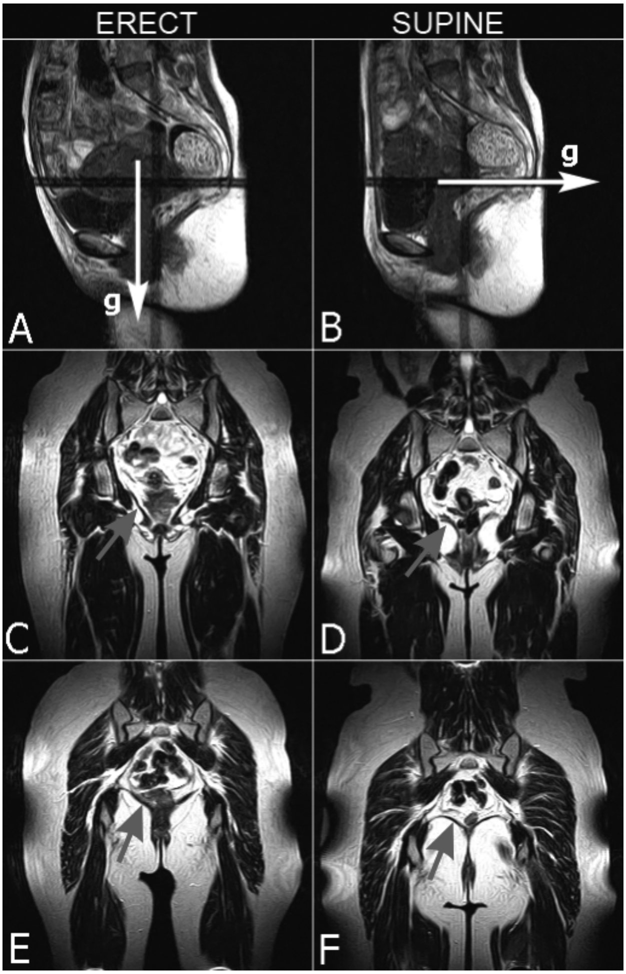

FIGURE 5.3: *The shape and position of the pelvic floor muscle (small arrows) is demonstrated on the corresponding MRI images in the rest condition in the erect position (left column) and supine position (right column). A slightly different shape of the pelvic floor compartment can be observed between the erect and supine positions (Image A and B). The most obvious difference in the position and shape of the diaphragma pelvis between the erect and supine positions is observed in the posterior part (m. coccygeus) of the diaphragma pelvis (Part 2) where the muscle assumes a dome shape in the supine position (Image F) while a basin shape can be found in the erect position (Image E). A similar shape difference is also present in Part 1 (Image C and D). This shape difference is caused by the weight of the internal organs. The mass of internal organs in the pelvic floor compartment pushes the diaphragma pelvis downwards during the erect position (gravity force g in Image A), while during the supine position the mass force is pointing to the back (gravity force g in Image B). This effect is present in both parts of the diaphragma pelvis (Images C, D, E, F).* ***A*** *- mid-sagittal slice in the erect position.* ***B*** *- mid-sagittal slice in the supine position.* ***C*** *- coronal slice in Part 1 of the diaphragma pelvis in the erect position.* ***D*** *- coronal slice in Part 1 of the diaphragma pelvis in the supine position.* ***E*** *- coronal slice in Part 2 of the diaphragma pelvis in the erect position.* ***F*** *- coronal slice in Part 2 of the diaphragma pelvis in the supine position.*

Figure 5.4 demonstrates the typical coronal MRI image of the female pelvis. The shape and position of the pelvic floor muscles are indicated. The most obvious difference is observed in the posterior part (m. coccygeus) of the diaphragma pelvis (Part 2) where the shape of the muscle assumes a dome shape in supine position (Image D), while a basin shape can be found in erect position (Image C). Also compare Images A and C, and B and D.

The position of the levator ani muscle in Condition b is always below the position observed in Condition a in both erect and supine position (see Figure 5.5). The position of the levator ani muscle in Condition c intersects with the muscle in Condition a in both parts in supine condition and in Part 1 in erect position (see Figure 5.5). In Part 2 in erect position the position of the muscle is above the position during Condition a. In erect position during rest, the muscle is always positioned below the muscle in supine condition (see Figure 5.5).

The IAP has a major role in the loading and the displacement of the pelvic floor muscles (Chapter 4). The effect of the IAP is larger than the weight of internal organs of the pelvic floor. This effect is found between Conditions b and c in both positions (erect and supine) and can be observed in Figure 5.3 and Figure 5.4.

5.4 Discussion

The main goal of this experiment was to investigate the effect of the loading of the pelvic floor by the weight of the internal organs and IAP in the erect and supine positions. All currently used clinical MRI scanners are designed for image acquisition in the supine position. The effect of the weight of the internal organs has been investigated in order to improve and to evaluate the diagnostic results. Most of the diagnostic imaging in the pelvic floor is performed in the rest condition. The pelvic floor is a dynamic system, which responds significantly to the loading and muscle activation (Chapter 4).

5.4.1 MRI measurements

The coronal slices are chosen since all muscle parts of the pelvic floor diaphragma are easily recognizable in this section, which is necessary for segmentation of the muscles. The pelvic floor organs are more easily recognizable in sagittal sections, but these slices cannot be used for muscle segmentation. In each condition, one mid-sagittal slice and several coronal slices were acquired, since the main goal of our study was to evaluate the position of the pelvic floor muscles and not the organs.

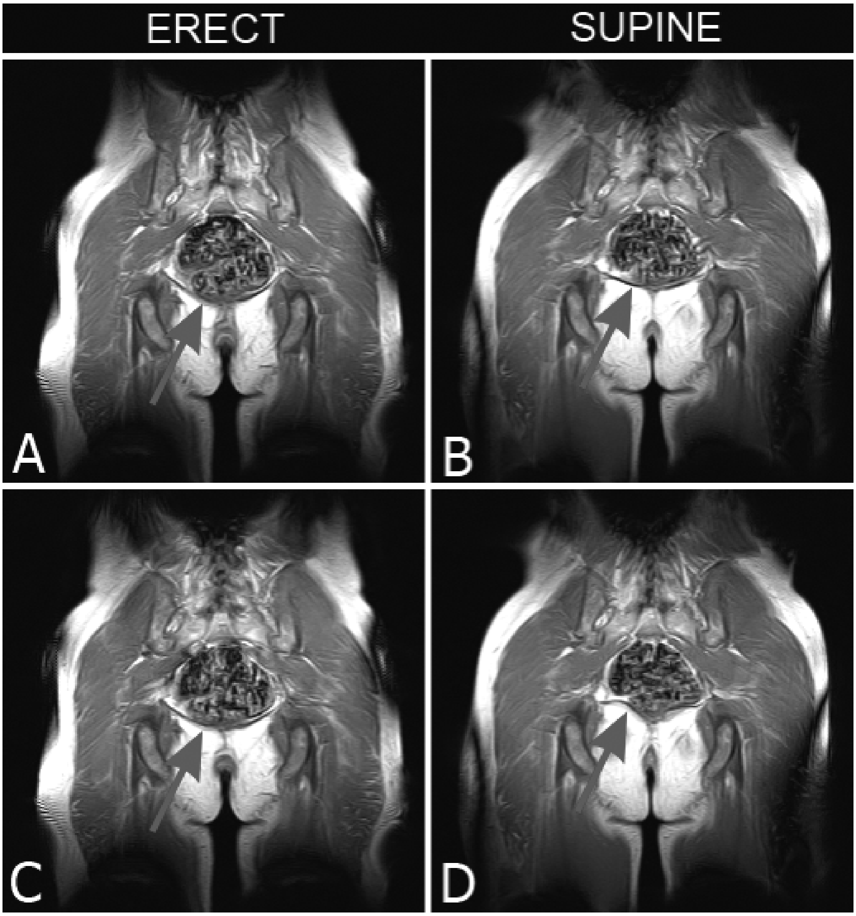

FIGURE 5.4: *Typical example of the coronal MRI images of the female pelvis where the shape and position of the pelvic floor muscle (small arrows) is demonstrated.* ***A*** *- coronal slice in Part 1 of the diaphragma pelvis during max IAP (Condition b) in the erect position.* ***B*** *- coronal slice in Part 1 of the diaphragma pelvis during max IAP (Condition b) in the supine position.* ***C*** *- coronal slice in Part 2 of the diaphragma pelvis during max ACT (Condition c) in the erect position.* ***D*** *- coronal slice in Part 2 of the diaphragma pelvis during max ACT (Condition c) in the supine position. The most obvious difference is observed in the posterior part (m. coccygeus) of the diaphragma pelvis (Part 2) where the shape of the muscle assumes dome shape in supine position (Image D) while a basin shape can be found in erect position (Image C). Also compare Images A and C, and B and D.*

Each subject was carefully instructed on how to perform all the conditions, particularly the dynamic conditions b and c. Prior to measurements, subjects practiced performing these conditions. However, the performance of these conditions cannot be measured, since only the position of the pelvic floor muscle was determined and not muscle activation and IAP. The only way to evaluate these effects is to measure the EMG activity of the muscle and IAP simultaneously (Chapter 4). We were not able to measure EMG within an MRI scanner because of the strong magnetic field affecting all electronic and metallic devices. IAP can be accurately measured using optical pressure sensors connected by optical cables with the measuring device, which must be positioned outside the MRI scanner. Unfortunately, we did not have such a device during this experiment.

All procedures used during this experiment were standard clinical procedures with low associated risks. Some difficulties were expected during breath holding and holding of the maximal level of the IAP in supine position. Some subjects did not find it comfortable in the MRI scanner because of the level of noise during scanning. Nevertheless, all subjects deal well with these inconveniences.

5.4.2 Data analysis

3D reconstruction based on semi-automated gradient-oriented single line segmentation of the MRI scans was performed as described in Section 5.2.1 on page 93. Segmentation of a thin layer muscle tissue such as m. levator ani and m. coccygeus is very difficult and no automatic segmentation tool is available. An inner surface border of muscle is chosen since the diaphragma pelvis is a flat structure and the inner surface of the muscle is well recognisable.

Since the position of the subject's pelvic region is slightly different in the erect and supine positions (see Figure 5.3A and B), the transformation of the data is necessary in order to obtain the data in the same co-ordinate system. The accuracy of this transformation depends on the number of selected corresponding points and the number of slices in the reference data set, which is important for the precision of the 3D reconstruction. To this end, at least four sets of corresponding bony landmarks are selected on the pelvic bone surface. A closed-form solution for the least-square problem of absolute orientation is calculated. It provides the best rigid-body transformation between two co-ordinate systems given measurements of the co-ordinates of a set of points that is not collinear (Horn, 1987). The solution uses unit quanterions to represent rotations.

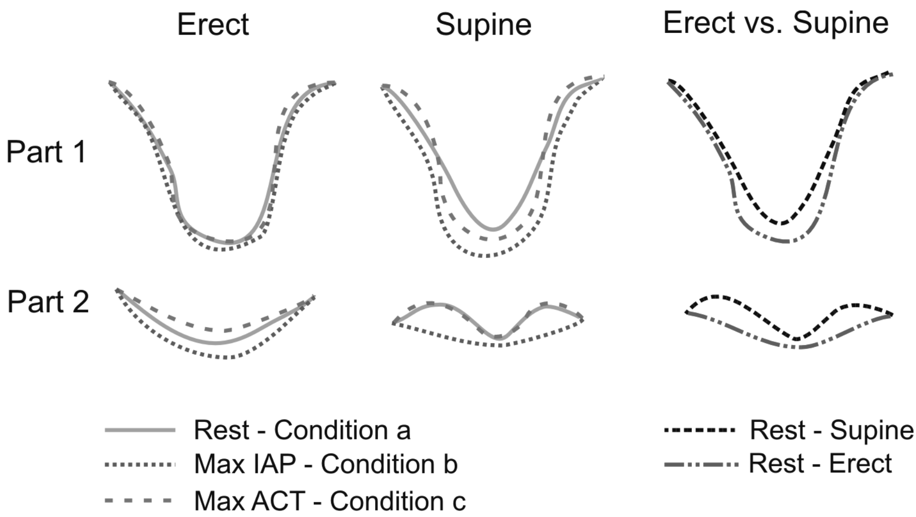

FIGURE 5.5: *Schema of the position of the pelvic floor muscles of the subject in erect and supine positions. The position of the muscle in all three conditions in Part 1 and Part 2 is displayed in erect and supine positions (on the left and in the middle). The difference in position of the muscle in rest between erect and supine position in both parts is displayed (on the right side). The mean displacement of the muscles is summarised in Table 5.2.*

Each surface representing the diaphragma pelvis is divided into two compartments as described in Section 5.2.1.2 on page 94, based on an anatomical division. The purpose of this division is to quantify the differences in the organ compartment (Part 1) and posterior compartment (Part 2). Since a numerical comparison is performed for the whole compartment, such a division can suppress local differences within the compartment. The whole group of subjects included healthy volunteers, therefore these local effects are considered negligible. The mean symmetric Hausdorff distance between the surfaces is used for quantifying the difference between particular conditions. Using the mean distance value can suppress local effects, however, it is a reproducible method for calculating the difference between two corresponding surfaces. A relatively high standard deviation for average displacement (see Table 5.2) was found in all conditions (a, b and c). This is presumably caused due to the inter-individual differences between the subjects. The position of the muscle in Condition c intersects with the muscle in Condition a. Therefore, it is difficult to make conclusions about the position of the muscle using the mean distance in Condition c.

A highly significant effect in position of the diaphragma pelvis was found between the erect and supine position. It is obviously caused due to the weight of internal organs as well as a shape difference. The weight of internal organs in the pelvic floor compartment is pushing the diaphragma pelvis downwards during erect position, while during the supine condition the weight force is pointing to the back (see Figure 5.3). This effect is present in both parts of the diaphragma pelvis and in all conditions.

Observing the results from Table 5.2, the contribution of IAP and weight of the internal organs might be estimated. The mean displacement of the pelvic floor in erect position in Condition b (max IAP) is 3.63 mm, whereas in supine position in Condition b is 2.53 mm. This suggests, that the displacement of the pelvic floor in erect position in Condition b is caused by IAP (two thirds of the load) and weight of internal organs (one third of the load). In previous study (Chapter 4), the IAP was determined in supine position during rest (2.9 kPa) and during Condition b (8.3 kPa) in healthy subjects. The IAP was determined using intra-rectal unisensor microtipcatheter placed in the rectum. Hypothetically, the level of the IAP during rest is related to the weight of internal organs, since these are pressing to the back, where the pressure sensor was placed. A level of 8.3 kPa was recorded during Condition b, but considering the weight of the organs (2.9 kPa) the pressure loading the pelvic floor due to IAP will be 5.4 kPa in a supine position. Therefore, it can be assumed that this pressure of 5.4 kPa will cause the mean displacement of the pelvic floor muscles of 2.53 mm in supine position (see Table 5.2). In contrary, the entire pressure of 8.3 kPa will load the pelvic floor in erect position, since the pelvic floor is also loaded by the weight of the internal organs. The pressure of 8.3 kPa will cause the mean displacement of 3.63 mm in erect position (see Table 5.2). The considerations above lead to the conclusion that the mean displacement of the pelvic floor is in relation with the IAP, which presents about two thirds of the loading, and with the weight of organs, which presents about one third of the load to the pelvic floor in erect position in Condition b. Only two thirds of the measured IAP is loading the pelvic floor in supine position.

Present clinical MRI evaluation of the pelvic floor muscles performed on patients in the supine position cannot provide the correct information about the functional behaviour of the pelvic floor, since it is not loaded.

In general, all presented results show that the weight of the internal organs (position of the subject), the level of IAP (Conditions a and b) and muscle activation (Condition c) have a significant influence on the displacement and shape of the pelvic floor muscles. This concludes, that the diaphragma pelvis is a dynamic system. The shape difference in particular parts of diaphragma pelvis (Figure 5.3 and Figure 5.4) is obviously caused due to the weight of the internal organs. The dome shape during rest in the supine position was already observed (Hjartardottir et. al, 1997). However, the diaphragma pelvis assumes the basin shape during all conditions in the erect position (see Figure 5.5).

Performing MRI scanning in erect position in rest and during holding the maximal level of the IAP can give us the best information about the position and the displacement of the pelvic floor muscles.

5.5 CONCLUSIONS

A highly significant effect in the position of the diaphragma pelvis was found between the erect and supine position. It is obviously caused due to the weight of internal organs.

Present clinical MRI evaluation of the pelvic floor muscles performed on patients in the supine position cannot provide the correct information about the functional behaviour of the pelvic floor, since it is not loaded.

Performing MRI scanning in supine position during holding the maximal level of the IAP provides diagnostic information about the position and the displacement of the pelvic floor muscles.

ACKNOWLEDGEMENTS

The authors wish to give special thanks to all volunteers participating during this study.

The study was realized thanks to co-operation with the CBFI. The MRI part of the project was funded by the European Commission Improving Human Potential Programme by Access to Research Infrastructures, granted to the University of Aberdeen under the title Centre for Biomedical Functional Imaging. The authors wish to thank the CBFI (Prof. Malcolm Pope) for offering the facilities to perform the vertical MRI measurements. Particularly Dr. Andrew Bromiley, Tom Davidson for co-operation during MRI measurements and Beverly McLennan and Lindsey Christie for performing the MRI scanning.

REFERENCES

Aspert, N., Santa-Cruz, D., Ebrahimi, T., 2002. MESH: Measruing errors between surfaces using the Hausdorff distance. In proc. of the IEEE ICME 2002, vol. 1, 705-708.

Botha, C.P., 2004. DeVIDE: The Delft Visualisation and Image processing Development Environment, tech. rep., Delft Technical University.

Hjartardottir, S., Nilsson, J., Petersen, C., Lingman, G., 1997. The female pelvic floor: A dome - not basin. Acta Obstet Gynecol Scand 76, 567-571.

Horn, B.K.P., 1987. Closed-form solution of absolute orientation using unit quanterions. J.Opt. Soc. Am. 4 (4), 629-642.

Olsen, A.L., Smith, V.J., Bergstorm, J.O., Colling, J.C., Clark, A.L., 1997. Epidemiology of surgically managed pelvic organ prolapse and urinary incontinence. Obstet Gynecol. 89, 501-506.

Van Leeuwen, J.L., Spoor, C.W., 1992. Modelling mechanically stable muscle architecture. Phil. Trans. R. Soc. Lond. B 336, 275-292.

Chapter 6

A FINITE ELEMENT MODEL OF HUMAN PELVIC FLOOR MUSCLES

Abstract

The main goal of this study is to understand the biomechanical behaviour of the pelvic floor muscles. The muscle behaviour is simulated as a displacement resulting to the loading by the intra-abdominal pressure (IAP) and the muscle activation. Also the internal stress and deformation in the muscle and connective tissue is calculated. We have developed a FE model of the pelvic floor muscles based on cadaver morphology and a constitutive model for the passive elastic behaviour of the human pelvic floor muscles. Thermal shortening in the muscle fibre direction is utilised to represent the muscle activation. One active and two passive layers are used in a multi-layer shell element, representing the active muscle fibres and passive tissue. This concept allows using an orthotropic active layer incorporated in a non-linear passive isotropic matrix formed of passive layers. The active muscle layer is modelled as an anisotropic material layer with defined stiffness in the muscle fibre direction. Three general conditions measured in healthy volunteers (Load-Case (LC) 1 - rest, LC2 maximal contraction of the pelvic floor muscles and LC3 - holding the maximal level of IAP) are simulated and validated using the experimental data.

The results show that the thermal shortening of the element, simulating a muscle force-length relationship is a simple and effective method for modelling contractile properties of the muscle tissue. The FE analysis of the pelvic floor muscles results in the muscles' displacements in relation to the level of the IAP and muscle activation, which are qualitatively and quantitatively in line with the MRI measurements. Width of the levator hiatus and displacement of the muscle is in a good agreement with experimentally determined values in parenthesis: Width [mm] in LC1 39.4 (34 ± 3.6), LC2 47.6 (47 ± 7.5) and LC3 42.4 (41.9 ± 6.1); the displacement [mm] in LC1 3.28 (not determined), LC2 2.8 (3.2 ± 0.4) and LC3 2.32 (2.8 ± 0.5) It is concluded that the present model describes the muscle forces and displacements well, validated by experimental results. The FE model will be used to simulate the pathological behaviour of patients with a genital prolapse, and to predict the effect of surgical interventions.

Keywords

Biomechanics of pelvic floor muscles; Finite element model; Muscle activation; Intra-abdominal pressure, EMG

6.1 INTRODUCTION

The human pelvic floor is a very complex structure composed of muscles and other connective tissues linked to the supported organs. The pelvic diaphragm consists of the levator ani muscle with its fascial covering. The levator ani muscle is largely responsible for supporting both pelvic and abdominal organs and acts synergistically with the striated muscle of the anterior abdominal wall, generating intra-abdominal pressure (IAP). Any increase in IAP e.g. caused by coughing or sneezing, is applied equally to all sides of the pelvic and abdominal walls. If the levator ani is pathologically weakened or temporarily inactivated, the pressure on one side of a pelvic organ may become greater than that on the other, permitting the organ to descend (genital prolapse).

Surgery for problems related to defective pelvic organ support is required for one in every nine women worldwide. Among these women, one in every four needs a second operation (Olsen et al., 1997). Despite the common occurrence of the genital prolapse, the structural defects responsible for its formation remain poorly understood.

The fundamental knowledge about the biomechanical behaviour of the pelvic floor muscles is missing. There is no knowledge describing the relation between the loading of these muscles and the muscle forces itself. Moreover, it is plausible that pelvic floor muscles have a fundamental influence in disorders like genital prolapse. Muscles, like many biological tissues undergo large deformations. A geometrically non-linear theory has to be used for modelling purposes. The constitutive equation (i.e. stress-strain relationship) is usually non-linear and anisotropic, and depends on neural activation. The geometry of the problem is very complex. Consequently, closed-form solution of the mathematical equations cannot be found.

A powerful tool to find good approximate numerical solutions for these equations is the finite-element (FE) method. The basis of this method is discretization of the continuum into finite elements and determination of the stresses and nodal forces of the elements. The main loading of the pelvic floor muscles is by the IAP. In addition there will be the load due to the weight of the internal organs. Muscles in joint systems (e.g. in the upper or lower extremities) are activated to exert forces at the bones in line with their muscle line of action. In contrast, the pelvic floor muscles are loaded perpendicular to the muscle line of action by the IAP. A simple representation of the muscle action by a (one-dimensional) muscle line of action is not appropriate. A sophisticated approach using a FE model of the muscle is necessary. In a FE model the relationship between the loading and muscle forces in three dimensions can be represented.

Continuum models based on FE theory have been applied to study the mechanical behaviour and function of isolated skeletal muscles. Several studies were performed to study the mechanical behaviour of the gastrocnemius medialis muscle of the rat (Vankan et al., 1996; Donkelaar et al., 1996) and the heart muscle tissue (Huyghe et al., 1991). Van der Linden et al. (1998) developed a two-dimensional muscle model. Johansson et al. (2000) developed a three-dimensional (3D) muscle elements. Recently, Yucesoy et al. (2002) developed a 3D FE model of skeletal muscle using a two-domain approach (the intra-cellular domain and the extra-cellular matrix domain). Oomens et al. (2003) published the simulations of 3D model describing the mechanical behaviour of a tibialis anterior muscle of rat. The results have been compared with experimentally determined strains at the surface of the rat muscle. The basic concept of these models is solving equilibrium equations on a FE continuum model of skeletal muscle. Muscle-tendon relationships, muscle fibre direction, shear stiffness and the muscle force-length relationships using for example Hill type model or Huxley sliding-filament theory are used as parameters. The FE models are validated using displacements and strains at the surface of the muscle determined in animal experiments.

No study has been found focusing on modelling of a thin flat muscle layer such as the pelvic floor muscles. The main goal of this study is to understand the biomechanical behaviour of the pelvic floor muscles. The approach is to simulate the biomechanical behaviour of the pelvic floor muscles as a response to the loading by the IAP and muscle activation. We have developed a FE model of the pelvic floor muscles based on cadaver morphology (Janda et al., 2003) and a constitutive model for the passive elastic behaviour of human pelvic floor muscles (Chapter 3). Unlike other studies, which used solid elements for bulky muscles, shell elements are used for modelling the flat pelvic floor muscle. The FE analysis of the pelvic floor muscles gives us the muscles' displacements in relation to the level of the IAP and muscle activation. It is extremely difficult to experimentally determine the displacement and strains of the muscle. This was only possible with MRI scanning. The experimental data (Chapters 4 and 5) have been used for validation of the FE model.

6.2 Materials and methods

A 3D FE model of the pelvic floor muscles is generated numerically using a commercial package MSC.Marc (Palo Alto, CA, USA). The FE model geometry is based on the experimental measurements describing the complete pelvic floor morphology (Janda et al., 2003). Two element types are used. Since the pelvic floor muscles are thin and flat, 4-node bilinear shell quad elements and 3-node bilinear triangular shell elements were used. These are three- and four-node shell elements with global displacements and rotations as degrees of freedom. Bilinear interpolation is used for the co-ordinates, displacements and the rotations. Due to its simple formulation when compared to the standard higher order shell elements, it is less computationally expensive and, therefore, very attractive in a non-linear analysis. The element is not very sensitive to distortion, particularly if the corner nodes lie in the same plane. The triangular shell element is used for the connective tissue parts (see Figure 6.1). The mapped FE mesh is generated in order to generate elements in the same direction as the muscle fibres as described in Janda et al. (2003). Thereafter, the local co-ordinate system of each element is oriented in line with the muscle fibre direction. The muscle fibre length is set to the optimal muscle fibre length for the particular muscle part (Janda et al., 2003). The thickness of the particular pelvic floor muscle is taken to be constant (t = 3 mm), based on the average thickness of the human pelvic floor muscles (Chapter 3).

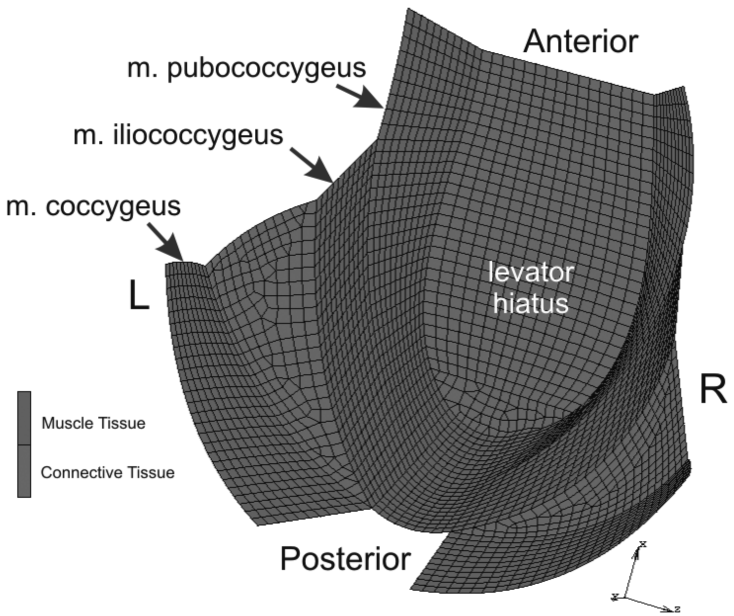

FIGURE 6.1: *Top back view of the mapped FE mesh of the pelvic floor muscles. Elements are generated in the same direction as the muscle fibres. The FE model geometry is based on the experimental measurements describing the complete pelvic floor morphology (Janda et al., 2003).*

To deal with anisotropic and active non-linear elastic behaviour of the pelvic floor muscles, the multi-layer thick shell element consists of two elastic isotropic passive layers (each 25% of the thickness of the element) and one anisotropic active layer (50% of the thickness of the element) (see Figure 6.2). It is assumed that the total stress in the muscle tissue is defined by a superposition of the passive stress in the plane of the muscle, and active stress that works only in the fibre direction. Because of this superposition, the thickness of the active layer is 3 mm and the gross thickness of both passive layers is 3 mm based on data described in Chapter 3. In the numerical model, the total thickness of the muscle multi-layer shell element is 6 mm representing passive and active properties, which are combined in the muscle layer. The larger thickness of the numerical model does not have an effect on the results. Since a shell element with seven integration points is used, the thickness of 6 mm does not affect the numerical precision of the model.

Non-linear large displacement updated Lagrange procedure is used for numerical calculations. The calculations of the model are performed by MSC.Marc FE package.

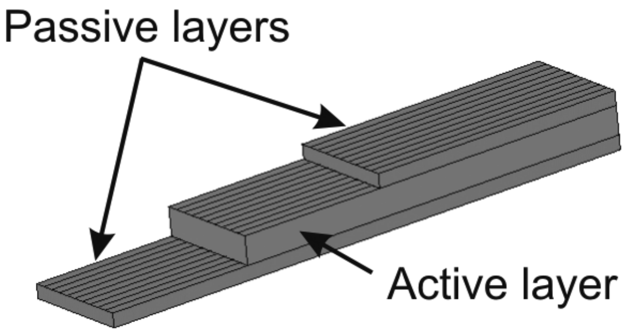

FIGURE 6.2: *The composite of the multi-layer shell element representing the pelvic floor muscles. An orthotropic active layer (50% of the element thickness) incorporated in a non-linear passive isotropic matrix formed by two passive layers (each 25% of the element thickness). The active layer generates stress only in the fibre direction. In the passive the layer stress in the fibre direction and perpendicular to the fibre direction can occur.*

6.2.1 MUSCLE TISSUE - PASSIVE

The Mooney-Rivlin (Mooney, 1940) Third Order Deformation (TOD) constitutive model (Chapter 3) is used for the isotropic non-linear passive layers (see also Figure 6.3). Model parameters are the result of tissue experiments on a fresh human cadaver specimen.

6.2.2 MUSCLE TISSUE - ACTIVE

In the context of the present paper, the active muscle stress is important. In the literature, Hill-type models are often chosen for the active stress. These are phenomenological models, accounting for the length-force and the velocity-force relationship of the muscle. In the present paper, a model based on a thermal shortening in the muscle fibre direction is utilised. The active muscle layer is modelled as an anisotropic material layer with defined stiffness in the muscle fibre direction. Young modulus in the muscle fibre direction E_1 is defined in relation to the particular level of the muscle activation (Equation 6.3), the modulus in other directions (E_2 and E_3) is set to the value close to zero (Equation 6.4):

$$\sigma_{max} = 0.37\ MPa \tag{6.1}$$

$$E_{max} = 9 \cdot \sigma_{max} \tag{6.2}$$

$$E_1 = act \cdot E_{max} \tag{6.3}$$

$$E_2 = E_3 = 0.00001\ MPa \tag{6.4}$$

σ_{max} is the active maximal stress in the muscle fibre (Weis and Hillen, 1985). E_{max} is the maximal derivative of the force-length curve representing the intramuscular intrinsic stiffness (Schouten et al., 2001). The muscle stiffness is not the derivation of force-length relationship but depends on cross-bridge properties and reflexive properties, and is assumed not to depend on muscle length. E_1 is calculated in consideration that the stiffness is scaled with the level of activation act (between 0 for no activation up to 1 for 100% activation of the muscle).

A coefficient of thermal shortening α_1=0.005 is introduced in the muscle fibre direction, while α_2=α_3=0 for other directions. The stress in the muscle fibre direction is calculated using the muscle activation and the muscle force-length relationship. The stress is imposed in the model by calculating the thermal strain ε_{TN} in a particular element, in accordance with the desired muscle activation, and the actual muscle strain ε_N. The force-length relationship curve (Figure 6.4) is modelled as a Gaussian curve using the following formula:

$$\sigma_N = E_1 \cdot (\varepsilon_N - \varepsilon_{TN}) \tag{6.5}$$

$$\sigma_N = act \cdot \sigma_{max} \cdot e^{-\left(\frac{\varepsilon_N}{lsh}\right)^2} \tag{6.6}$$

where σ_N is a stress in the muscle fibre direction, ε_N is a strain with respect to the muscle optimum length, ε_{TN} is a thermal strain for particular element *N* and *lsh* is a parameter of the curve (*lsh* = 0.3). The activation *act* is a given variable and strain ε_N is calculated by solving the FE model. Muscle force-length relationship (Equation 6.6) and relation between stress and strain (Equation 6.5) are constants (see Figure 6.4).

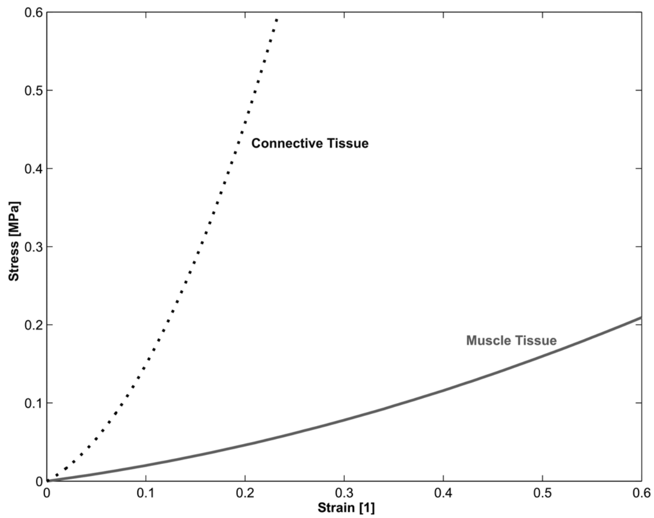

FIGURE 6.3: *The representative equibiaxial stress-strain response for passive material properties of the pelvic floor muscles and connective tissue (raw data fits). The data were used for fitting third order deformation Mooney-Rivlin material model (Table 6.1).*

A user sub-routine is written in Fortran (Digital Visual Fortran 6.0). It is solves for ε_{TN} until equilibrium between the external load (IAP), deformation and muscle stress is obtained. The strain ε_N in the muscle fibre direction is calculated in each element to fulfil the muscle force-length relationship as described in Equation 6.6. With given coefficient of the thermal shortening α_1, the temperature difference is calculated and an increment of the new value is updated as a new state variable. Adaptive step value is used for calculating the temperature increment of each element.

6.2.3 PASSIVE CONNECTIVE TISSUE

Non-linear elastic isotropic material parameters are used for modelling the passive connective tissue. Those material properties are obtained from previous measurements on the passive pelvic floor muscle tissue as described in (Chapter 3). The stress-strain data (see Figure 6.3) are fitted using the non-linear regression routine available in the MSC.Marc FE package. This is used to determine five material constants of the Mooney-Rivlin TOD model summarised in Table 6.1.

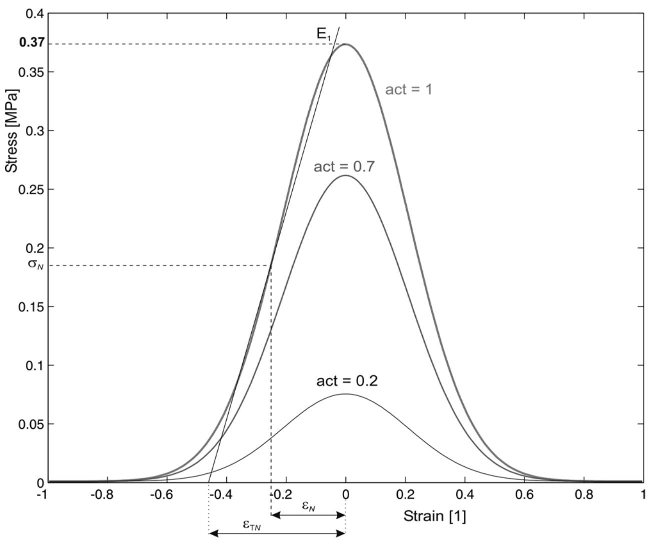

FIGURE 6.4: *The force-length relationship curve is modelled as a Gaussian curve using Equation 6.6. Three particular examples are displayed for three different levels of activation (100%, 70% and 20%).* σ *represents the stress in the muscle fibre direction and* ε *the strain in the muscle direction. The top of each curve represents the maximal optimal stress for particular level of the muscle activation.* σ_N *is a stress in the muscle fibre direction,* ε_N *is the strain and* ε_{TN} *is a thermal strain for particular element N.* E_1 *is Young modulus in the muscle fibre direction, which represents the intrinsic and reflexive contributions to muscle stiffness, and scales with muscle activation. In order to comply with the force - length curve, a value for* ε_{TN} *is calculated iteratively such that the resulting muscle force is in accordance with the prescribed muscle activation and the muscle strain* ε_N *calculated by the FE model.*

6.2.4 Loading

The pelvic floor muscles are firmly attached to the bone and to the arcus tendineus, therefore displacements on this boundary are zero but rotations are allowed. The perineum is modelled as rigid.

The main loading of the pelvic floor muscles is by the IAP and the weight of the internal organs (Chapters 4 and 5). Chapter 5 concluded that the mean displacement of the pelvic floor is in relation to the IAP, which represents about two thirds of the loading, and with the weight of organs, which represents about one third of the load to the pelvic floor in erect position during maximal IAP. Only two thirds of the measured IAP is loading the pelvic floor in supine position during maximal IAP, since the weight of the organs is not loading the pelvic floor, but does affect the recordings with a rectal pressure sensor. The loading pressure on the pelvic floor is modelled using Equation 6.7:

$$p_{load} = p_{recorded} - p_{weight} \tag{6.7}$$

where p_{load} is the pressure loading the pelvic floor, $p_{recorded}$ is the IAP determined during measurements in supine position (Chapter 4) and p_{weight} = 2.9 kPa is the equivalent pressure calculated as an effect of the weight of internal organs. p_{weight} is related to the level of the $p_{recorded}$ recorded in the rest condition (i.e. p_{load} = 0 (rest), whereas $p_{weight} = p_{recorded}$ = 2.9 kPa).

Table 6.1: *Elastic constants describing the non-linear passive elastic behaviour of the connective tissue and muscle tissue used in FE model (see also Figure 6.3). The non-linear regression routines in MSC.Marc (Palo Alto, CA) are used in order to determine material constants for Mooney-Rivlin deformation model. Third order deformation model provided the best fit of the experimental data. The least square error for particular fit is also given.*

	Mooney-Rivlin TOD			
	Passive Connective Tissue		Passive Muscle Tissue	
	Best-fit values [MPa]	Pos. const. [MPa]	Best-fit values [MPa]	Pos. const. [MPa]
a_{10}	1.54499	0.262221	-0.0155102	0
a_{01}	-1.42902	0	0.0298809	0.0220045
a_{11}	0.0888792	0.387745	0.0020027	0.000181295
a_{20}	0.38841	0.392656	-0.000419854	0.00023415
a_{30}	-0.00841026	0	-0.000633591	0.000384789
Error	0	0.06	0	0.1

The FE model was loaded with the objective to obtain equilibrium between loading, level of activation and the displacement of the pelvic floor muscles. The load is stepwise increased; otherwise the FE model would crash due to the large deformations. The IAP, modelled as a hydrostatic pressure, is increasing from zero to the desired level. A decrease of the temperature results in shortening of the muscle elements in the muscle fibre direction. The thermal loading is applied only on the muscle tissue, while the IAP is applied on whole structure including passive connective tissue.

Then, the force in the muscle fibre due to muscle activation is calculated as described in Section 6.2.2 on page 113. The necessary ε_{TN} in accordance with the muscle activation is calculated iteratively. The displacement is calculated in each single iteration. Finally, a static equilibrium between loading, muscle activation and displacement will result.

6.2.5 SIMULATED LOAD-CASES

To illustrate the potential of this model, three loading examples are presented. The muscle is loaded by hydrostatic pressure at three different levels of activation.

The level of the muscle activation is calculated based on experimental measurements in the pelvic floor (Chapter 4). The average EMG activity during maximal activation of the muscle (max ACT) in the healthy volunteer is considered to be 100% (reference value). The levels of activation for healthy volunteers for other conditions like rest and holding of maximal level of the IAP (max IAP) are calculated with respect to the reference value of 100%. The pressure loading the pelvic floor is taken from the measurements using Equation 6.7. The IAP recorded in rest is used as a p_{weight}. The following load-cases are simulated in order to understand the biomechanical behaviour of the pelvic floor muscle and to validate FE model using the experimental data from Chapter 4:

Load-Case 1 (LC1) Rest: The muscle is loaded with the pressure of 0.01 kPa (IAP of 2.9 kPa was determined during measurements and it is considered to be p_{weight}) and level of activation of 29% (act = 0.29). This load-case represents response of the healthy muscle during rest in the supine position. It also simulates the effect of the reconstruction of the muscle tone compared to the cadaver geometry.

Load-Case 2 (LC2) Maximal IAP: The muscle is loaded with the pressure of 5.4 kPa (IAP of 8.3 kPa was determined during measurements = $p_{recorded}$) and level of activation of 87% (act = 0.87). This load-case represents response of the healthy muscle during max IAP in the supine position.

Load-Case 3 (LC3) Maximal ACT: The muscle is loaded with pressure of 1.3 kPa (IAP of 4.2 kPa was determined during measurements = $p_{recorded}$) and fully activated (act = 1). This load-case represents response of the healthy muscle during max ACT in the supine position.

6.2.6 Validation of the model

The displacement of the muscles and the width (W) of the levator hiatus are calculated. The depth (D) is determined from the centre of the line connecting both femur centroids to the lowest border of the levator ani muscle (Chapter 4). The width W of the levator hiatus is determined as a distance of the left and right borders of the levator ani muscle perpendicular to D at 50% of the length of D. The mean displacement and width W has been recorded using MRI in ten healthy volunteers (Chapter 4), and will be compared to the results of all three load-cases described in Section 6.2.5 on page 117. The mean displacement is calculated in LC2 and LC3 with respect to LC1 using a MATLAB^{TM} 6.1 software from The Mathworks Inc. The mean displacement in LC1 is calculated with respect to the unloaded state, which corresponds to the cadaver muscle geometry without a muscle tone.

6.3 Results

The graphical results of the three loading cases are presented in Figure 6.5 and Figure 6.6. In all loading cases, the stress in the muscle fibre direction reached equilibrium with respect to the level of activation and external load. Stress is uniformly distributed over all muscle fibres (see Figure 6.5A, C and E), since they have all the same activation and sustain the same external load. The global displacement is presented in Figure 6.5B, D and F. The largest displacement (with respect to the cadaver geometry) in the LC1 is observed on both sides of the iliococcygeus muscle (see Figure 6.5B). However, the largest displacement in LC2, where the maximum pressure of 5.4 kPa takes place, is observed in the connective tissue of the levator hiatus. In the LC3 where the activation of the muscle reach 100%, the largest displacement is observed in both the iliococcygeus muscle and the connective tissue of the rear part of the pelvic floor.

The strain in the fibre and transverse direction of the muscle is presented in Figure 6.6. The strain in the transverse direction is higher than in the muscle fibre direction in all loadcases (LC1, LC2 and LC3). Due to the muscle activation, the muscle will shorten and the stress will increase in its fibre direction.

However, the same internal stress must be reached in the perpendicular direction. This can be achieved when the connective tissue is strained further.

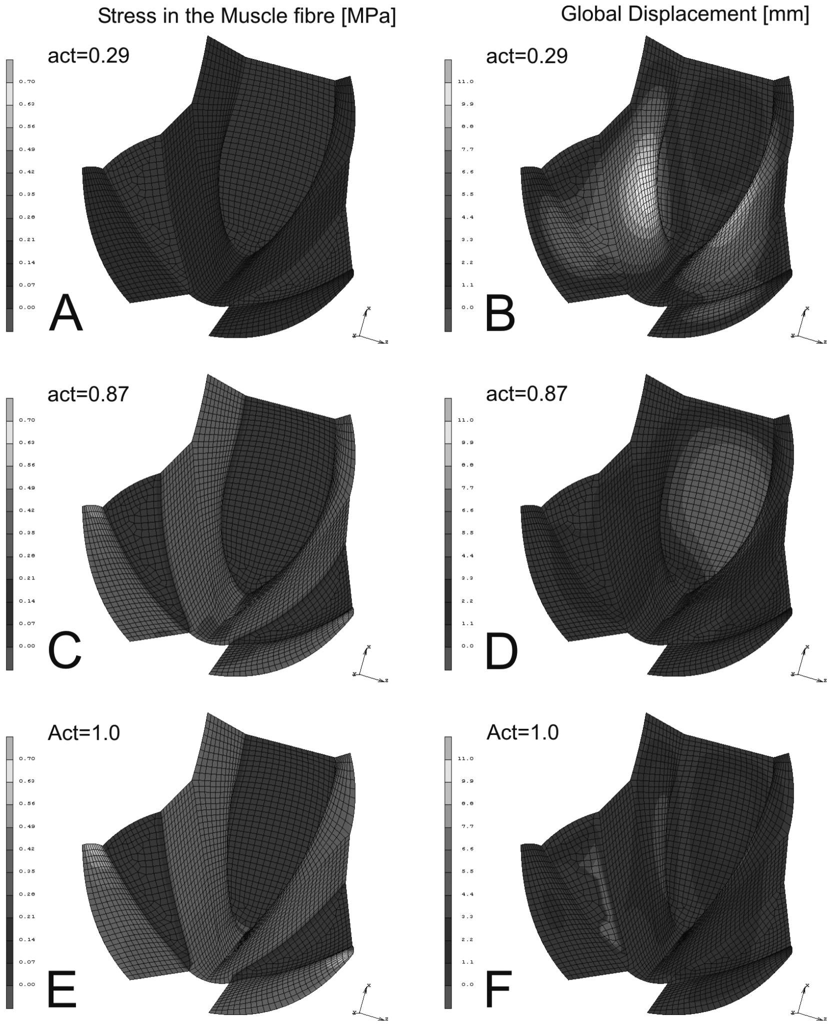

FIGURE 6.5: *Graphical results of the FE analysis of the pelvic floor muscles. The stress in the muscle fibre direction in MPa is displayed in the left column, displacement in millimeters in the right column. The 'active' stress in the connective tissue is zero in image A, C and E, since it is passive tissue. The same scale is used for all three load-cases. Three particular examples are displayed for three conditions: LC1 (rest): 29% activation, 0.01 kPa load - Images A and B; LC2 (max IAP): 87% activation, 5.4 kPa load - Images C and D; LC3 (max ACT): 100% activation, 1.3 kPa load - Images E and F).*

The width W of the levator hiatus and the mean displacement of the muscle calculated in the model for all three conditions and the experimental data from Chapter 4 are summarised in Table 6.2. For LC2 and LC3 the difference in width between model prediction and experiment is small (less than 1 mm), and the difference in mean displacement is also smaller than 0.5 mm. In LC1 (rest condition) the difference in width is 5 mm. The displacement in LC1 (rest) with respect to the cadaver geometry (no muscle tone) is 3.28 mm.

TABLE 6.2: *The results of the width W and mean displacement (with respect to LC1) in all three load-cases compared to the experimental data from Chapter 4.*

	Loading Case	LC1	LC2	LC3
FE model	Width W [mm]	39.4	47.6	42.4
	Mean displacement [mm]	3.28	2.8	2.32
Experimental measurements	Width W [mm]	34 ± 6.1	47 ± 7.5	41.9 ± 6.1
	Mean displacement [mm]	×	3.2 ± 0.4	2.8 ± 0.5

6.4 DISCUSSION

The main objective of the presented paper is to explain the concept of the FE modelling of the pelvic floor muscles and its ability to analyse the biomechanical behaviour of such a complex structure as the pelvic floor musculature. The pelvic floor is composed of muscles and other connective tissues linked to the supported organs. One of the major complexities of such structure is caused by the difficult constitutive behaviour of the material. This is particularly true for muscle, because apart from non-linear passive properties, it has an active property. Muscle is able to generate force depending not only on its length but also on its activation. The active stress is implemented using thermal strain ε_N representing the force-length relation and activation. The coupling of this stress with the deformation makes this type of analysis complicated.

6.4.1 FE MODEL

The descriptive model includes reflexive and contractile properties of the muscle, incorporated in the Young's modulus E_1. A concept based on thermal shortening of the muscle in the muscle fibre direction is chosen using a standard FE code (MSC.Marc). This concept solves the muscle force using an optimisation method, as described in Section 6.2 on page 110. Thermal shortening of the element using a muscle force-length relationship is a simple and effective method for simulating contractile properties of the muscle tissue.

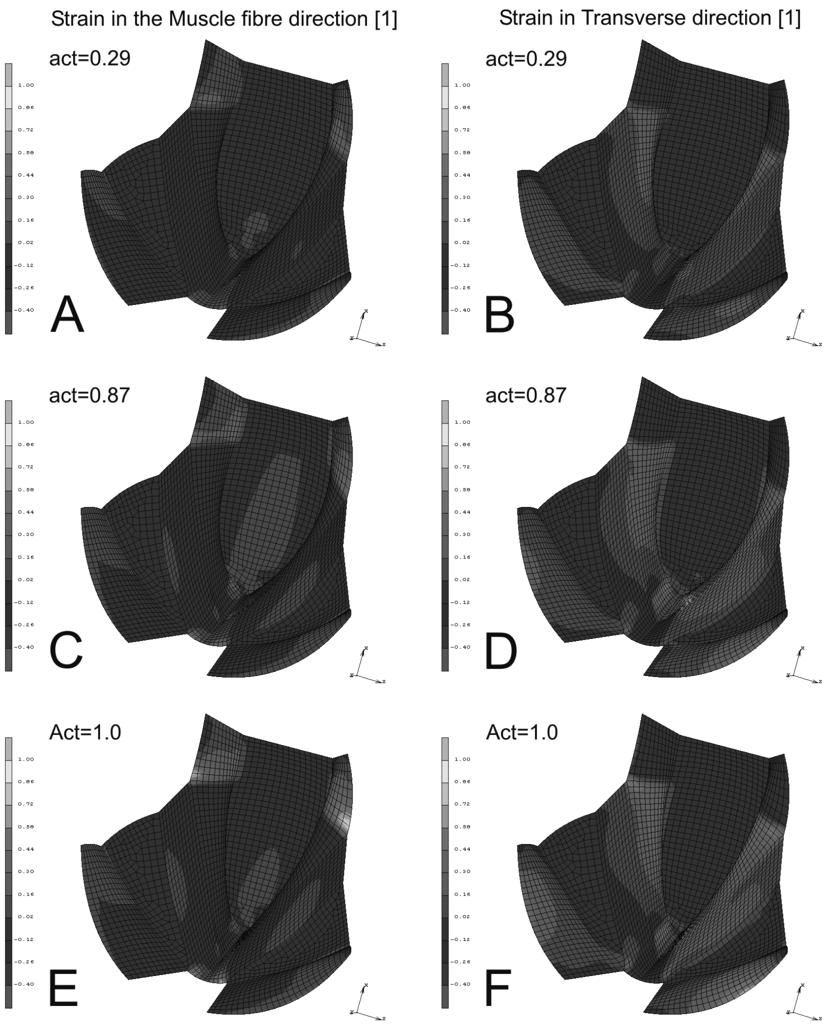

FIGURE 6.6: *Graphical results of the FE analysis of the pelvic floor muscles. The strain in the muscle fibre direction is displayed in the left column, strain in the transverse fibre direction in the right column. The same scale is used for all load-cases. The strain in the connective tissue is displayed in principal directions (the local co-ordinate system). Three particular examples are displayed for three conditions: LC1 (rest): activation 29%, load 0.01 kPa - Images A and B; LC2 (max IAP): activation 87%, load 5.4 kPa - Images C and D; LC3 (max ACT): activation 100%, load 1.3 kPa - Images E and F).*

The convergence of the optimisation method depends mainly on the temperature difference as a new state variable in each optimisation step. The maximal increment of the thermal strain was found to be $\Delta\varepsilon_{TN} = 0.00025$ which corresponds to the temperature increment of about 0.05 K. This is caused presumably due to very complex geometry of the pelvic floor and the large deformations.

The FE muscle model is quite complex with many material parameters, and is difficult to validate. For contracting muscle, much simpler models, which were successful, have been used in the past. Many musculoskeletal models e.g. in gait analysis problems can be solved using 1D-line elements for muscle with simple contraction model. However, the pelvic floor is loaded perpendicular to the muscle line of action by IAP and, therefore, a simple representation of the muscle action by a 1D-line elements is not appropriate. A sophisticated approach using a FE model of the muscle is necessary.

The advantage of the present concept is to model both non-linear passive and active properties of the muscle using a standard FE code. Since an element with non-linear and orthotropic properties is not available in standard FE code, we have used a multi layer shell element with both active and passive layers. This concept allows using an orthotropic active layer incorporated in a non-linear passive isotropic matrix formed of passive layers.

6.4.2 FE analysis of the pelvic floor

The stress in the muscle fibre reached the equilibrium level with respect to the level of activation in all loading cases (see Figure 6.5). However, there are some spots with higher stress than the maximal stress in the muscle fibre (see Figure 6.5). These artefacts (stress concentration) are situated mostly at the attachment sites (an effect of the boundary conditions) in the posterior part of the coccygeus muscle (attached to spina ischiadica). These are presumably caused due to the constant thickness of the element. Since the pelvic floor muscles are flat, have no tendon and because of the trapezoid shape, the muscle must be thicker when the width is smaller if assuming a constant number of fibres. Simulations shown that these artefacts disappear if constant cross-section area of the muscle is considered, assuming that the thickness of the muscle is not constant i.e. it is growing with the decreasing width.

The largest displacement is observed in LC1 in the iliococcygeus and pubococcygeus muscle (Figure 6.5B). In this load-case, the activation of the muscle is 29% and the loading pressure is very low. A small pressure of 10 Pa is used for numerical stability of the FE model. The main loading in the LC1 is due to the muscle activation. Therefore, the largest displacement is observed in the muscle tissue on both sides of the pelvic floor. This is in agreement with the clinical observations (see also Chapter 4). The largest displacement in LC2 is observed in the connective tissue of the levator hiatus. In this load-case, the pelvic floor is loaded by the maximal pressure of the 5.4 kPa, while the muscles are highly activated. The passive connective tissue obtains the necessary stress through larger deformations, and displaces in a downward direction. In the LC3 where the activation of the muscle reach 100%, the largest displacement is observed in both the iliococcygeus muscle and the connective tissue of the rear part of the pelvic floor. Again, since there is not a large load of the structure, the contracting muscle parts will displace most in the upward direction.

The displacement of the connective tissue parts depend only on the passive properties. Increasing pressure loading the pelvic floor generates increasing displacement of the connective tissue of the levator hiatus. In the muscle parts, the displacement is in relation to the muscle activation. When the muscle activation is increasing the upward muscle displacement is increasing as well (see Figure 6.5). The global displacement is, however, also depending on the pressure loading the pelvic floor. If the pressure is increasing the (upward) displacement is decreasing. The levator hiatus is closing with increasing activation of the muscle tissues (see Figure 6.5B, D and F). This is in agreement with the clinical observations. The muscle is the only active component in the pelvic floor. Therefore, the displacement of the muscle, particularly in the anterior part of the levator ani muscle plays obviously a crucial role in the support of the organs in the pelvic floor. The opening and closing of the levator hiatus is dependent on the activation of the muscle. When the activation is decreasing, the width of the levator hiatus is increasing and vice versa.

The strain in the muscle fibre and transverse direction of the muscle is presented in Figure 6.6. The strain in the muscle fibre direction reached the equilibrium level with respect to the muscle force-length relationships (Equation 6.6) for each element. The lower strain in the muscle fibre direction compared to the transverse direction is caused by reinforcement through the active layer of the muscle tissue. When the level of muscle activation is increasing the strain in the muscle fibre is decreasing. The strain in the transverse direction is higher than in the muscle fibre direction as observed in Figure 6.6. The strain in the transverse direction is solely dependent on the passive properties of the muscle tissue.

6.4.3 MUSCLE ACTIVATION

Activation of the pelvic floor muscles is necessary to increase the IAP (also during activities like coughing, sneezing etc.). Whether the muscles are lengthened or shortened, which will result in downward or upward movement of the pelvic floor respectively, depends on the level of the IAP and the level of muscle activation. There is a direct relation between the pressure difference between the inside and outside of the intra-abdominal compartment, the tensile stress in the wall of the compartment and the curvature of the wall of the compartment (Equation 6.8) described by Van Leeuwen and Spoor (1992):

$$c_f = -\frac{dp}{\sigma_f \cdot dr} \tag{6.8}$$

where $c_f = 1/R_f$ is the local curvature (R_f = local radius of curvature), dp is the pressure difference, σ_f is the stress in the muscle and dr represents the muscle thickness. If the muscles are activated, the tensile stress will increase in the muscle direction and the curvature will decrease for the same IAP (which also depends on the activation of the abdominal muscles). However, in the muscle the stress perpendicular to the fiber direction (transverse direction) is not actively controlled, and will be lower. From Equation 6.8 it can be seen that as a result the curvature will be higher. The combination of curvatures in the fiber direction and perpendicular to the fiber direction will result in the typical basin and dome shapes of the pelvic floor muscle (Hjartardottir et al., 1997). In pathological cases like genital prolapse the displacement was not different from healthy subjects, but the width W (which is mainly affected by the connective tissue) was different.

Since the relation between stress σ and strain ε is utilised using a linear Hook law (Equation 6.5, see also Figure 6.4), the solution is not dependent on modulus E_1 i.e. the intrinsic and reflexive muscle stiffness. This linear relation is used in muscle force-length relationship (Figure 6.4 and Equation 6.6) and it will be important for later dynamics simulations, when perturbations are present like in walking or coughing. The positive value of E is used for numerical stability of the model.

Loss of muscle tone after death has been addressed by studying some cadavers during the phase of rigor mortis (DeLancey, 1999). There is a difference in the pelvic floor topology between the cadaver and the living subject. In the biomechanical model based on the FE theory, the muscle position is reconstructed to the in vivo situation by imposing the appropriate level of muscle activation. In the FE model, the loading forces and muscle forces are simulated, and the muscle found a new position depending on the load condition and simulated muscle activation. That solved the problem of the loss of the muscle tone based on a cadaver geometry data.

Muscle consists of more than 70% water and behaves as nearly incompressible. Nearly incompressible material behaviour can lead to so-called locking of element in a numerical procedure. This becomes visible as oscillations in the displacement fields (Oomens et al., 2003). For this reason fully incompressible material model (Mooney-Rivlin TOD) is used. The advantage of such a constitutive model is that it can describe non-linear elastic material properties of the passive muscle and connective tissue. The disadvantage is an isotropic model for the passive muscle tissue. This is, however, partly solved using the anisotropic active layer incorporated in multi-layer composite element as described in Section 6.4.1 on page 120.

6.4.4 VALIDATION

The FE model described above is validated using the experimental data obtained from Chapter 4. The width W of the levator hiatus and the mean displacement with respect to the rest condition of the pelvic floor muscles are measured. The simultaneously recorded EMG data and the level of the IAP are used as an input for the numerical model.

The width W corresponds very well with the experimental measurements in LC2 and LC3 (see Table 6.2). In the LC1, the width W calculated by the FE model is larger than measured in Chapter 4. This effect can be caused by the stiffness of the connective tissue of the levator hiatus in the FE model. The connective tissue has an influence on the borders of the muscle. If the stiffness of this connective tissue is decreasing, the muscle is able to close the levator hiatus more easily and, therefore, the width W is decreasing if the pressure is loading the pelvic floor (Chapter 7).

The mean displacement of the pelvic floor muscles is summarised in Table 6.2 and compared with data from Chapter 4. The displacement in LC2 and LC3 is in good agreement with the experimental measurements. In the LC1, the mean displacement is calculated with respect to the fully relaxed muscle, with lost tone (cadaver geometry). This condition is obviously not determined experimentally in Chapter 4.

In the next study, more load-cases will be analysed in order to confirm the hypothesis that the activation of the pelvic floor muscles play a crucial role in the pelvic floor support. It is also important to test the effect of the various stiffness of the passive connective tissue in the pelvic floor. The results from these analyses will be validated using experimentally determined displacements from MRI measurements (Chapters 4 and 5) and EMG activity of the muscle (Chapter 4) in patients and healthy subjects.

6.5 CONCLUSIONS

The relation between input variables: loading (by IAP etc.) and muscle activation and output variables: displacement of the pelvic floor muscles was iteratively determined by FE model. This relation describes the biomechanical behaviour of the pelvic floor.

The results of the FE simulations (Width of the levator hiatus and displacement of the muscle) are in good agreement with experimentally determined values on healthy subjects in parenthesis: Width [mm] in rest: 39.4 (34 ± 3.6), max IAP: 47.6 (47 ± 7.5) and max ACT: 42.4 (41.9 ± 6.1); the displacement [mm] in rest: 3.28 (not determined), max IAP: 2.8 (3.2 ± 0.4) and max ACT: 2.32 (2.8 ± 0.5).

The model can be used for further studying of the function of the pelvic floor and for understanding the substance of disease such as genital prolapse.

REFERENCES

DeLancey, J.O.L., 1999. Structural anatomy of the posterior pelvic compartment as it relates to rectocele. Am J Obstet Gynecol. Vol 180, No.4, 815-823.

Donkelaar, C.C.v., Drost, M.R., Mameren, H.v., Tuinenburg, C.F., Janssen, J.D., Huson, A., 1996. Three-dimensional reconstruction of the rat triceps surae muscle and finite element mesh generation of the gastrocnemius medialis muscle. European Journal of Morphology 34, 31-37.

Hjartardottir, S., Nilsson, J., Petersen, C., Lingman, G. (1997). The female pelvic floor: A dome - not basin. Acta Obstet Gynecol Scand 76, 567-571.

Huyghe, J.M., van Campen, D.H., Arts, T., Heethaar, R.M., 1991. A two-phase finite element model of the diastolic left ventricle. Journal of Biomechanics 24, 527-538.

Janda, S., Van der Helm, F.C.T., de Blok, S.B, 2003: Measuring morphological parameters of the pelvic floor for FE modelling purposes. Journal of Biomechanics, 36/6, 749-757.

Johansson, T., Meier, P., Blickhan, R., 2000. A finite-element model for the mechanical analysis of skeletal muscles. Journal of Theoretical Biology 206, 131-149.

Mooney, M., 1940. A theory of large elastic deformation. Journal of Applied Physics 11, 582-591.

Olsen, A.L., Smith, V.J., Bergstorm, J.O., Colling, J.C., Clark, A.L., 1997. Epidemiology of surgically managed pelvic organ prolapse and urinary incontinence. Obstet Gynecol. 89, 501-506.

Oomens, C.W.J., Maenhout, M, van Oijen, C.H., Dorst, M.R., Baaijens, F.P., 2003. Finite element modelling of contracting skeletal muscle. Phil. Trans. R. Soc. Lond. B 358, 1453-1460.

Schouten, A.C., de Vlugt, E., van der Helm, F.C.T., Brouwn, G.G., 2001. Optimal posture control of a musculo-skeletal arm model. Biol. Cybern., 84, 143-152.

Van der Helm, F.C.T., 1994. A finite element musculoskeletal model of the shoulder mechanism. J. Biomechanics 27(5), 551-569.

Van der Linden, B.J., Koopman, H.F., Huijing, P.A., Grootenboer, H.J., 1998. Revised planimetric model of unipennate skeletal muscle: a mechanical approach. Clinical Biomechanics 13, 256-260.

Van Leeuwen, J.L., Spoor, C.W., 1992. Modelling mechanically stable muscle architecture. Phil. Trans. R. Soc. Lond. B 336, 275-292.

Vankan, W.J., Huyghe, J.M., van Donkelaar, C.C., Drost, M.R., Janssen, J.D., Huson, A., 1998. Mechanical blood-tissue interaction in contracting muscles: a model study. Journal of Biomechanics 31, 401-409.

Weis, W.A., Hillen, B., 1985. Cross-sectional areas and estimated intrinsic strength of the human jaw muscles. Acta Morph. Neerl.-Scand 23: 267-274.

Yucesoy, C.A., Koopman, B.H.F.J.M., Huijing, P.A., Grootenboer, H.J., 2002. Three-dimensional finite element modelling of skeletal muscle using a two-domain approach: linked fiber-matrix mesh model. Journal of Biomechanics 35, 1253-1262.

Chapter 7

BIOMECHANICAL ANALYSIS OF THE PELVIC FLOOR MUSCULATURE

Abstract

The goal of this study is to understand the development of the genital prolapse as a result of the biomechanical loading of the pelvic floor musculature. 12 specific load-cases are analysed using a biomechanical model based on FE theory. These load-cases describe the effect of the level of the muscle activation and intra-abdominal pressure (IAP) on the shape and displacement of the pelvic floor. These load -cases were also experimentally determined in both healthy subjects and patients. The load-cases could accurately be described by the FE model and validated using the experimental data. Width of the levator hiatus and displacement of the muscle are in a good agreement with experimentally determined values (healthy subject data used for validation: H1a - rest, H2a - max contraction of the pelvic floor muscles and H3a - holding the max level of IAP) in parenthesis: Width [mm] in H1a 39.4 (34 ± 3.6), H2a 47.6 (47 ± 7.5) and H3a 42.4 (41.9 ± 6.1); the displacement [mm] in H1a 3.28 (not determined), H2a 2.8 (3.2 ± 0.4) and H3a 2.32 (2.8 ± 0.5). The hypothesis was tested that genital prolapse might result from compliant connective tissue; Two types of connective tissue with different stiffness are tested. The results show that the muscle tissue as the only active component in the pelvic floor plays a major role in the support of the organs in the pelvic floor. When the muscle activation is increasing the upward muscle displacement is increasing as well. The levator hiatus is closing with increasing activation of the muscle tissues if the pressure is constant.

It leads to the conclusions, that: 1) Decreasing muscle activation leads to the increasing width of the levator hiatus, which is associated with the development of genital prolapse. 2) The compliance of the connective tissue of the levator hiatus has not a significant effect on the width of hiatus, therefore has not a significant effect on the development of genital prolapse. 3) The muscle training is efficient since the muscle plays a crucial role in pelvic organ support. 4) Muscle activation is a major factor responsible for the enlargement of the levator hiatus. Therefore, the surgeon has to focus on the levator hiatus width, which should be reduced by use of mesh prosthesis in order to minimize the development of the genital prolapse. Design of a new biomaterial mesh prostheses for surgical repair of the genital prolapse can be based on predictions of the FE model.

Keywords

Genital prolapse; Pelvic floor muscles; Finite element model

7.1 INTRODUCTION

The pelvic floor in humans is a very complex muscular structure. The levator ani muscle with its fascial covering constitutes the pelvic diaphragm. It is largely responsible for supporting both pelvic and abdominal organs and acts synergistically with the striated muscle of the anterior abdominal wall generating intra-abdominal pressure (IAP). Any increase in IAP e.g. caused by coughing or sneezing, is applied equally to all sides of the pelvic and abdominal wall. If the levator ani is pathologically weakened or temporarily inactivated a genital prolapse can occur. Genital prolapse is a major cause of morbidity in women. Genital prolapse is a condition in which pelvic organs (vagina, uterus, bladder, etc.), normally supported by the pelvic floor muscles, protrude outside the pelvic floor into or through the vagina.

One in every nine women requires surgery for problems related to defective pelvic organ support (Olsen et al., 1997). Various surgical procedures have been advocated for repair of pelvic floor organ prolapse (genital prolapse) depending on the site of the defect (Richardson et al., 1976, Hurt, 1997). Prolapse can recur postoperatively in up to 34% of cases (Shull et al., 1994). It is possible that the recurrences may be the results of failure to identify the causative lesion in the pelvic floor before operation (Hoyte et al., 2000). Despite the common occurrence of genital prolapse, the structural defects responsible for its formation remain poorly understood. Besides, damage to the levator ani muscle is associated with genital prolapse, which has been documented on dissections (Halban and Tandler, 1907), with radiography (Berglas and Rubin, 1953), and in neuromuscular studies (Smith et al., 1989). Since genital prolapse occurs through the urogenital hiatus in the levator ani muscle, it seems possible that loss of the levator ani muscles' ability to close hiatus is a factor contributing to prolapse (DeLancey and Hurd, 1998). It was concluded that increasing pelvic organ prolapse is associated with increasing urogenital hiatus size; the hiatus is larger after several failed operations than after successful surgery or single failure. However, the factor responsible for enlargement of the urogenital hiatus remains to be determined (DeLancey and Hurd, 1998).

The biomechanical behaviour of the pelvic floor muscles was recently analysed (Chapter 6). It is expected that pelvic floor muscles have a fundamental influence in disorders like genital prolapse. The main loading of the pelvic floor muscles is due to IAP. In addition there will be the load due to the weight of the internal organs. To study the complex biomechanical behaviour of the pelvic floor muscles and to investigate the effectiveness of reconstructive surgery, a computer model based on the finite-element (FE) theory was developed (Chapter 6). In a FE model the relationship between the loading and muscle forces in three dimensions can be represented. The model is able to predict the position of the pelvic floor depending on the load (e.g. IAP) and activation of the muscles. Thus far, no other three-dimensional models have been proposed to analyse the biomechanical behaviour of the pelvic floor.

The main goal of this study is to understand the development of the genital prolapse as a result of the biomechanical loading of the pelvic floor musculature. Genital prolapse is likely to be related to the displacement of the pelvic floor and the width of the levator hiatus.

The following questions are raised:

1. What is the effect on the width of the levator hiatus if the muscle is insufficiently activated?
2. What is the effect on width of the levator hiatus if the connective tissue in the levator hiatus is more compliant than normal?

And finally clinical questions arise:

3. Is muscle training effective if there is a problem in connective tissue of the levator hiatus?
4. On what spot in the diaphragma pelvis the surgeon has to focus on during reconstructive surgery if:
   a) The muscle activation is insufficient (the muscle is not able to generate enough force) and the connective tissue has a normal compliancy;
   b) The muscle activation is normal (muscle is able to generate enough force) but the connective tissue of the levator hiatus is more compliant?

In order to answer these questions a biomechanical model of the pelvic floor based on FE theory was developed (Chapter 6). The model has been validated using experimental data describing the displacement of the pelvic floor muscles in relation to the level of IAP and muscle activation during several conditions (Chapters 4 and 5).

7.2 Materials and methods

A FE model of the pelvic floor muscles developed in Chapter 6 is used for biomechanical analysis of the pelvic floor muscles. This model is able to represent both non-linear and active properties of the muscle using a standard FE code multi layer shell element. A thermal shortening in the muscle fibre direction is utilised for simulating active muscle properties. The force in the muscle fibre is calculated in order to obtain the optimal muscle force for particular level of the muscle activation (Chapter 6).

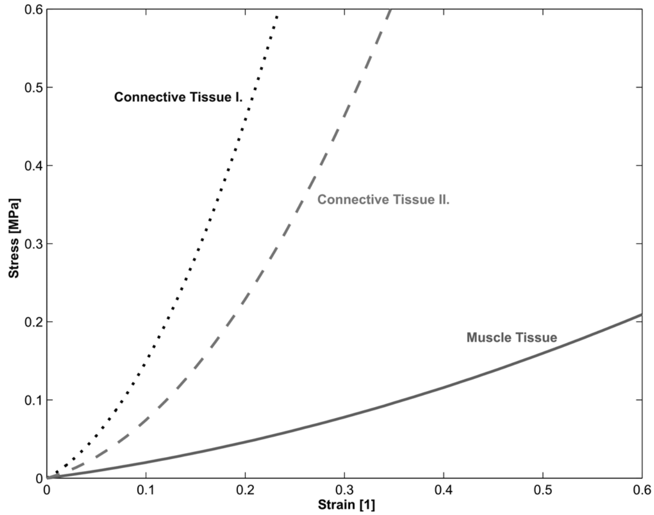

FIGURE 7.1: *The representative equibiaxial stress-strain response for passive material properties of the pelvic floor muscles and uniaxial stress-strain response for passive connective tissue (raw data fits). Connective tissue I. represent measured values on normal specimen (stiff); connective tissue II. represents approximately two times more compliant tissue. The data were used for fitting third order deformation Mooney-Rivlin material model (Table 7.1).*

7.2.1 PASSIVE CONNECTIVE TISSUE

Passive connective tissue of the pelvic floor is assumed to be isotropic. Non-linear elastic isotropic material parameters are used for modelling the passive connective tissue. Two types of connective tissue with different stiffness - stiff (Connective tissue I.) and compliant (Connective tissue II.) are chosen (see Figure 7.1). The material properties of connective tissue are obtained from previous measurements (unpublished data) on the passive pelvic floor muscle tissue as described in Chapter 3. Connective tissue I. is determined by uniaxial tensile test (described in Chapter 3) of the pelvic floor connective tissue in the levator hiatus region of healthy specimen. The connective tissue II. is calculated to be approximately two times lower in stiffness than connective tissue I. The stress-strain data (see Figure 7.1) are fitted using the non-linear regression routine available in the MSC.Marc FE package. This is used to determine five material constants of the Mooney-Rivlin (Mooney, 1940) Third Order Deformation (TOD) model summarised in Table 7.1. Positive constants are used (Chapter 3).

TABLE 7.1: *Elastic constants describing the non-linear passive elastic behaviour of the connective tissue and muscle tissue used in FE model (see also Figure 7.1). The non-linear regression routines in MSC.Marc (Palo Alto, CA) are used in order to determine material constants for Mooney-Rivlin deformation model. Third order deformation model (TOD) provided the best fit of the experimental data. The least square error for particular fit is also given.*

	Mooney-Rivlin TOD					
	Passive Connective Tissue I.		Passive Connective Tissue II.		Passive Muscle Tissue	
	Best-fit values [MPa]	Pos. const. [MPa]	Best-fit values [MPa]	Pos. const. [MPa]	Best-fit values [MPa]	Pos. const. [MPa]
a_{10}	1.54499	0.262221	0.774016	0.131757	-0.0155102	0
a_{01}	-1.42902	0	-0.715201	0	0.0298809	0.0220045
a_{11}	0.0888792	0.387745	0.0445678	0.212103	0.0020027	0.000181295
a_{20}	0.38841	0.392656	0.38841	0.184141	-0.000419854	0.00023415
a_{30}	-0.00841026	0	0.194134	0	-0.000633591	0.000384789
Error	0	0.06	0	0.05	0	0.1

7.2.2 LOADING

The pelvic floor muscles are firmly attached to the bone and to the arcus tendineus, therefore displacements on this boundary are zero but rotations are allowed. The perineum is modelled as rigid with free rotations. The main loading of the pelvic floor muscles is by the IAP and the weight of the internal organs (Chapters 4 and 5). Chapter 5 concluded that the displacement of the pelvic floor is in relation with the IAP, which presents about two thirds of the loading, and with the weight of organs, which presents about one third of the load to the pelvic floor in erect position. Only two thirds of the measured IAP is loading the pelvic floor in supine position, because the weight of the organs is also pressing on the rectal pressure sensor, whereas the weight does not load the pelvic floor. The loading pressure on the pelvic floor is modelled using Equation 7.1:

$$p_{load} = p_{recorded} - p_{weight} \tag{7.1}$$

where p_{load} is the pressure loading the pelvic floor, $p_{recorded}$ is the IAP determined during measurements in supine position (Chapter 4) and p_{weight} is the equivalent pressure calculated as an effect of the weight of internal organs. p_{weight} is equal to the level of the $p_{recorded}$ recorded in the rest condition (i.e. $p_{load} = 0$).

The FE model will iterate until equilibrium is obtained between loading, level of activation and the displacement of the pelvic floor muscles. The IAP is modelled as a hydrostatic pressure. Imposing a thermal loading on the muscle elements simulates muscle activation. A decrease of the temperature results increased tensile stress of the muscle elements in the muscle fibre direction. The thermal loading is applied only on the muscle tissue, while the IAP is applied on whole structure including the passive connective tissue.

The thermal loading is calculated iteratively such that the resulting force complies with the given muscle activation and the resulting muscle length calculated by the FE model, given the muscle force-length relationship as described in Chapter 6.

7.2.3 SIMULATED LOAD-CASES

The muscle activation, IAP and position of the pelvic floor are based on experimental measurements (Chapter 4). The average EMG activity during maximal activation of the muscle (Max ACT) in the healthy volunteer is considered to be 100% (reference value). The levels of activation for both healthy volunteers and patients for other conditions like rest and holding of maximal level of the IAP (Max IAP) are calculated with respect to the reference value of 100%. The pressure loading the pelvic floor is calculated using Equation 7.1. The IAP recorded in rest is used as a p_{weight}. Load-cases based on EMG and IAP measurements (Chapter 4) are summarised in Table 7.2. Those are simulated in order to understand the biomechanical behaviour of the pelvic floor muscle and to answer question from Section 7.1 on page 131.

7.2.4 VALIDATION

The mean displacement and the width W of the levator hiatus calculated by the FE model are validated using the MRI data from Chapter 4. The distance (depth - D) is determined from the centre of the line connecting both femur centroids to the lowest border of the levator ani muscle (Chapter 4, see Figure 4.2 on page 73). The width W of the levator hiatus is determined as a distance of the left and right borders of the levator ani muscle perpendicular to D at 50% of the length of D.

TABLE 7.2: *Description of the all load-cases used for analysing the biomechanical behaviour of the pelvic floor muscles. The input parameters and short description of the conditions are given. The IAP and activation levels are based on results of experimental measurements in the pelvic floor (Chapter 4).*

Load case No.:	IAP [kPa]	Activation [%]	Connective tissue type	Condition description
H1a	0.01	29	I.	Healthy subject muscle and strong connective tissue in the pelvic floor during rest
H1b	0.01	29	II.	Healthy subject muscle and compliant connective tissue in the pelvic floor during rest.
H2a	5.4	87	I.	Healthy subject muscle and strong connective tissue in the pelvic floor during max IAP
H2b	5.4	87	II.	Healthy subject muscle and compliant connective tissue in the pelvic floor during max IAP
H3a	1.3	100	I.	Healthy subject muscle and strong connective tissue in the pelvic floor during max ACT
H3b	1.3	100	II.	Healthy subject muscle and compliant connective tissue in the pelvic floor during max ACT
P1a	0.3	23	I.	Patient muscle activation and strong connective tissue in the pelvic floor during rest
P1b	0.3	23	II.	Patient muscle activation and compliant connective tissue in the pelvic floor during rest
P2a	3.9	54	I.	Patient muscle activation and strong connective tissue in the pelvic floor during max IAP
P2b	3.9	54	II.	Patient muscle activation and compliant connective tissue in the pelvic floor during max IAP
P3a	1.2	70	I.	Patient muscle activation and strong connective tissue in the pelvic floor during max ACT
P3b	1.2	70	II.	Patient muscle activation and compliant connective tissue in the pelvic floor during max ACT

The mean displacement of the muscle tissue in the FE model is calculated with respect to the rest condition (load-cases: H1a, H1b, P1a, P1b) using a MATLAB^{TM} 6.1 software from The Mathworks Inc. H2a and H3a are calculated with respect to H1a, in H2b and H3b with respect to H1b, in P2a and P3a with respect to P1a and in P2b and P3b with respect to P1b. The mean displacement in H1a, H1b, P1a and P1b is calculated with respect to the unloaded state (act = 0), which corresponds to the cadaver muscle geometry without a muscle tone.

The width W and the mean displacement of muscle for both healthy subjects (H1a, H2a and H3a) and patients without cystocele (P1a, P2a and P3a) and with cystocele (P1b, P2b and P3b) are compared with the results of all 12 load-cases (see Table 7.2).

7.3 RESULTS

The graphical results of all twelve simulated load-cases are presented in Figures 7.2, 7.3, 7.4 and 7.5. In all loading cases, the stress and deformation in the muscle fibre reached equilibrium with respect to the level of activation and IAP. Stress is uniformly distributed over all muscle fibres (see left column in Figures 7.2 to 7.5). The global displacement is presented in the right columns in Figures 7.2 to 7.5.

The displacement of the pelvic floor muscles and the width W of the levator hiatus calculated by the FE model for all three conditions (rest, max IAP and max ACT) in the load-cases H1a, H2a and H3a are in a good agreement with the experimentally determined data of healthy subjects. These are summarised in Table 7.3.

TABLE 7.3: *The results of the width W and mean displacement in all three load-cases compared to the experimental data obtained from healthy subjects and patients in Chapter 4.*

	FE model		Experimental measurements	
Load case No.:	Width W [mm]	Mean displace-ment [mm]	Width W [mm]	Mean displacement [mm]
H1a	39.4	3.28	34 ± 3.6	×
H1b	39.5	3.35	×	×
H2a	47.6	2.8	47 ± 7.5	3.2 ± 0.4
H2b	47.5	2.84	×	×
H3a	42.4	2.32	41.9 ± 6.1	2.8 ± 0.5
H3b	42.1	2.33	×	×
P1a	48.9	2.88	36.7 ± 3.5	×
P1b	49	2.94	45.3 ± 6.7	×
P2a	56.5	2.31	51.3 ± 3.1	2.8 ± 0.6
P2b	56.2	2.35	57.6 ± 7.3	2.9 ± 0.7
P3a	52.3	2.16	49.3 ± 2.3	2.4 ± 0.5
P3b	51.6	2.18	51.5 ± 8.6	2.7 ± 0.5

The largest displacement (11.1 mm) with respect to the cadaver geometry is observed in the Rest condition H1b on both sides of the iliococcygeus muscle (see Figure 7.3B). In the Max IAP condition the largest displacement in caudal direction with respect to the Rest condition H1b (7.4 mm) is observed in H2b (see Figure 7.3D). In this condition, where the maximum pressure of all load-cases of 5.4 kPa takes place, the maximal displacement is observed in the connective tissue of the levator hiatus. In the Max ACT condition the largest displacement in cranial direction (6.5 mm) is observed in H3b (see Figure 7.3F). In this condition, where the activation of the muscle reach maximum of all load-cases (100%), the largest displacement is observed in both the iliococcygeus muscle and the connective tissue of the posterior part of the pelvic floor.

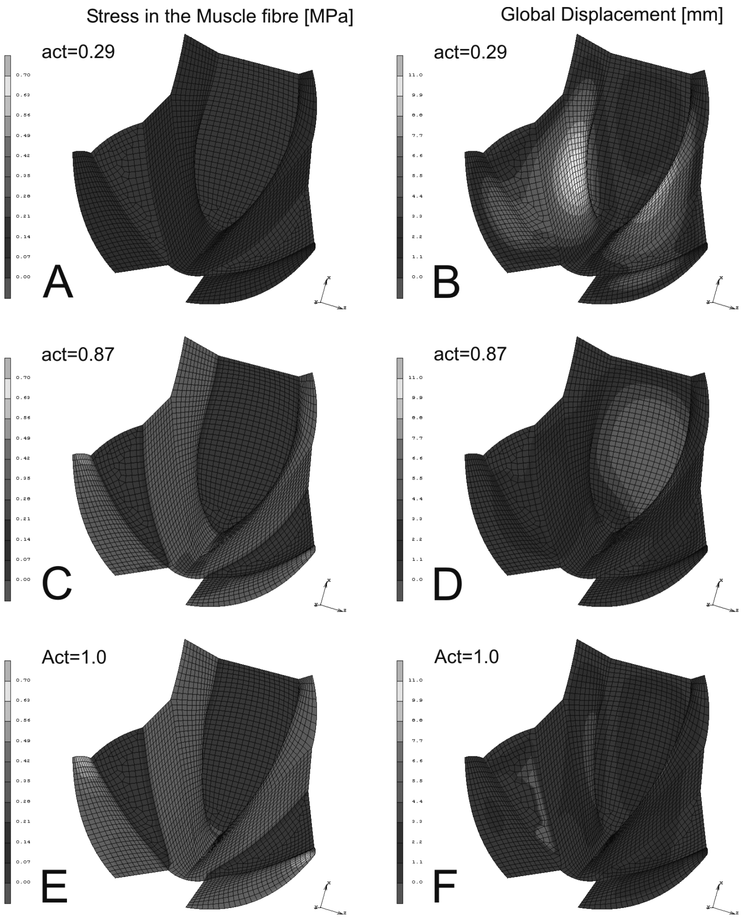

FIGURE 7.2: *Healthy subject muscle activation and stiff connective tissue during all three conditions (see also Table 7.2). Connective tissue I. is used in all displayed conditions. The stress in the muscle fibre direction in MPa is displayed in the left column, displacement in millimetres in the right column. Load-cases H1a (Images A and B), H2a (Images C and D) and H3a (Images E and F) are displayed for three different levels of the muscle activation (29% - Rest condition, 87% - Max IAP condition, and 100% - Max ACT condition). The stress in the connective tissue is zero since it is not an active tissue. The same scale is used for all three load-cases.*

The width W of the levator hiatus and the mean displacement of the muscle calculated in the model for all three conditions and compared to the experimental data from Chapter 4. The results are summarised in Table 7.3. The largest mean displacement (3.35 mm) is observed in H1b (Rest condition). The largest width W of the levator hiatus (56.5 mm) is observed in P2a (Max IAP condition).

7.4 DISCUSSION

The FE model developed in this study is designed specifically to study the fundamental biomechanical behaviour of the pelvic floor muscles. The quasi-static model consists of the pelvic floor muscles and connective tissue of the diaphragma pelvis. This simplification is sufficient to satisfy the main goals of this study. The other structures such as organs inside the pelvic floor and connections of these organs to the muscles are not included. The pelvic region is very complicated structure, where the support of the organs is maintained in three levels (i.e. hanging apparatus of the uterus etc.) as described by DeLancey 1992. The pelvic floor muscle is the only active structure in this region responsible for supporting the organs. Therefore, if the muscle is not active, the other structures (mostly passive collagen, connective and fat tissues) cannot fully support the internal organs and resist to the higher levels of IAP pushing the organs downward. The weight of the organs is incorporated in the hydrostatic pressure loading the pelvic floor. For the future studies, however, a more sophisticated model including internal organs might be necessary. Dynamics effects of moving organs might be included as well.

There are two main hypothesises concerning the development of the genital prolapse. Genital prolapse can occur due to compliant muscle (muscle pathology) or the degradation of the connective tissue (connective tissue pathology). In this study, 12 load-cases are analysed in order to confirm the hypothesis that the activation of the pelvic floor muscles play a crucial role in the pelvic floor support. Two types of connective tissue with different stiffness are tested in order to describe an effect of the influence of the passive connective tissue in the pelvic floor. The results from these analyses are validated using experimentally determined displacements from MRI measurements (Chapters 4 and 5) and EMG activity of the muscle (Chapter 4).

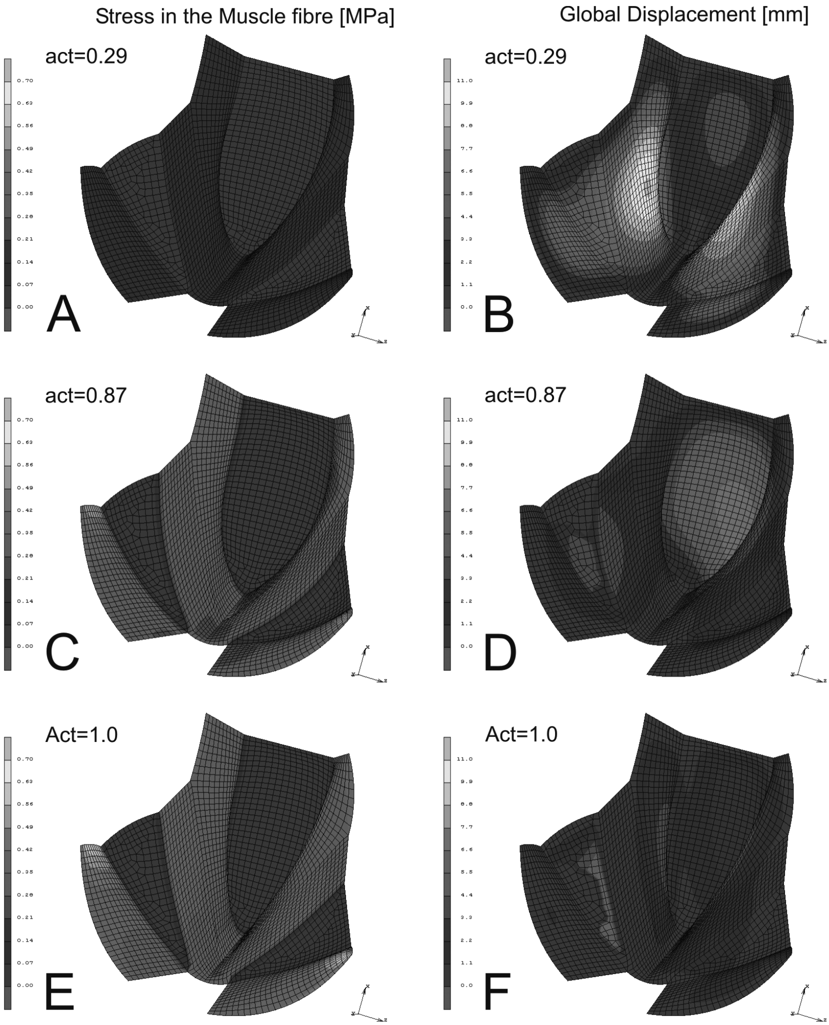

FIGURE 7.3: *Healthy subject muscle activation and a compliant connective tissue during all three conditions (see also Table 7.2). Connective tissue II. is used in all displayed conditions. Graphical results of the FE analysis of the pelvic floor muscles. The stress in the muscle fibre direction in MPa is displayed in the left column, displacement in millimetres in the right column. Load-cases H1b (Images A and B), H2b (Images C and D) and H3b (Images E and F) are displayed for three different levels of the muscle activation (29% - Rest condition, 87% - Max IAP condition, and 100% - Max ACT condition). The stress in the connective tissue is zero since it is not an active tissue. The same scale is used for all three load-cases.*

7.4.1 LOAD-CASES ANALYSIS

The FE model is validated using the data of healthy subjects (load-cases H1a, H2a and H3a). In order to provide a good prediction for patients, following adjustments were performed: The muscle activation of a compliant muscle obtained from experimental measurements were utilised (load-cases P1a, P2a and P3a). Furthermore, the effect of the quality of the connective tissue of the diaphragma pelvis was tested utilizing two types of this tissue with the difference in stiffness. This represents the strong and compliant connective tissue. The quality of the connective tissue was tested for both healthy and patient muscle activation (load-cases H1b, H2b, H3b, P1b, P2b and P3b). These adjustments are necessary to understand the effects of the muscle activation and connective tissue influence to the behaviour of the pelvic floor muscles and to the mechanism of the development of genital prolapse.

The stress in the muscle fibre reached the equilibrium level with respect to the level of activation in all loading cases (see Figures 7.2 to 7.5). However, there are some spots with higher stress than the maximal stress in the muscle fibre. These artefacts are caused due to constant thickness of element and disappear if constant cross-section area of the muscle is considered (Chapter 6). The active stress distribution in the muscles depends on the active as well as passive muscle material properties, level of the muscle activation and level of the loading pressure. It is not affected by the material properties of the connective tissue (see Figures 7.2 to 7.5 - for example, there is no difference in the stress in the muscle fibre between H1a and H1b, H2a and H2b etc.).

The largest displacement of the muscle in all load-cases with respect to the cadaver geometry (without the muscle tone) is observed in the Rest condition on both sides of the iliococcygeus muscle (see Figures 7.2B to 7.5B). In these load-cases, the activation of the muscle is 29% (in H1a, H1b) and 23% (in P1a, P1b) and the loading pressure is low or approaching zero (see Table 7.2). The main loading in the rest position is due to the muscle activation. Therefore, the largest displacement is observed in the anterior part of the muscle tissue on both sides of the pelvic floor. This is in agreement with the clinical observations using the MRI scanner (Chapter 4). In the simulated rest position the muscle position is reconstructed to the in vivo situation by imposing the appropriate level of muscle activation. There is a difference in the pelvic floor topology between the cadaver and the living subject. Loss of muscle tone after death was addressed by studying some cadavers during the phase of rigor mortis (DeLancey, 1999).

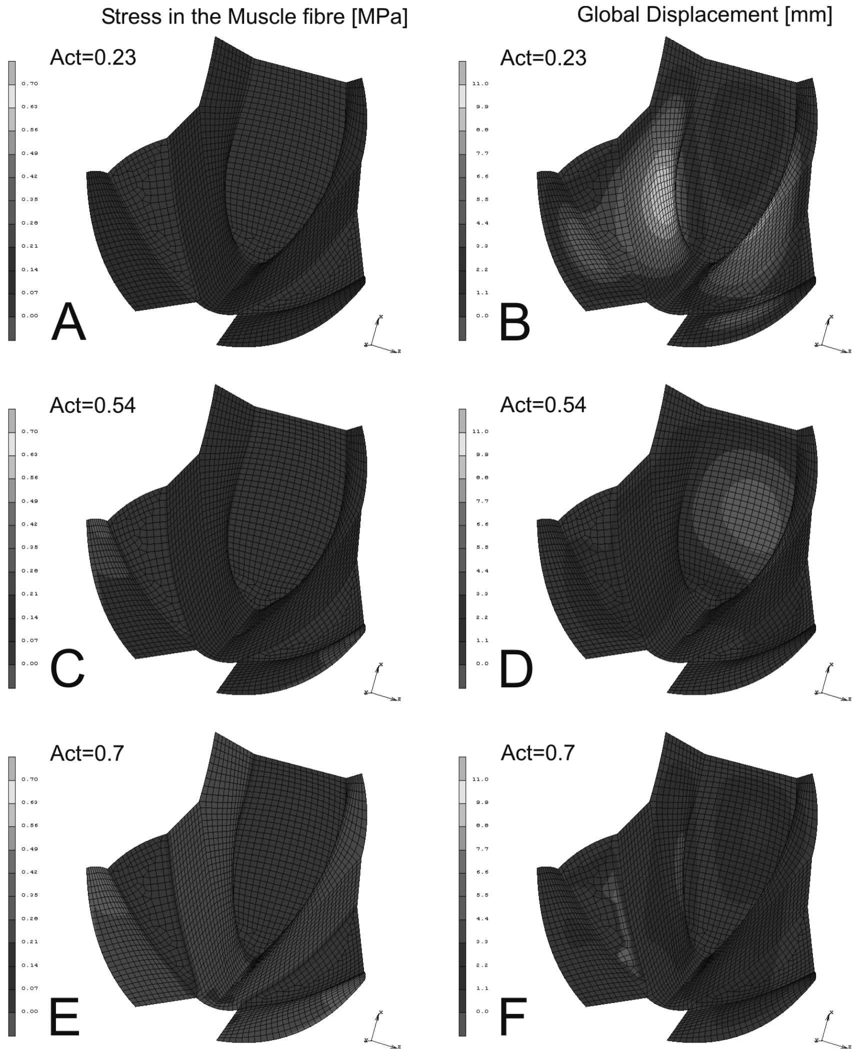

FIGURE 7.4: *Patient muscle activation and strong connective tissue during all three conditions (see also Table 7.2). Connective tissue I. is used in all displayed conditions. The stress in the muscle fibre direction in MPa is displayed in the left column, displacement in millimetres in the right column. Load-cases P1a (Images A and B), P2a (Images C and D) and P3a (Images E and F) are displayed for three different levels of the muscle activation (23% - Rest condition, 54% - Max IAP condition, and 70% - Max ACT condition). The stress in the connective tissue is zero since it is not an active tissue. The same scale is used for all three load-cases.*

In the Max IAP condition, the largest displacement with respect to the rest position is observed in H2b (see Figure 7.3D). In this condition, the pelvic floor is loaded by maximum pressure of all load-cases (5.4 kPa). The maximal displacement in all load-cases in this condition (H2a, H2b, P2a and P2b) is observed in the connective tissue of the levator hiatus. The pelvic floor is loaded by high pressure while the muscle activation is 54% up to 87% (see Table 7.2). The displacement of the connective tissue parts depends only on the passive material properties. Increasing pressure loading the pelvic floor generates increasing displacement of the connective tissue of the levator hiatus. The decreasing stiffness of the connective tissue (stiff vs. compliant connective tissue) results in the larger anterior displacement in this region (see Figures 7.2D, 7.3D, 7.4D and 7.5D). The quality of the connective tissue has an influence on the anterior part of the diaphragma pelvis, foremost on the levator hiatus tissue. The larger displacement of the connective tissue affects the displacement of the muscle parts, primarily in the transverse direction. However, there is not a significant difference in the mean displacement of the muscle in load-cases H2b and P2b with respect to H2a and P2a (see Table 7.3). This difference is however very small. This effect is observed in all conditions during all load-cases.

In the Max ACT condition, the largest displacement is observed in H3b (see Figure 7.3F). In this condition, where the activation of the muscle reach maximum of all load-cases - 100%, the largest displacement is observed in both the iliococcygeus muscle and the connective tissue of the posterior part of the diaphragma pelvis.

In the muscle parts, the displacement is in relation with the muscle activation. Considering the constant level of IAP it can be stated that, when the muscle activation is increasing the muscle is moving upwards (Figures 7.2 to 7.5). The global displacement is however also depending on the pressure loading the pelvic floor. If the pressure is increasing, the displacement is decreasing (the muscle is moving downwards thus in opposite direction to the direction of the muscle contraction). The levator hiatus is closing with increasing activation of the muscle tissue (see Figure 7.5B, D and F). This is in agreement with the clinical observations. The muscle is the only active component in the pelvic floor. Therefore, the displacement of the muscle, particularly in the anterior part of the levator ani muscle plays obviously a crucial role in the support of the organs in the pelvic floor. The opening and closing of the levator hiatus is dependent on the activation of the muscle. When the activation is decreasing, the width of the levator hiatus is increasing and vice versa.

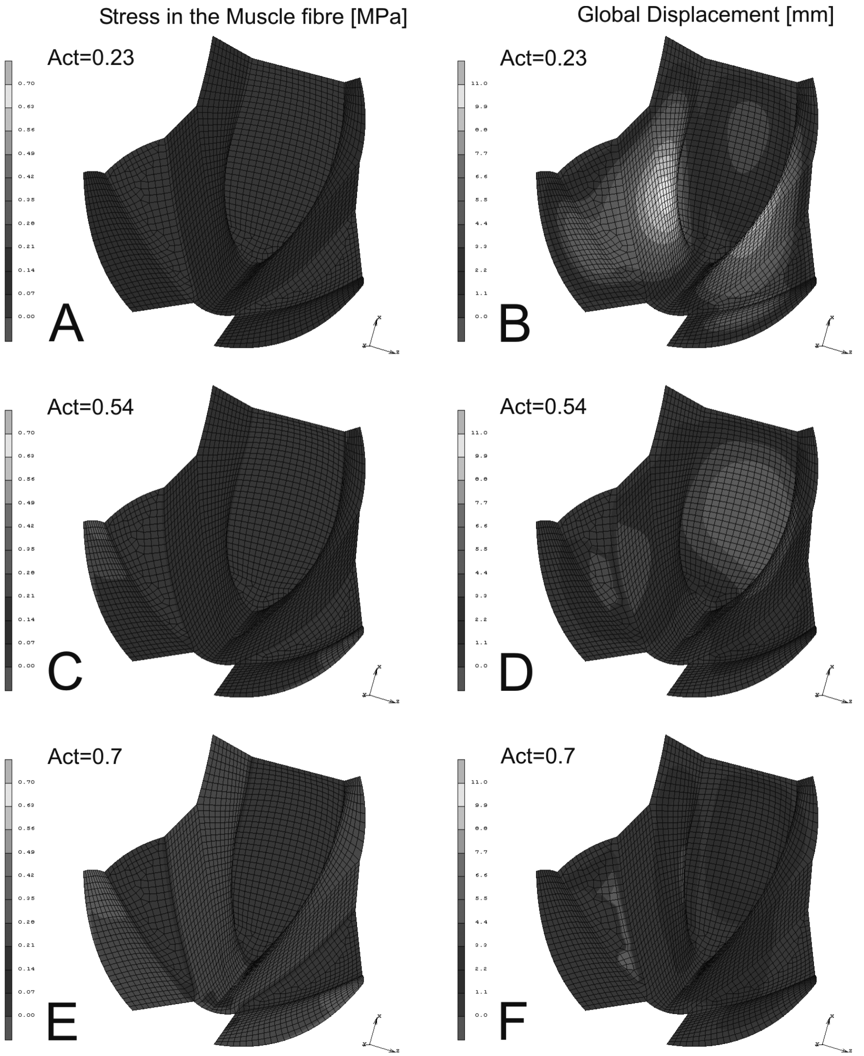

FIGURE 7.5: *Patient muscle activation and compliant connective tissue during all three conditions (see also Table 7.2). Connective tissue II. is used in all displayed conditions. The stress in the muscle fibre direction in MPa is displayed in the left column, displacement in millimetres in the right column. Load-cases P1b (Images A and B), P2b (Images C and D) and P3b (Images E and F) are displayed for three different levels of the muscle activation (23% - Rest condition, 54% - Max IAP condition, and 70% - Max ACT condition). The stress in the connective tissue is zero since it is not an active tissue. The same scale is used for all three load-cases.*

In Chapter 4 it was concluded that there is no significant difference in the displacement in relation to the IAP but there is a larger width of the levator hiatus in the group of patients with cystocele. The width W of the levator hiatus and the mean displacement with respect to the rest condition of the pelvic floor muscles are determined for all load-cases and validated using the experimental data obtained from Chapter 4. These are the only parameters obtained in vivo using the MRI data. Experimental data were obtained only for H1a, H2a, H3a, P1a, P2a and P3a (see Table 7.3 and Chapter 4).

The width W corresponds very good with the experimental measurements in all load-cases (if data available) except H1a (see Table 7.3). In the H1a, the width W calculated by FE model is larger than measured in Chapter 4. This effect can be caused by the stiffness of the connective tissue of the levator hiatus in the FE model. The results of simulations H1a vs. H1b, H2a vs. H2b, H3a vs. H3b, P1a vs. P1b, P2a vs. P2b and P3a vs. P3b show no significant difference in the width of the levator hiatus associated to the quality of the connective tissue (stiff vs. compliant tissue). Therefore, the stiffness of the connective tissue has not a significant effect on the width of the levator hiatus. It only has a small influence on the displacement of the connective tissue of the levator hiatus. The IAP loading the pelvic floor and the weight of the internal organs play a role in this case. Stiffness of the connective tissue plays a minor role in the support of the organs in the pelvic floor.

The mean displacement of the pelvic floor muscles is summarised in Table 7.3 and compared with the data from Chapter 4. Experimental data were obtained only for H2a, H3a, P2a, P3a, P2b and P3b (see Table 7.3 and Chapter 4). The displacement in all load-cases is in a good agreement with the experimental measurements. In the H1a, H1b, P1a and P1b, the mean displacement is calculated with respect to the fully relaxed muscle, which lost the tone (cadaver geometry). This condition is not determined in experimental data (Chapter 4) and cannot be validated.

7.4.2 CLINICAL QUESTIONS

The main goal of this study is to understand the development of the genital prolapse and to answer the questions arose from previous studies (e.g. Chapter 4):

Question 1) What is the effect on the width of the levator hiatus if the muscle is insufficiently activated?

Answer: Revising the results of the simulations, we can directly compare the load-cases H1a vs. P1a, H2a vs. P2a and H3a vs. P3a, where the muscle is activated either as a healthy or patient (decreased muscle activation, and/or muscle atrophy). The width of the levator hiatus in P1a, P2a and P3a is always larger than in comparable condition H1a, H2a and H3a. The opening and closing of the levator hiatus depends primarily on the activation of the muscle and the pressure loading the pelvic floor. When the activation is decreasing, the width of the levator hiatus is increasing and vice versa. In max IAP condition if the pressure is increasing (e.g. during coughing, sneezing) the width of the levator hiatus is increasing as well. The behaviour of the levator hiatus (opening and closing) depends particularly on the anterior part of the levator ani muscle. The muscle is the only active component in the pelvic floor. Therefore, the muscle activation, particularly in the anterior part of the levator ani muscle plays obviously a crucial role in the support of the organs in the pelvic floor. Any lack of the organ support can lead to the development of pelvic floor diseases particularly to the genital prolapse. This leads to the conclusion, that decreasing muscle activation leads to the increasing width of the levator hiatus, which is associated with genital prolapse.

Question 2) What is the effect on width of the levator hiatus if the connective tissue in the levator hiatus is more compliant than normal?

Answer: To answer this question, the results of following simulations are discussed: H1a vs. H1b, H2a vs. H2b, H3a vs. H3b, P1a vs. P1b, P2a vs. P2b and P3a vs. P3b. The results show no significant difference in the width of the levator hiatus associated to the quality of the connective tissue (stiff vs. compliant tissue). Therefore, the stiffness of the connective tissue has a minor effect on the width of the levator hiatus. It only has a small influence on the displacement of the connective tissue of the levator hiatus. It also slightly affects the displacement of the pelvic floor muscle. The IAP loading the pelvic floor and the weight of the internal organs play a role in this case. Stiffness of the connective tissue plays a minor role in the support of the organs in the pelvic floor. It can be concluded, that the quality of the connective tissue of the levator hiatus has not a significant effect on the width of hiatus, which is associated with genital prolapse.

<u>And finally clinical questions arise:</u>
Question 3) Is muscle training effective if there is a problem in connective tissue of the levator hiatus?

Answer: In Question 2 it was concluded, that the quality of the connective tissue of the levator hiatus has not a significant effect on the width of hiatus, therefore has not a significant effect on the development of genital prolapse. If there is a problem in connective tissue of the levator hiatus, only the muscle provides the support of the pelvic floor organs. The muscle training can improve the condition of the muscle tissue. It can be concluded, that the muscle training is efficient since the muscle plays a crucial role in pelvic organ support. This conclusion is based on the results from following load-cases: H1b vs. P1b, H2b vs. P2b, and H3b vs. P3b.

Question 4) On what spot in the diaphragma pelvis the surgeon has to focus on during reconstructive surgery if:

a)The muscle activation is insufficient (the muscle is not able to generate enough force) and the connective tissue has a normal compliancy;

b) The muscle activation is normal (muscle is able to generate enough force) but the connective tissue of the levator hiatus is more compliant?

Answer 4a: Revising the results of load-cases P1a, P2a and P3a, where the muscle activation is lower than in healthy subjects (H1a, H2a and H3a) and the strong connective tissue is utilised, we can state, that the decreased muscle activation leads to the increasing width of the levator hiatus, which is associated with the development of genital prolapse. Muscle activation is a major factor responsible for the enlargement of the levator hiatus. Therefore, the surgeon has to focus on the levator hiatus width, which should be reduced in order to minimize the development of the genital prolapse. If the muscle cannot maintain the pelvic organ support, the surgical intervention is necessary. The organs inside the pelvic floor should be kept in place by use of a surgical procedure. The way to resolve this problem is a use of the mesh prosthesis, which can improve the support of the pelvic floor organs. Recent prostheses used for genital prolapse repair are very stiff and provide very poor results, since the whole pelvic floor is a dynamic system. Design of new biomaterial prostheses for surgical repair of the genital prolapse can be based on predictions of the FE model. The shape, design and proper placing in the pelvic floor should be optimised using the computer model.

Answer 4b: Revising the results of load-cases H1b, H2b and H3b, where the muscle activation is normal (corresponding to activation recorded in healthy subjects) but the compliant connective tissue of the levator hiatus is utilised, we can state, that the quality of the connective tissue of the levator hiatus has not a significant effect on the width of hiatus, therefore has not a significant effect on the development of genital prolapse. The surgeon has to focus on the levator ani muscle, in order to improve the muscle function. The muscle is responsible for support of the pelvic floor organs. A good quality of the muscle minimizes dispositions to the development of the genital prolapse. The muscle training can improve the quality and function of the muscle tissue. In the future, the effect of training should be evaluated as a part of the development of an optimal handling of patients with pelvic floor complaints and diseases.

7.5 Conclusion

Decreasing muscle activation leads to the increasing width of the levator hiatus, which is associated with the development of genital prolapse.

The compliance of the connective tissue of the levator hiatus has not a significant effect on the width of hiatus, therefore has not a significant effect on the development of genital prolapse.

The muscle strengthening is efficient since the muscle plays a crucial role in pelvic organ support.

Muscle activation is a major factor responsible for the enlargement of the levator hiatus. Therefore, the surgeon has to focus on the levator hiatus width, which should be reduced by use of mesh prosthesis in order to minimize the development of the genital prolapse. Design of a new biomaterial mesh prostheses for surgical repair of the genital prolapse can be based on predictions of the FE model.

A good quality of the muscle minimizes dispositions to the development of the genital prolapse even if there is a problem related to the compliant connective tissue of levator hiatus. The muscle training can improve the quality and function of the muscle tissue.

References

Berglas, B., Rubin, I.C., 1953. Study of the supportive structures of the uterus by levator myography. Surg Gynecol Obstet. 97: 677-692.

DeLancey J.O.L., 1992. Anatomic aspects of vaginal eversion after hysterectomy. Am J Obstet Gynecol. 166: 1717-28.

DeLancey, J.O.L., Hurd, W.W., 1998. Size of the Urogenital Hiatus in the Levator Ani Muscles in Normal Women and Women With Pelvic Organ Prolapse. Obstet Gynecol. 91: 364-368.

DeLancey, J.O.L., 1999. Structural anatomy of the posterior pelvic compartment as it relates to rectocele. Am J Obstet Gynecol. Vol 180, No.4, 815-823.

Halban, J., Tandler, J., 1907. Anatomie und atiologie der genital prolapse beim weibe. Wilhelm Braunmuller.

Hoyte, L., Schierlitz, L., Zou, K., Flesh, G., Fielding, J.R., 2001. Two- and 3-dimensional MRI comparison of levator ani structure, volume, and integrity in women with stress incontinence and prolapse. Am J Obstet Gynecol. 185, 11-19.

Hurt, W.G., 1997. Anterior colporrhaphy. In: Gershenson D, edior. Operative techniques in gynecologic surgery. Philadelphia: WB Saunders (vol 2).

Janda, S., Van der Helm, F.C.T., de Blok, S.B, 2003: Measuring morphological parameters of the pelvic floor for FE modelling purposes. Journal of Biomechanics, 36/6, 749-757.

Mooney, M., 1940. A theory of large elastic deformation. Journal of Applied Physics 11, 582-591.

Olsen, A.L., Smith, V.J., Bergstorm, J.O., Colling, J.C., Clark, A.L., 1997. Epidemiology of surgically managed pelvic organ prolapse and urinary incontinence. Obstet Gynecol. 89, 501-506.

Richardson, A.C., Lyon, J.B., Williams, N.E., 1976. A new look at pelvic relaxation. Am J Obstet Gynecol, 126, 568-573.

Shull, B.L., Benn, S.J., Kuehl, T.J., 1994. Surgical management of prolapse of the anterior vaginal segment: an analysis of support defects, operative morbidity, and anatomic outcome. Am J Obstet Gynecol. 171, 1429-1439.

Chapter 8

GENERAL DISCUSSION AND FI-NAL CONCLUSIONS

8.1 Goal and the approach of the thesis

The presented study was motivated by the two main goals described in the first chapter. The first research goal of the thesis was to understand the complex biomechanical behaviour of the pelvic floor muscles. The second goal was to study the mechanism of the pelvic organ prolapse (genital prolapse). In the previous chapters separate elements contributing to these goals were discussed and separate conclusions were presented. In this General discussion and final conclusions chapter, the two main goals will be discussed with respect to the validity of the mathematical model based on the finite-element (FE) theory used for studying the biomechanical behaviour of the pelvic floor, the mechanism of the pelvic organ prolapse, the fundamental principle of the behaviour of the pelvic floor muscles and the validity of the experimental data.

The FE model is presented in Chapters 6 and 7. The experimental data concerning the pelvic floor morphology (Chapter 2), muscle properties (Chapter 3) and loading data (Chapters 4 and 5) are necessary as well as boundary condition as an input for FE analysis (Chapters 6 and 7). The displacement and the forces in diaphragma pelvis are calculated in Chapters 6 and 7. By means of this model, the biomechanical behaviour of the pelvic floor, the understanding of the development of the genital prolapse and the fundamental clinical questions, which arose from previous studies, are discussed.

The model is able to simulate several pathological conditions such as changes in loading, activation of the levator ani muscle and the development of the pelvic organ prolapse. Results of the analyses were validated using from magnetic resonance imaging (MRI) and electromyography (EMG) data obtained from experimental measurements performed on healthy volunteers as well as on patients (Chapters 4 and 5). The strength of the FE model is the potential to predict the effect of surgical interventions and give insight into the function of pelvic floor muscles.

8.2 Final inspection of the goals

The pelvic floor in humans is a very complex muscular structure. It is largely responsible for supporting both pelvic and abdominal organs and acts synergistically with the striated muscle of the anterior abdominal wall to generate the intra-abdominal pressure (IAP). It is hypothesized that if the levator ani is pathologically weakened or temporarily inactivated, or the connective tissue of the pelvic floor is not able to maintain support of the organs, a genital prolapse can occur. Genital prolapse is a major cause of morbidity in women.

Although the major attention is on the pelvic floor compartment and the pelvic floor pathology, the behaviour of the diaphragma pelvis was not yet understood. The major problem is the complexity of the pelvic floor caused by the complex 3D shape of the pelvic floor, the relation between active muscle tissue and connective tissue, the complex loading by the IAP and organs acting perpendicularly to the muscle fibres etc. It was expected that the pelvic floor muscles have a fundamental influence in disorders like genital prolapse.

The main loading of the pelvic floor muscles is due to IAP and the weight of the internal organs. Muscles in joint systems (e.g. in the upper or lower extremities) are activated to exert forces at the bones in line with their muscle line of action. In contrast, the pelvic floor muscles are loaded perpendicular to the muscle line of action by the IAP. A simple representation of the muscle action by a (one-dimensional) muscle line of action is not appropriate, but a more sophisticated approach using a FE model of the muscle is necessary. In a FE model the relationship between the loading and muscle forces in three dimensions can be represented. The model is able to predict the position of the pelvic floor depending on the load (e.g. IAP) and activation of the muscles and to answer clinical questions resulting from previous studies during the research work on this study.

The model is able to give us the insight to the fundamental behaviour of the diaphragma pelvis (pelvic floor muscles and connective tissue). The factors (compliant muscle and connective tissue) contributing to the development of the genital prolapse were described in Chapter 7, based on the simulations of the several load-cases arose from observation from the experimental measurements performed on healthy volunteers and patients. The results from FE simulations were validated using the MRI and EMG data of healthy subjects obtained during three conditions (rest, max IAP and max activation (ACT) of the pelvic floor muscles) described in Chapters 4 and 5.

During the development of the computer model, several lacks of the necessary model parameters came out. Particularly, the complete geometry of the pelvic floor was not exactly determined (i.e. direction of the muscle fibres, muscle fibre length etc.), the material parameters of the muscle (foremost passive as well as active material properties) were unknown. The loading of the diaphragma pelvis during several specified conditions (i.e. rest, performing maximal IAP and performing maximal activation) in both supine and erect position and the effect of loading of the pelvic floor by the weight of the internal organs were unknown, or not exactly determined. The loading of the diaphragma pelvis is used as an input for the model. The displacement and stress distribution of the pelvic diaphragma is the output of the model. Determining all these parameters are described in the particular studies (Chapters 2 to 5). These were mostly designed to uncover missing data and knowledge with the main focus on the input and validation of the FE model. However, they separately describe, with their limitations, the particular topic as mentioned above.

The main conclusions are separately described in every single chapter and summarised in Section 8.3 on page 154. The limitations are discussed in Section 8.4 on page 158 and the future directions are discussed in Section 8.5 on page 165.

8.3 Conclusions

Discussing the results of this thesis it is concluded, that:

- Decreasing muscle activation leads to the increasing width of the levator hiatus, which is associated with the development of genital prolapse.
- The compliance of the connective tissue of the levator hiatus has not a significant effect on the width of hiatus, therefore has not a significant effect on the development of genital prolapse.
- The muscle strengthening is efficient since the muscle plays a crucial role in pelvic organ support.
- Muscle activation is a major factor responsible for the enlargement of the levator hiatus. Therefore, the surgeon has to focus on the levator hiatus width, which should be reduced by use of mesh prosthesis in order to minimize the development of genital prolapse. Design of a new biomaterial mesh prostheses for surgical repair of the genital prolapse can be based on predictions of the FE model.
- A good quality of the muscle minimizes dispositions to the development of genital prolapse even if there is a problem related to the compliant connective tissue of levator hiatus. The muscle training can improve the quality and function of the muscle tissue.
- Increased muscle activation resulted in an upward motion (dome shape) of the pelvic floor. Increased IAP (e.g. due to simultaneous activation of the abdominal and pelvic floor muscles) resulted in a downward motion of the pelvic floor (basin shape).
- The results of the FE simulations are in a good agreement with the experimental measurements for healthy subjects as well as for patients.
- The muscle tissue as the only active component in the pelvic floor plays a major role in the support of the organs in the pelvic floor.

- The model can be used for further studying of the function of the pelvic floor and for understanding the substance of disease such as genital prolapse.

8.3.1 CONCLUSIONS: GOAL BY GOAL

The goal of ***Chapter 2*** ("Measuring morphological parameters of the pelvic floor for FE modelling purposes") was to obtain a complete data set needed for studying the complex biomechanical behaviour of the pelvic floor muscles using a computer model based on the FE theory.
<u>It is concluded, that:</u>

- The produced data set is not only important for biomechanical modelling of the pelvic floor muscles and to investigate the effectiveness of the reconstructive surgery, but it also describes the geometry of muscle fibres that is useful for functional analysis of the pelvic floor in general.
- In the cadaver study data were obtained about the muscle fiber direction and optimal fiber length. These data are indispensable for developing a FE model, but can not be obtained in an MRI study.
- By the use of many reference landmarks (e.g. spina iliaca anterior superior, symphysis pubica, promontorium, os coccygeus etc.) all these morphological data concerning fibre directions and optimal fibre length can be morphed onto the geometrical data based on segmentation from MRI scans.

The goal of ***Chapter 3*** ("A constitutive model for the passive elastic behaviour of human pelvic floor muscles") was to derive passive material parameters of the pelvic floor muscles.
<u>It is concluded, that:</u>

- The produced data set describes the passive elastic material properties of the pelvic diaphragm. The constitutive model based on these data is necessary for building a mathematical model based on FE theory.
- Material properties of the muscle in the fibre direction are greatly affected by rigor mortis. Therefore, passive muscle properties can only be determined in transverse direction. The passive material properties in the muscle fibre direction can be derived from transverse direction data. Active muscle properties must be derived using a muscle model relating activation and muscle length.
- The presented elastic constants in a Mooney-Rivlin Third Order Deformation Model, describing the non-linear passive elastic behaviour of the

pelvic floor muscles, represent a good fit of the experimental data. A bi-axial material model is necessary for a thin layer like the pelvic floor.

The goal of ***Chapter 4*** ("Pelvic floor muscle displacement in relation to the level of the intra-abdominal pressure and muscle activation) was to analyse the behaviour of the pelvic floor in patients and healthy volunteers.
<u>It is concluded, that:</u>

- The presented results demonstrate: 1) significantly lower muscle activation (EMG activity) in the patient group; 2) no difference in the mean displacement in relation to the level of IAP; 3) No significant difference was found in the level of the IAP between both groups. 4) Larger width W of the levator hiatus in group of patients with cystocele but no difference in the depth D of the levator hiatus.
- The level of IAP is also determined by the abdominal muscles, and is equal for patients and healthy subjects. The increased width of the levator hiatus might be the result of the reduced muscle activation, or of more compliant connective tissue.
- Performing MRI scanning in the rest and during holding the maximal level of the IAP provides the best information about the position and the displacement of the pelvic floor muscles. The combination of EMG, IAP and the width W of levator hiatus in these two conditions can be used for diagnostic purposes.

The goal of ***Chapter 5*** ("Loading effect of the weight of the internal organs on the pelvic floor in erect and supine positions") was to investigate the effect of the loading of the pelvic floor due to the weight of the internal organs in the erect and supine positions.
<u>It is concluded, that:</u>

- A highly significant effect in the position of the diaphragma pelvis was found between the erect and supine position. It is obviously caused due to the weight of internal organs.
- Present clinical MRI evaluation of the pelvic floor muscles performed on patients in the supine position cannot provide the correct information about the functional behaviour of the pelvic floor, since it is not loaded.
- Performing MRI scanning in supine position during holding the maximal level of the IAP provides diagnostic information about the position and the displacement of the pelvic floor muscles.

The goal of ***Chapter 6*** ("A finite element model of human pelvic floor muscles") was to understand the biomechanical behaviour of the pelvic floor muscles.

<u>It is concluded that:</u>

- The relation between input variables: loading (by IAP etc.) and muscle activation and output variables: displacement of the pelvic floor muscles was iteratively determined by FE model. This relation describes the biomechanical behaviour of the pelvic floor.
- The results of the FE simulations (Width of the levator hiatus and displacement of the muscle) are in good agreement with experimentally determined values on healthy subjects in parenthesis: Width [mm] in rest: 39.4 (34 ± 3.6), max IAP: 47.6 (47 ± 7.5) and max ACT: 42.4 (41.9 ± 6.1); the displacement [mm] in rest: 3.28 (not determined), max IAP: 2.8 (3.2 ± 0.4) and max ACT: 2.32 (2.8 ± 0.5).
- The model can be used for further studying of the function of the pelvic floor and for understanding the substance of disease such as genital prolapse.

The goal of ***Chapter 7*** ("Biomechanical analysis of the pelvic floor musculature") was to understand the development of the genital prolapse and to answer the questions resulting from previous studies.

<u>It is concluded that:</u>

- Decreasing muscle activation leads to the increasing width of the levator hiatus, which is associated with the development of genital prolapse.
- The compliance of the connective tissue of the levator hiatus has not a significant effect on the width of hiatus, therefore has not a significant effect on the development of genital prolapse.
- The muscle strengthening is efficient since the muscle plays a crucial role in pelvic organ support.
- Muscle activation is a major factor responsible for the enlargement of the levator hiatus. Therefore, the surgeon has to focus on the levator hiatus width, which should be reduced by use of mesh prosthesis in order to minimize the development of the genital prolapse. Design of a new biomaterial mesh prostheses for surgical repair of the genital prolapse can be based on predictions of the FE model.
- A good quality of the muscle minimizes dispositions to the development of the genital prolapse even if there is a problem related to the compliant connective tissue of levator hiatus. The muscle training can improve the quality and function of the muscle tissue.

8.4 Limitations

8.4.1 Pelvic floor morphology

When a FE model is developed for a living patient or healthy subject, the only way to obtain morphological parameters is using MRI scans. However, important parameters like the optimum muscle length and fibre orientation cannot be obtained from MRI scans, and must be imported from a cadaver study. Therefore, it is important to enable a link between the present cadaver study and MRI studies. The bony landmarks enable the construction of a local co-ordinate system of the pelvis. MRI data were described with respect to this local co-ordinate system, as well as the geometrical and muscle data in this cadaver study. The similarity between the data sets was good.

In this thesis, the measurements were performed on only one cadaver specimen, which is relevant for purposes of FE modelling. A previous anatomical study (De Blok, 1982) showed that there is no significant inter-individual and intra-individual difference in pelvic floor morphology. However, additional cadaver studies focusing on pelvic floor morphology and also material properties are needed to demonstrate if the present data set is sufficient for a 'generic' model. Otherwise, new data acquisition methods must be developed to obtain e.g. optimum length and fibre orientation in vivo, in order to build patient-specific models.

The experimental measurement of the pelvic floor structures was performed in a specimen fixed by injection embalming. These specimens are known to exhibit distorted spatial relationships (Richter, 1966) and these topographic relationships do not correspond to the data available from living women. After embalming, the m. levator ani, as well as the sphincter muscles (e.g. m. sphincter ani externus and m. sphincter ani internus) lose their tone (Figure 8.1A and B). All internal organs and structures move downwards, because they lack support by the pelvic diaphragma. In the biomechanical model based on the FE theory, the muscle position can be reconstructed by imposing the appropriate muscle tone.

The real geometry and architecture of the most muscles and connective tissues are highly complex. However, the muscles studied in this thesis were modelled only as flat shells with constant thickness. This represents a simplification of the real situation as the model in its present form make only limited use of the third dimension, despite the use of 3D elements. More realistic 3D geometry of the pelvic floor muscles is needed in order to improve the relevance of modelling the muscle function in vivo. Nevertheless, the results of the present FE model are in a good qualitative agreement with the experimental measurements suggesting that the principles of muscle modelling were taken into account adequately.

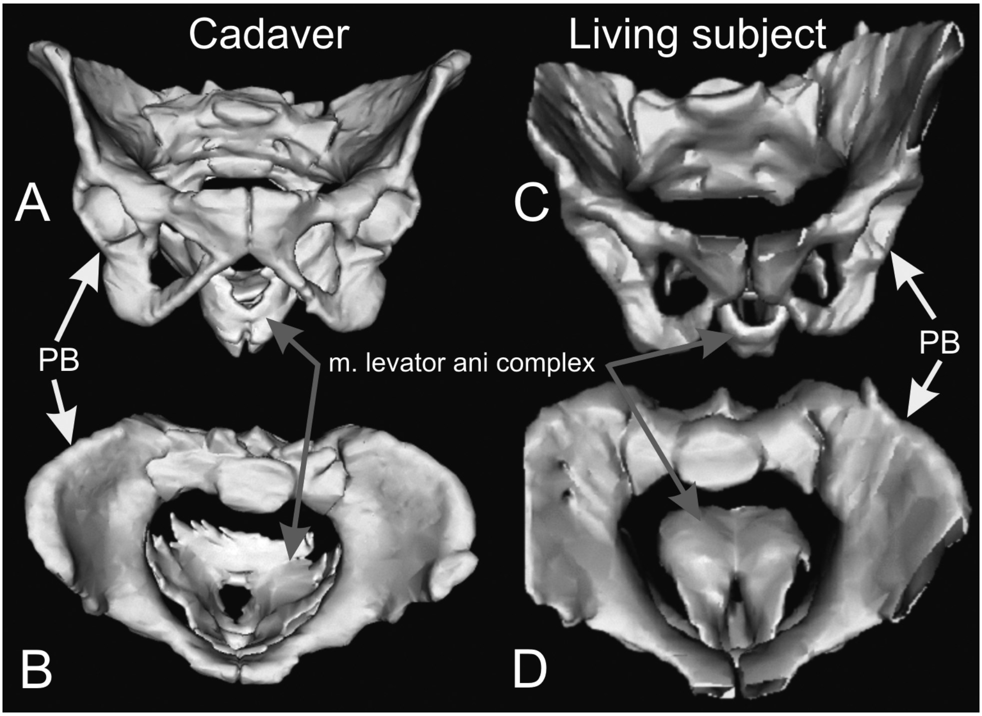

FIGURE 8.1: *The 3D reconstruction of the pelvic bone (PB) and m. levator ani complex using experimental data from the MRI, for a cadaver (A and B) and the rest position of a healthy subject (C and D). It can be seen that in the cadaver geometry the loss of muscle tone results in a basin shape, whereas in the subject even a slight muscle tone results in a dome shape in the rest position. The cadaver geometry - basin shape (specimen from Chapter 2) on the left side: **A** - frontal view, **B** - top view. The living subject - the dome shape (subject No.: 1 from Chapter 4) on the right side. **C** - frontal view, **D** - top view.*

8.4.2 MATERIAL PROPERTIES OF THE MUSCLE

Continuum models based on FE theory are applied to study the mechanical behaviour and function of skeletal muscle. Biomechanical analysis of soft tissue requires quantification of their 3D material properties, i.e. stress-strain behaviour. This necessitates accurate determination of stresses and strains under multiaxial loading, since uniaxial data do not uniquely characterize 3D properties. However, multiaxial stress-strain data do not exist for the muscle tissue. The reasons for this include the complex geometry and composite nature of such tissue.

Our study was performed on three fresh cadaver specimens. This material is very difficult to obtain. The goal of this study was not to describe population specific properties of the pelvic floor muscle but to get a first estimate of the parameter values and the feasibility of the material model. Therefore, we considered, that for developing a constitutive model of these muscles three specimens should be sufficient. In the future work, more specimens should be tested and the inter-individual comparison will also be provided. The other limitation relates to the tissue testing itself. The specimens should be very fresh in order to minimize the effect of the rigor-mortis process, which can affect the mechanical properties (Chapter 3). The tissue testing should be performed at the body temperature rather than at the room temperature as performed in this thesis. For such testing, a more sophisticated laboratory equipment and set-up is needed than was at our disposal during the measurements. Avoiding all these limitations can lead to a more accurate data set. In addition, a large amount of specimens could describe population specific properties, which was not the goal of present thesis.

In this thesis, the Mooney-Rivlin Third Order Deformation (TOD) constitutive model was used for modelling the passive material parameters of the muscle and connective tissue. The benefit of such model is the ability to describe passive non-linear elastic material properties of the soft tissue. The disadvantage is its natural incompressibility and isotropy. The limitation due to isotropy was solved using a composite material with one orthotropic active muscle layer incorporated into two passive isotropic layers representing passive muscle properties (Chapter 6).

8.4.3 Loading of the pelvic floor

The main loading of the pelvic floor muscles is by the IAP and the weight of the internal organs (Chapters 4 and 5). In Chapter 5 it was concluded that the mean displacement of the pelvic floor is in relation with the IAP, which presents about two thirds of the loading, and with the weight of organs, which presents about one third of the load to the pelvic floor in erect position during maximal IAP. Only two thirds of the measured IAP is loading the pelvic floor in supine position, since the weight of the organs is not loading the pelvic floor. Unfortunately, the IAP could not be determined during these measurements, since we had no access to an optical catheter pressure sensor, which can be used within the MRI scanner and can quantitatively approve this conclusion.

The IAP was measured inside the rectum. If the intestine wall between abdomen and rectum is not tensed, the pressure in the rectum is equal to the IAP. The sensor was inserted well beyond the anal sphincters.

Muscles in joint systems (e.g. in the upper or lower extremities) are activated to exert forces at the bones in line with their muscle line of action. In contrast, the pelvic floor muscles are loaded perpendicular to the muscle line of action by the IAP. Therefore, IAP was modelled as a hydrostatical pressure loading the muscle elements perpendicular to the fibre direction. During the experimental measurements, the IAP was determined using an intra-rectal catheter placed in the rectum (approximately 4 cm). Before insertion, the pressure was set to zero, in order to calibrate the level of the IAP in relation to the atmospheric pressure. During rest, an IAP of 2.9 ± 1.3 kPa was recorded by the sensor. Since there was no muscle activity, the recorded IAP is presumably due to the internal organs pressing on the sensor in the rectum. However, in the supine position the organs are not loading the pelvic floor, which can be seen on MRI by the dome shape of the pelvic floor. Hence, it was concluded that in all supine IAP measurements, the weight of the organs should be subtracted from the recorded IAP, in order to derive the correct loading of the pelvic floor musculature.

In the experiments we could not record IAP and EMG in the MRI machine. Therefore we were limited to three experimental conditions, which we assumed to be repeatable inside and outside the MRI: Rest, maximal IAP and maximal activation without the IAP (by releasing the abdominal muscles). In the max IAP condition, one third of the load was estimated to be from the weight of the internal organs. In real-life supine conditions, the weight of the organs is likely to be the main loading source. However, extreme conditions like coughing were demonstrated to result in maximal IAP (Chapter 4).

8.4.4 EMG MEASUREMENTS

A two-channel perineal surface EMG was measured using a modular urodynamics system. The dual electrodes composed of two circular electrodes placed on one supporting fabric strip were used. These electrodes were placed lengthwise in ventral-dorsal direction approximately 1 cm anterior to the anus. Electrodes are placed on both left and right side of the perineum. The limitation of this type of measurements is a relatively large distance between the electrode and the muscle tissue. This space is usually filled with skin, subcutaneous fat and other connective tissues, which can vary between subject and cannot be exactly determined. It may affect the EMG measurements.

Since the space for placing electrodes is very limited, the local description of the activation of a particular muscle parts is impossible. The only way to solve this problem is a usage of needle electrodes. However, the placing of such electrodes into the muscle (thickness of about 3 mm) is very difficult and must be evaluated for example by ultrasound. Finally, the usage of needles during the experiment is an invasive method, which is not favourable for subjects (volunteers).

Surface EMG was found to be one of the best ways to measure activity of the levator ani muscle (Voorham-van der Zalm et al., 2004). The use of vaginal or rectal electrodes is not accurate enough since these electrodes measure sphincter activity and the activity of structures other than the levator ani muscle (Voorham-van der Zalm et al., 2004). The EMG data in microvolts were used for further analysis, since it is not possible to normalise the EMG signal e.g. with respect to maximal EMG and maximal force within this study. No proper maximal EMG could be obtained as reference, and there is not any absolute reference in the muscle strength. Max level of IAP cannot be used to determine the muscle activity and force.

8.4.5 MRI MEASUREMENTS

Several T1 and T2-weighted gradient-echo or fast spin-echo MRI sequences were performed in order to obtain the position of the pelvic floor muscles. The measurements were performed using various MRI scanners with magnetic field strength from 0.7 up to 1.5T. The special FONAR the Indomitable Stand-Up™ MRI scanner at the Positional MRI Centre, Woodend Hospital, Aberdeen, Scotland was used for scanning in both erect and supine position of the subject. The major limitation of the MRI measurements is a poor resolution (time factor) of the scans, especially during fast MRI sessions, when the session time is limited. In these sessions, only about seven slices were recorded within the time of 20s, which is insufficient for reconstruction of the local coordinate system.

Coronal slices are chosen since all muscle parts of the pelvic floor diaphragma are easily recognizable in this section, which is necessary for segmentation of the muscles. Pelvic floor organs are much better recognizable in sagittal sections, but these slices cannot be used for muscle segmentation. Visualizing the pelvic floor organs can more accurately indicate the severity of the prolapse. Obtaining both coronal and sagittal sections during one session will be beneficial for exact reconstruction of the pelvic floor and the organs.

3D reconstruction based on semi-automated gradient-oriented single line segmentation of the MRI scans was performed. Segmentation of a thin layer muscle tissue such as m. levator ani and m. coccygeus is very difficult and no automatic segmentation tool is available. An inner surface border of muscle is chosen since the diaphragma pelvis is a flat structure and the inner surface of the muscle is quite well recognisable. Certain level of skill is needed for segmenting such tissue.

Each subject was carefully instructed on how to perform all the experimental conditions. The subjects practised these conditions prior the measurements. However, the performance of these conditions cannot be measured, since only the position of the pelvic floor muscle was determined and not muscle activation and IAP. The only way to evaluate these effects is to measure the EMG activity of the muscle and IAP simultaneously with the MRI (Chapter 4). However, we were not able to measure EMG within an MRI scanner because of the strong magnetic field affecting all electronic and metallic devices. IAP can be accurately measured using optical pressure sensors connected by optical cables with the measuring device, which must be positioned outside the MRI scanner. Unfortunately, we did not have such a device during this experiment.

8.4.6 Finite element modelling

In order to understand a complex system, it is often useful to extract most of its essential features and use them to create a simplified representation like a model of the system. Simplifications have to be made in accordance with the goal of the modelling and the related limitations should be accounted for while interpreting the results. Such a model allows one to observe more closely the behaviour of the system and to make predictions regarding its performance under altered input conditions and different system parameters. Modelling is widely used in biomechanics (Prendergast, 1997). The attractiveness of modelling is that many research questions can be tested (heuristic purpose of a model) and the number of human experimental subjects can be limited. The great virtue of models is the heuristic purpose, besides predicting specific aspects of complex function. Another big advantage of a model is a freedom of the researcher to make the model as simple or as complex as his questions require or as detailed as the outcome require.

The FE modelling of the muscle mechanics has been successfully used (e.g. Huyghe et al., 1991; Vankan et al., 1998; Gielen, 1998; van der Linden, 1998; Yucesoy et al., 2002; Oomens et al., 2003). The advantage of the FE approach is the consideration of the muscle tissue as a continuum that accounts for material and geometrical non-linearity and its capability of studying mechanics of skeletal muscle under various conditions.

The FE model developed in this thesis was designed specifically to study the fundamental biomechanical behaviour of the pelvic floor muscles. The quasi-static model consists of the pelvic floor muscles and connective tissue of the diaphragma pelvis. This simplification is sufficient to satisfy the main goals of this study. The other structures such as organs inside the pelvic floor and connections of these organs to the muscles are not included. The hydrostatic pressure represents the weight of the internal organs and the IAP. The pelvic region is very complicated structure, where the support of the organs is maintained in three levels (i.e. hanging apparatus of the uterus etc.) as described by DeLancey (1992). The pelvic floor muscle is the only active structure in this region responsible for supporting the organs. Therefore, if the muscle is not active, the other structures (mostly passive collagen, connective and fat tissues) cannot fully support the internal organs and resist to the higher levels of IAP. For the future studies, however, a more sophisticated model including internal organs is necessary. Dynamics effect should be included as well.

8.4.7 Validation

Validation of any model is one of the most important issues. For this reason, the experimental measurements were performed in order to gather so far missing data. The data from these measurements (Chapters 2 to 5) were used for both input and validation of the FE model. We have determined the EMG activity of the muscle, IAP loading the pelvic floor and the displacement of the muscle using the MRI scanner (Chapter 4 and 5). Since we were not able to measure EMG and IAP within the MRI scanner the experiment (described in Chapter 4) was split into two parts. In the first part, the EMG and IAP were recorded simultaneously. MRI recordings were performed in the second part in the same conditions. An optical catheter pressure sensor could in the future record the IAP in the MRI machine, and verify that the IAP is equal in the two sessions. However, we did not have this device available during our study. Other limitations result from measuring only three repeatable conditions (rest, max IAP and max ACT see Chapters 4 and 5). The relatively long duration of these conditions (approximately 20s) can affect the precision of the measurements and quality of image acquisition. This can be solved using an optical pressure sensor and very fast MRI sequences (high quality MRI scanner with the high static magnetic field strength).

In the FE model the displacement of the pelvic floor muscles and the width of the levator hiatus were calculated. These results were validated with the MRI data obtained from experimental measurements on healthy subjects. The mean symmetric Hausdorff distance between the surfaces is used for quantifying the difference between all three conditions (rest, max IAP, max ACT) during MRI measurements. Using the mean distance value can suppress local effects, however, it is a reproducible method for calculating the difference between two corresponding surfaces. A relatively high standard deviation for average displacement was found in all three conditions. This is presumably caused due to the inter-individual differences. For diagnostic purposes, rest and max IAP conditions seem to be the most proper, since they can give us all necessary information about the position and displacement of the muscle. Width of the levator hiatus and displacement of the muscle are in a good agreement with experimentally determined values on healthy subjects in parenthesis: Width [mm] in rest: 39.4 (34 ± 3.6), max IAP: 47.6 (47 ± 7.5) and max ACT: 42.4 (41.9 ± 6.1); the displacement [mm] in rest: 3.28 (not determined), max IAP: 2.8 (3.2 ± 0.4) and max ACT: 2.32 (2.8 ± 0.5).

8.5 FUTURE DIRECTIONS

The main goal of a future project will be to obtain more knowledge concerning pelvic floor functional behaviour and the mechanisms of diseases in the pelvic floor in order to improve diagnostic and therapeutic tools and techniques. The aim is to investigate the dynamic biomechanical behaviour of the pelvic floor and to develop a new mesh prosthesis for surgical repair of the pelvic organ prolapse (genital prolapse). Novel surgical and conservative approaches based on detailed knowledge concerning several dysfunctional diseases of the pelvic floor will be developed using a computer model based on the FE theory and dynamic model incorporating muscle dynamics and reflexes.

In this thesis we developed a quasi-static FE model of the pelvic floor muscles based on cadaver measurements. However, the FE model is only a static model describing the relation between muscle forces and activation, stresses and strains. No dynamic properties and no control mechanisms are included.

8.5.1 DYNAMIC BIOMECHANICAL MODEL

For modelling the dynamic behaviour of the pelvic floor a more sophisticated computer model must be developed. Since the pelvic diaphragm is obviously a dynamic structure, as observed in this thesis using MRI, these dynamic effects must be described and imported into the computer model. There is no knowledge about the dynamic behaviour of the pelvic floor so far. Computer modelling based on accurate experimental data obtained from both cadaver and living subject studies is a very promising approach.

The pressure difference inside and outside the abdomen will be related to the force distribution within pelvic floor muscles. The pressure difference is directly related to the tensile forces and to the curvature in the abdominal and pelvic wall. The tensile forces will be higher in the muscle fibre direction than perpendicular to the fibre direction (transverse direction). If the tensile forces are higher, the curvature will be smaller. Hence, the largest curvatures in the pelvic floor (prolapse) will be noticed in the direction in which the smallest tensile forces are present. This will give an indication of possible weak spots, and might be noticed already on MRI scans. Tensile force in the fibre direction can be increased by muscle activation, which will. Tensile forces perpendicular to the fibre direction or in the connective tissue cannot be changed actively, and the curvature cannot be influenced. Knowledge of the fibre direction and accurate MRI measurements of the pelvic floor curvature in patients with a prolapse might give an indication if the prolapse is caused by muscle weakness (through insufficient activation or atrophy) or by increased compliance of the connective tissue.

Changes in IAP and the weight of internal organs e.g. through walking or running, will result in changes of muscle force, either through intrinsic muscle properties (muscle visco-elasticity) or through reflexive properties. Reflexes are the result of a closed-loop feedback system, in which the stretch and force of the muscle fibres is detected by muscle spindles and Golgi tendon organs, respectively. This information is fed back to the Central Nervous Systems, which will increase the muscle activation.

The function of an intact feedback system can only be measured by injecting perturbations into the system, and measure the response inside the system. At Delft University of Technology, a methodology has been developed to measure the contribution of intrinsic and reflexive muscle properties, and estimate the position, velocity and force feedback gains (Van der Helm et al., 2002). Thus far, the methodology has been applied to the human arm, wrist and ankle, and was used to e.g. determine reflex properties in patients with neurological disorders like Complex Regional Pain Syndrome, Parkinson's disease and Cerebrovascular Accident (Schouten et al., 2003). External force pertubations are exerted e.g. to the hand by a robotic manipulator. The hand force, hand position and EMG are being measured. Using advanced closed-loop identification algorithms (De Vlugt et al., 2003ab), transfer functions in the frequency domain from force to position, and from position to EMG can be determined. From these transfer functions, parameters like the muscle stiffness and viscosity, reflex gains (position, velocity and force) and reflex time-delays can be accurately estimated. The Variance-Accounted-For values of these models are typical in the order of 90%.

In the future project it should be attempted to apply the same methodology in order to distinguish the intrinsic and reflexive properties of the pelvic floor musculature. The subject will requested to maintain a certain IAP, and receives visual feedback about the magnitude. Force perturbations are imposed to the abdomen, resulting in pressure fluctuations. Simultaneously, the IAP, pelvic floor muscle EMG and the displacement of the pelvic floor (by ultrasound) will be recorded. Dynamic transfer functions will be fitted to the measurement data, and parameters determining the intrinsic and reflexive properties will be estimated.

In the arm experiments it was shown that the reflexes were modulated as a response to the frequency content of the perturbation (Van der Helm et al., 2002) or as a response to environmental conditions (change of external mass and viscosity). To our knowledge, no research group has ever measured the reflexes of the pelvic floor musculature in vivo, nor has been looking into the modulation. It will be a challenge to find experimental conditions in which the reflexes are modulated. In addition, it will be interesting to investigate the different dynamic and reflexive properties of the striated and smooth muscle fibres present in the pelvic floor musculature.

A new dynamic computer model in combination with the FE model should be developed. For such model, the basic morphological, material and reflex (dynamic) properties of the pelvic floor are necessary. The morphological and passive material data of the pelvic floor were already determined (Janda et al., 2003). The new experiments will be designed in order to obtain the dynamic biomechanical behaviour of the pelvic floor muscles. This will be necessary for improvement of training of the pelvic floor musculature and for development of new biomaterial prostheses.

8.5.2 NEW SURGICAL TREATMENTS

Recent prostheses used for genital prolapse repair are very stiff and provide very poor results, since the whole pelvic floor is dynamic system. Design of new biomaterial prostheses for surgical repair of the genital prolapse can be based on predictions of the FE model. The passive uniaxial as well as bi-axial material properties of the pelvic floor muscle were determined in this thesis. This data set describes the basis hyperelastic material behaviour of these muscles and will be used as an input for design of the suitable biomaterial used for mesh prosthesis. The shape, design and proper placing in the pelvic floor will be optimized using the computer model. The effects of the new surgical mesh prosthesis on the displacements of the pelvic floor will be developed and tested using the computer model. Ultimately, a new surgical technique might be developed in order to place such prostheses laparoscopically in order to benefit from the minimally invasive surgical techniques. The new instruments for placing such prosthesis need to be designed and tested using cadaver models.

Conservative therapies (e.g. training, bio-feedback training, electrostimulation) are widely used in clinical treatment of the patient with pelvic floor complaints and disorders. However, the biomechanical effects of these techniques on pelvic floor have not been measured. The results of these therapies have not been evaluated since experimental methods and models were lacking. In the future, the effect of training will be evaluated as a part of the development of an optimal handling of patients with pelvic floor complaints and diseases in collaboration with Department of Physiotherapy (LUMC and OLVG Hospitals). The MRI (positional MRI), IAP measurements and EMG can be used for evaluation of the pre-operative training effectives. The novel diagnostic schedule should be developed in order to optimal decision of further treatment (for example planning the pelvic floor surgery if necessary).

REFERENCES

De Blok, S., 1982. The connective tissue of the adult female pelvic region. A dissectional analysis. Acta Morphol Neerl Scand. 20(2), 191-212.

DeLancey J.O.L., 1992. Anatomic aspects of vaginal eversion after hysterectomy. Am J Obstet Gynecol. 166: 1717-28.

De Vlugt, E., Schouten, A.C., Van der Helm, F.C.T., 2003a. Closed-loop multivariable system identification for the characterization of the dynamic arm compliance using continuous force disturbances: a model study. Journal of Neuroscience Methods 122: 123-140.

De Vlugt, E., Schouten, A.C., Van der Helm, F.C.T., Teerhuis, P.C., Brouwn, G.G., 2003b. A force-controlled planar haptic device for movement control analysis of the human arm. Journal of Neuroscience Methods 129: 151-168.

Gielen, S., 1998. A continuum approach to the mechanics of contracting skeletal muscle. (Phd thesis). Eindhoven University of Technology, The Netherlands.

Huyghe, J.M., van Campen, D.H., Arts, T., Heethaar, R.M., 1991. A two-phase finite element model of the diastolic left ventricle. Journal of Biomechanics 24, 527-538.

Janda, S., Van der Helm, F.C.T., de Blok, S.B, 2003: Measuring morphological parameters of the pelvic floor for FE modelling purposes. Journal of Biomechanics, 36/6, 749-757.

Oomens, C.W.J., Maenhout, M, van Oijen, C.H., Dorst, M.R., Baaijens, F.P., 2003. Finite element modelling of contracting skeletal muscle. Phil. Trans. R. Soc. Lond. B 358, 1453-1460.

Prendergast, P.J., 1997. Finite element models in tissue mechanics and orthopaedic implants design. Clinical Biomechanics, Vol. 12, No. 5, 343-366.

Richter, K., 1966. Lebendige anatomie der vagina. Geburtshilfe frauenheilkd 26, 1213-1223.

Schouten, A.C., Van de Beek, W.J.T., Van Hilten, J.J., Van der Helm, F.C.T., 2003. Proprioceptive reflexes in patients with reflex sympathetic dystrophy. Exo Brain Res 151: 1-8.

Van der Helm, F.C.T., Schouten, A.C., de Vlugt, E., Brouwn, G.G., 2002. Identification of intrinsic and reflexive components of human arm dynamics during postural control. Journal of Neuroscience Methods 119: 1-14.

Van der Linden, B.J., Koopman, H.F., Huijing, P.A., Grootenboer, H.J., 1998. Revised planimetric model of unipennate skeletal muscle: a mechanical approach. Clinical Biomechanics 13, 256-260.

Vankan, W.J., Huyghe, J.M., van Donkelaar, C.C., Drost, M.R., Janssen, J.D., Huson, A., 1998. Mechanical blood-tissue interaction in contracting muscles: a model study. Journal of Biomechanics 31, 401-409.

Voorham-Van der Zalm, P.J., Pelger, R.C.M., Van Heeswijk-Faase, I.C., Wasser, M.N.J.M., Ouwerkerk, T.J., Verhoef, J., Delemarre, H.B.V.M., Lycklama a Nijeholt, G.A.B., 2004. Placement of probes in electro stimulation and biofeedback training. Accepted by the International urogynecology journal and pelvic floor dysfunction.

Yucesoy, C.A., Koopman, B.H.F.J.M., Huijing, P.A., Grootenboer, H.J., 2002. Three-dimensional finite element modelling of skeletal muscle using a two-domain approach: linked fiber-matrix mesh model. Journal of Biomechanics 35, 1253-1262.

Colour Figures

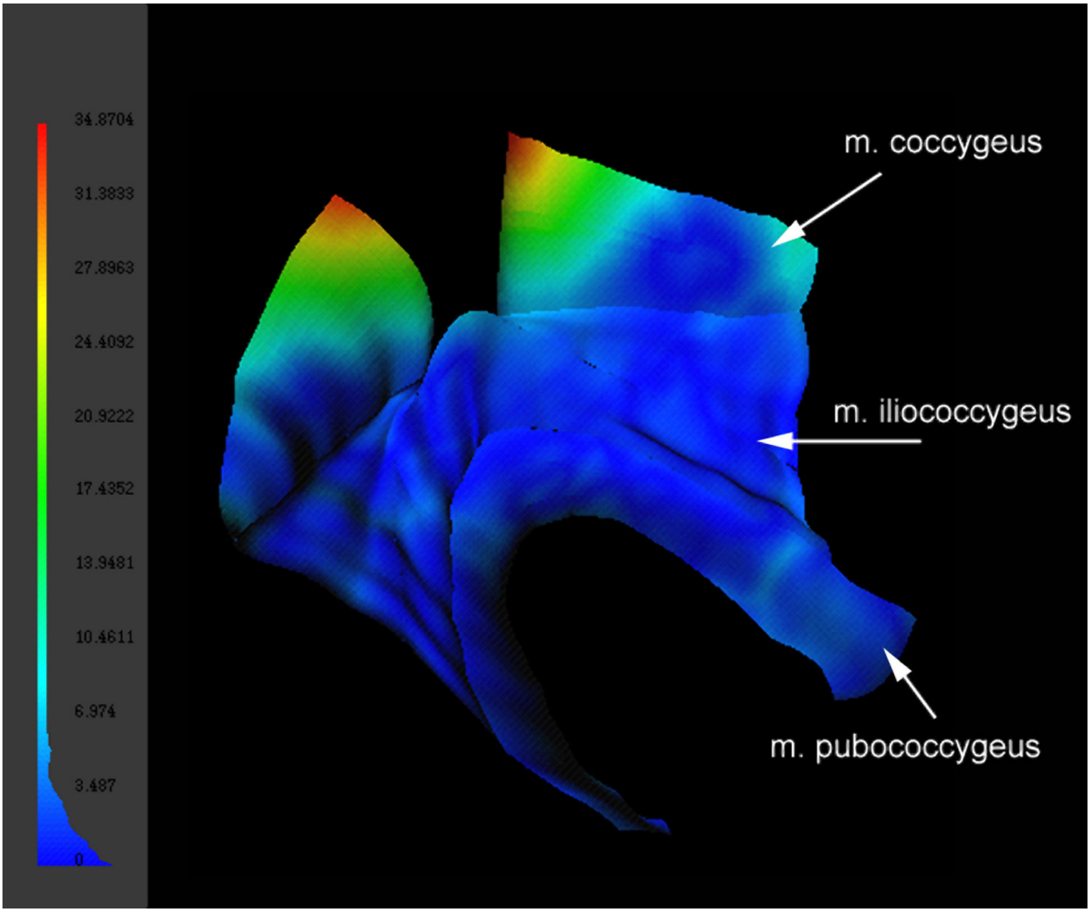

FIGURE 2.6: *The graphical results output from the Metro tool software (Cignoni, 1998). Surface distance-to-distance maximum error colour bar on the left side, the graphical visualisation of the error distribution in the 3D reconstruction of the pelvic floor muscles based on the palpator measurements on the right side. Mean surface-to-surface distance square error is 3.9 mm (see also Table 2.3). The maximal error of 34.9 mm is due to a missing coccygeus muscle part in the 3D reconstruction of the pelvic floor muscles based on MRI data set.*

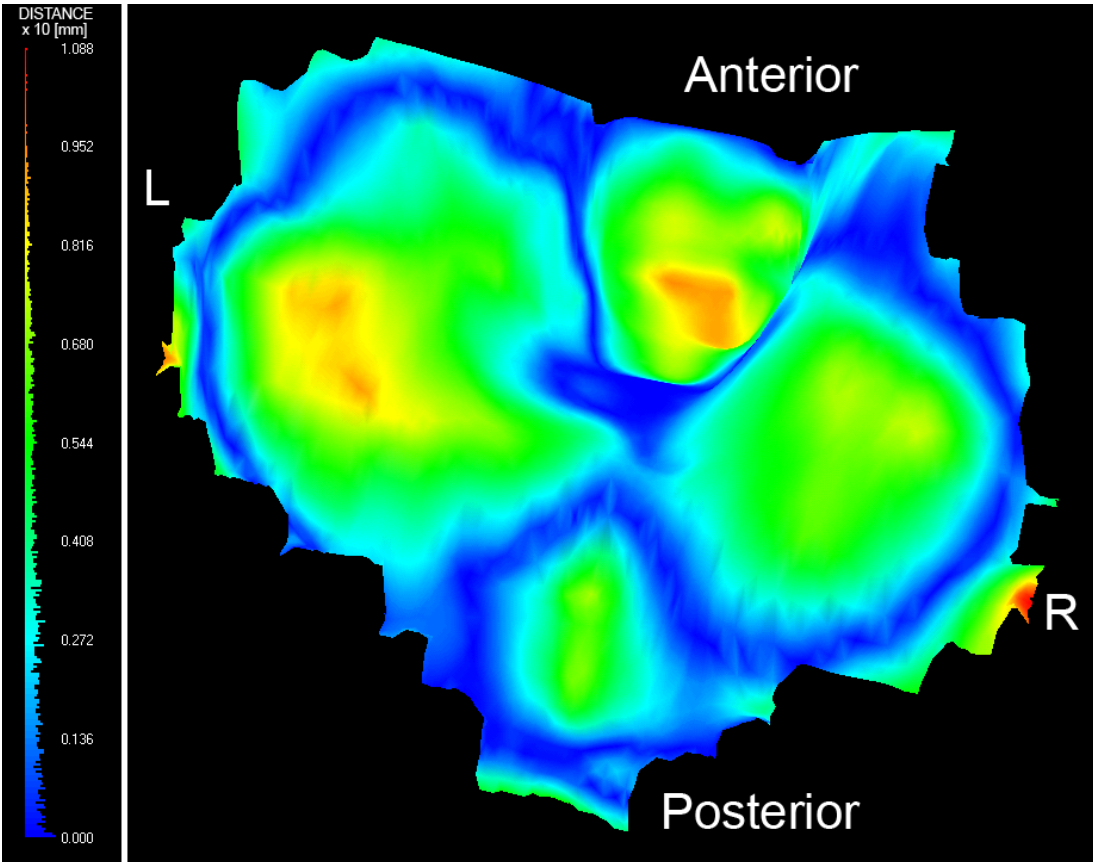

FIGURE 5.2: *An example of the graphical results output from the MESH tool software (Aspert et al., 2002). Surface symmetric Hausdorff distance maximum error colour bar on the left side, the graphical visualisation of the error distribution in the 3D reconstruction of the pelvic floor muscles based on the single line segmentation of the MRI data on the right side. In this particular example the surface model of the whole diaphragma pelvis is compared between the erect and supine positions.*

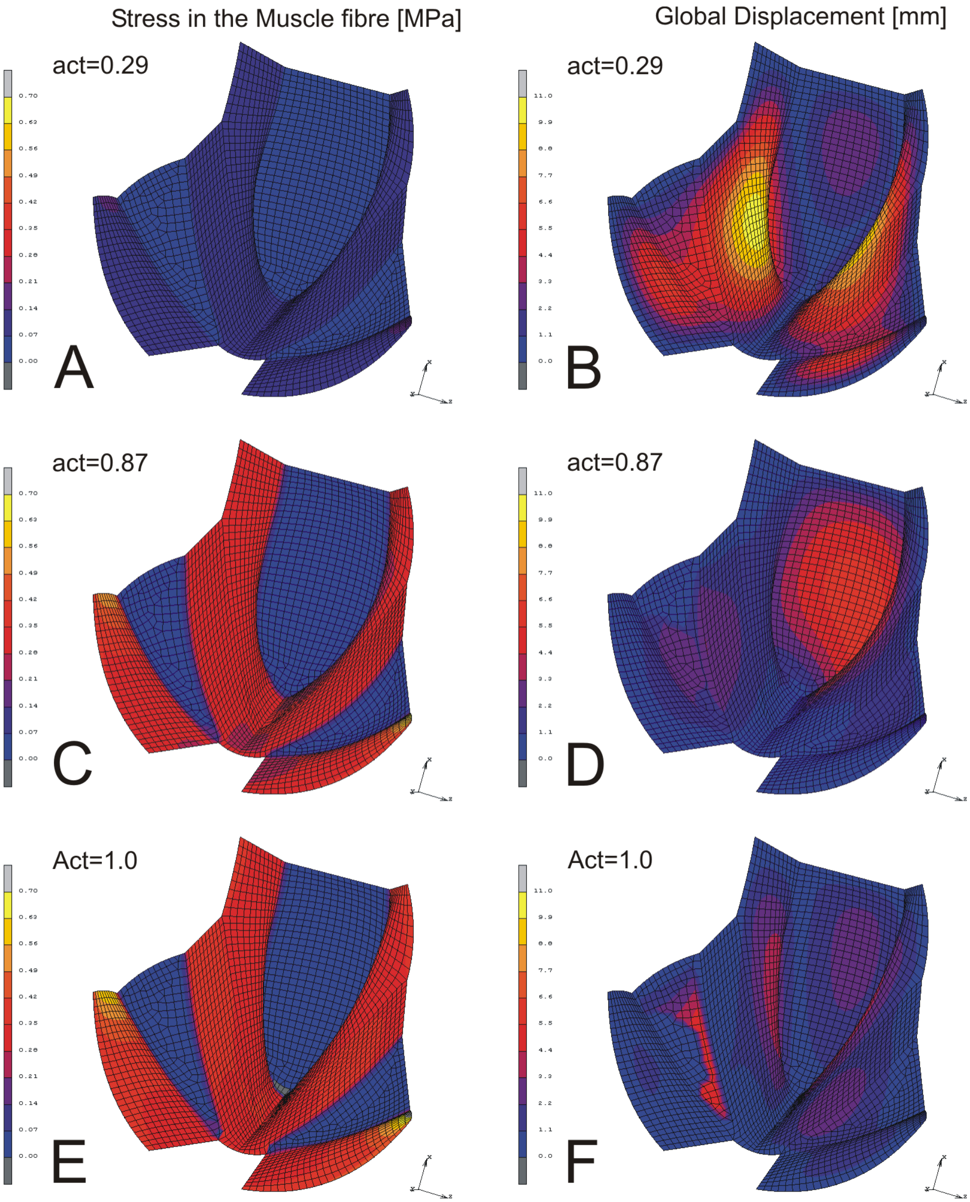

FIGURE 6.5: *Graphical results of the FE analysis of the pelvic floor muscles. The stress in the muscle fibre direction in MPa is displayed in the left column, displacement in millimeters in the right column. The 'active' stress in the connective tissue is zero in image A, C and E, since it is passive tissue. The same scale is used for all three load-cases. Three particular examples are displayed for three conditions: LC1 (rest): 29% activation, 0.01 kPa load - Images A and B; LC2 (max IAP): 87% activation, 5.4 kPa load - Images C and D; LC3 (max ACT): 100% activation, 1.3 kPa load - Images E and F).*

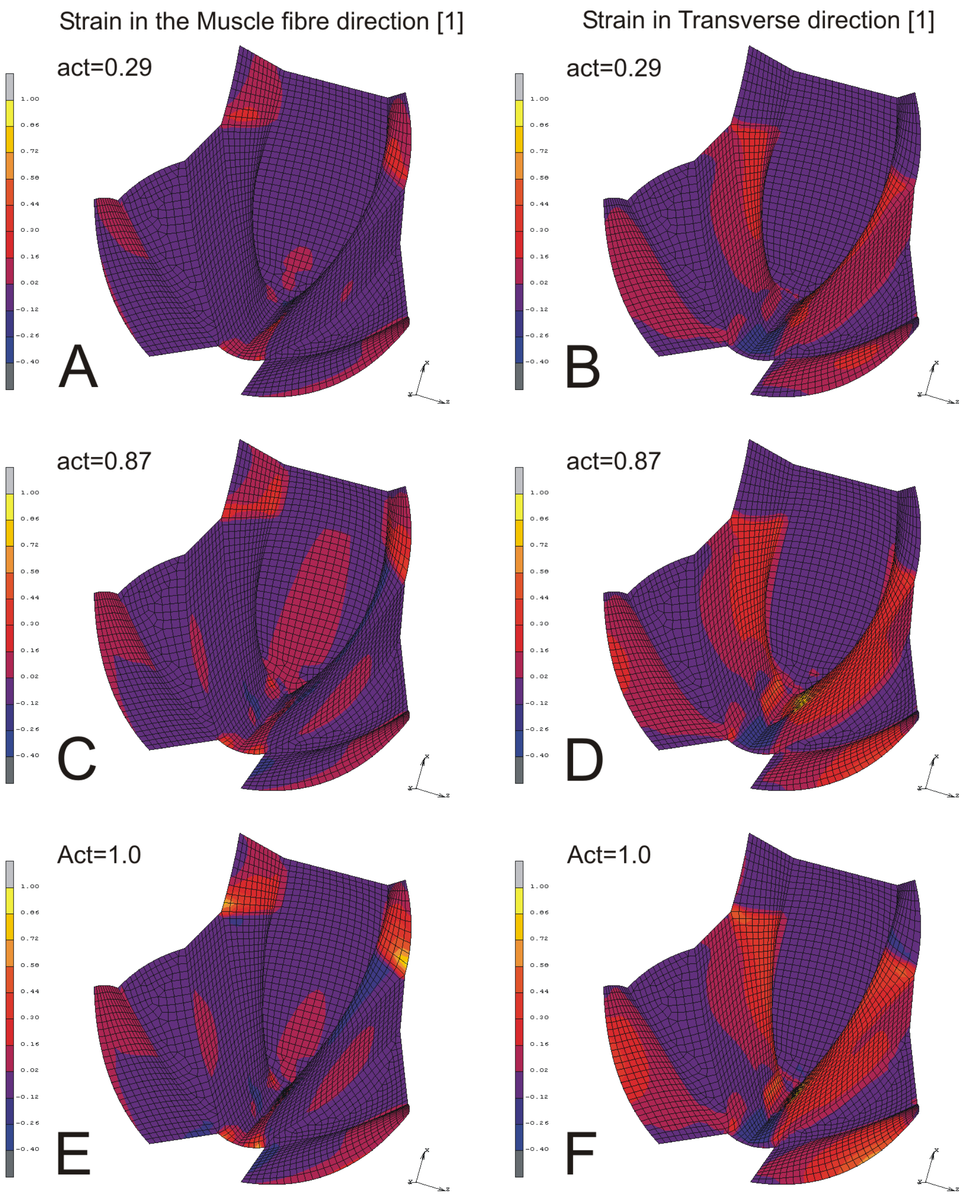

FIGURE 6.6: *Graphical results of the FE analysis of the pelvic floor muscles. The strain in the muscle fibre direction is displayed in the left column, strain in the transverse fibre direction in the right column. The same scale is used for all load-cases. The strain in the connective tissue is displayed in principal directions (the local co-ordinate system). Three particular examples are displayed for three conditions: LC1 (rest): activation 29%, load 0.01 kPa - Images A and B; LC2 (max IAP): activation 87%, load 5.4 kPa - Images C and D; LC3 (max ACT): activation 100%, load 1.3 kPa - Images E and F).*

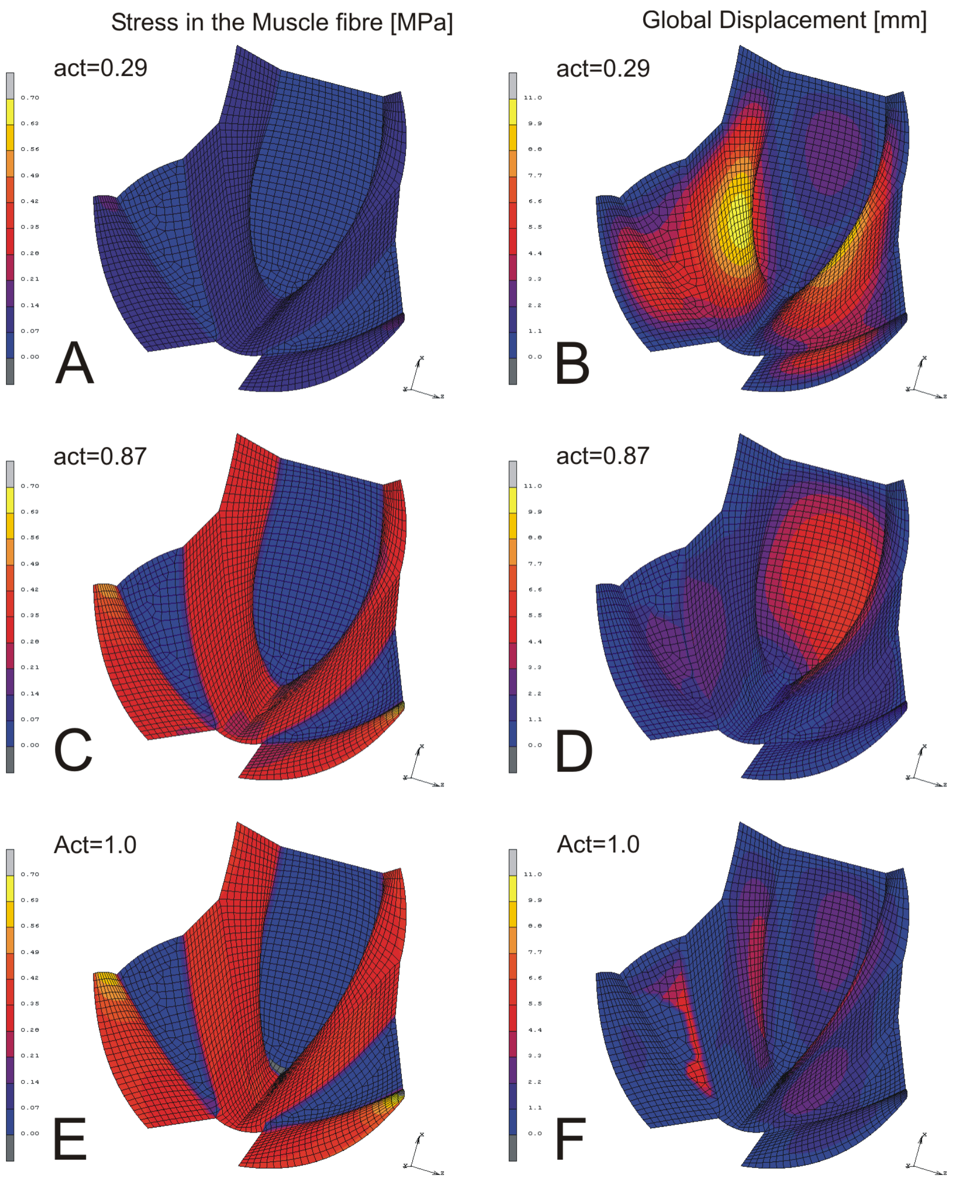

FIGURE 7.2: *Healthy subject muscle activation and stiff connective tissue during all three conditions (see also Table 7.2). Connective tissue I. is used in all displayed conditions. The stress in the muscle fibre direction in MPa is displayed in the left column, displacement in millimetres in the right column. Load-cases H1a (Images A and B), H2a (Images C and D) and H3a (Images E and F) are displayed for three different levels of the muscle activation (29% - Rest condition, 87% - Max IAP condition, and 100% - Max ACT condition). The stress in the connective tissue is zero since it is not an active tissue. The same scale is used for all three load-cases.*

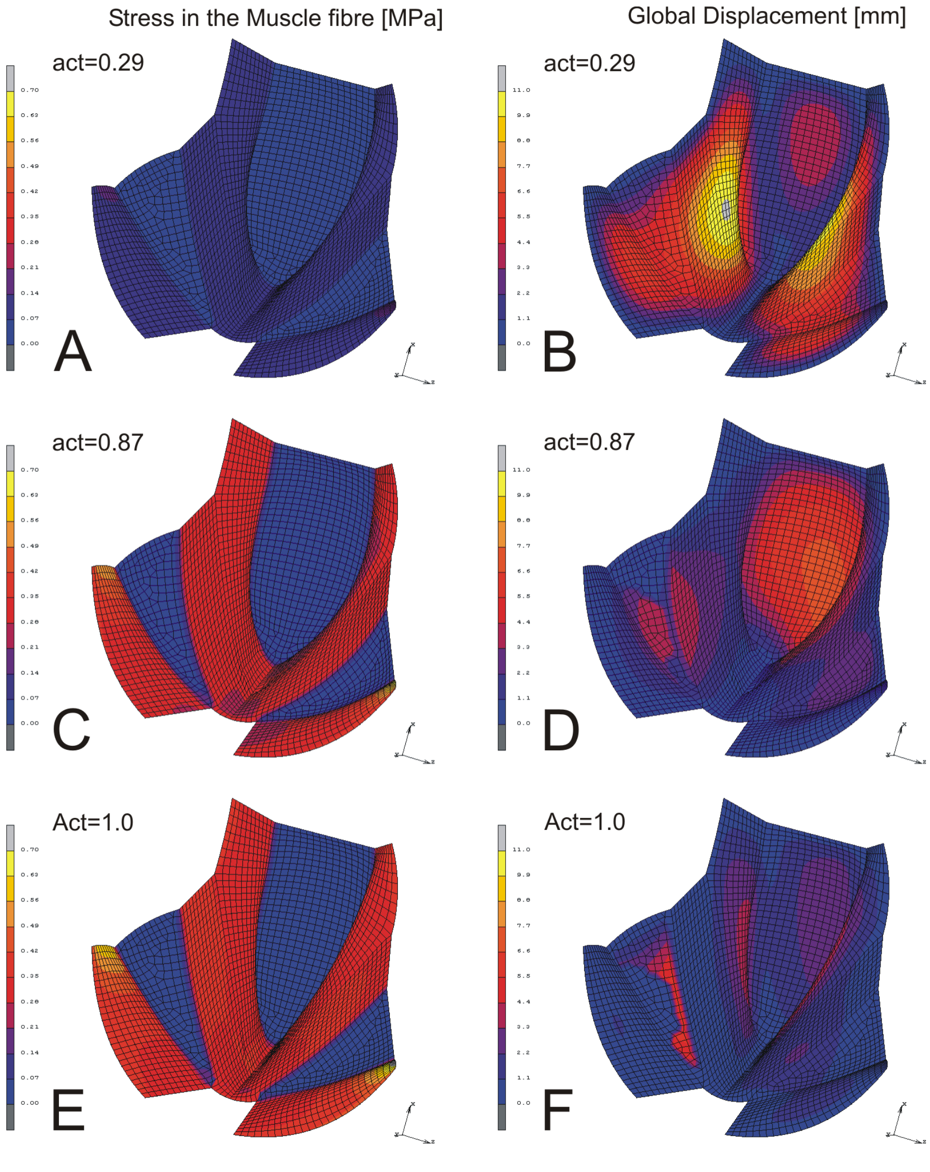

FIGURE 7.3: *Healthy subject muscle activation and a compliant connective tissue during all three conditions (see also Table 7.2). Connective tissue II. is used in all displayed conditions. Graphical results of the FE analysis of the pelvic floor muscles. The stress in the muscle fibre direction in MPa is displayed in the left column, displacement in millimetres in the right column. Load-cases H1b (Images A and B), H2b (Images C and D) and H3b (Images E and F) are displayed for three different levels of the muscle activation (29% - Rest condition, 87% - Max IAP condition, and 100% - Max ACT condition). The stress in the connective tissue is zero since it is not an active tissue. The same scale is used for all three load-cases.*

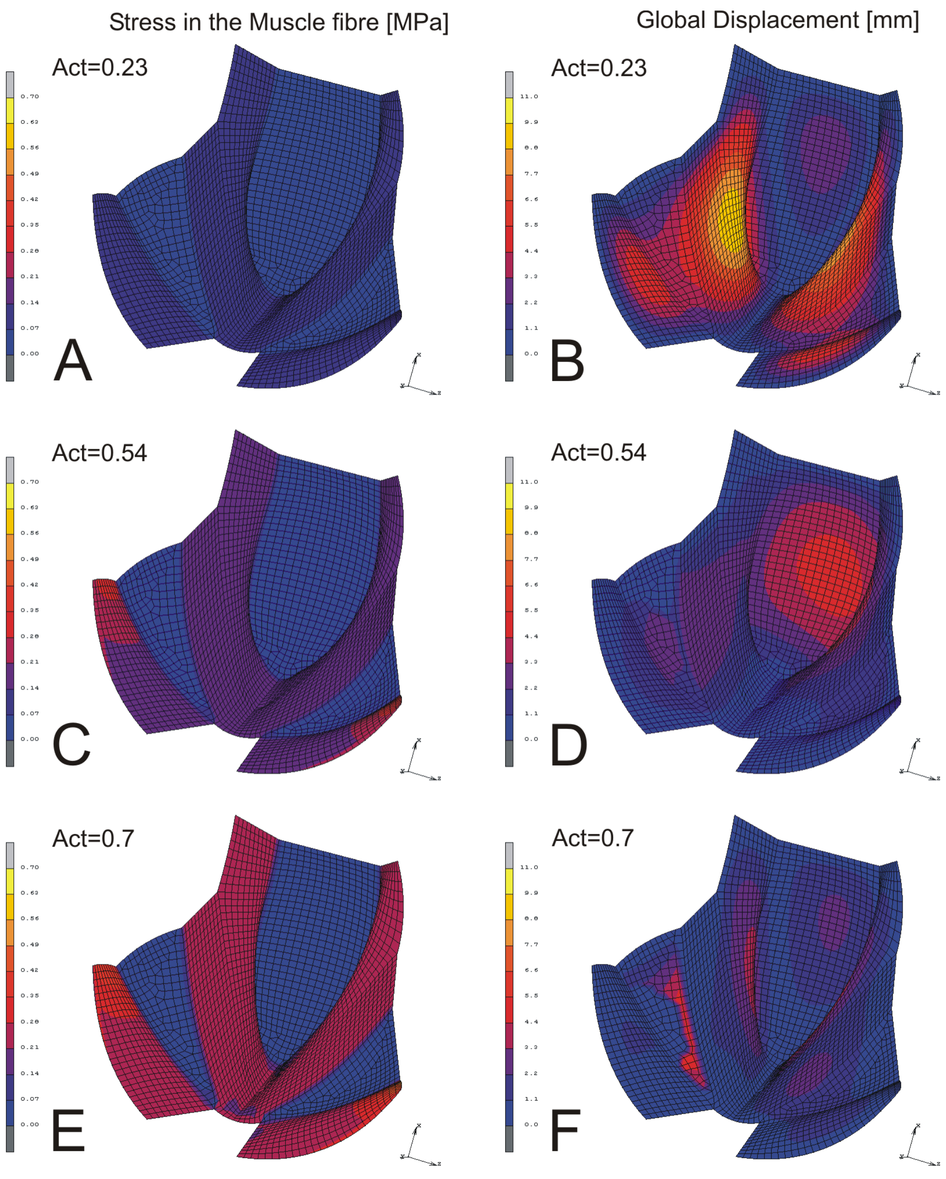

FIGURE 7.4: *Patient muscle activation and strong connective tissue during all three conditions (see also Table 7.2). Connective tissue I. is used in all displayed conditions. The stress in the muscle fibre direction in MPa is displayed in the left column, displacement in millimetres in the right column. Load-cases P1a (Images A and B), P2a (Images C and D) and P3a (Images E and F) are displayed for three different levels of the muscle activation (23% - Rest condition, 54% - Max IAP condition, and 70% - Max ACT condition). The stress in the connective tissue is zero since it is not an active tissue. The same scale is used for all three load-cases.*

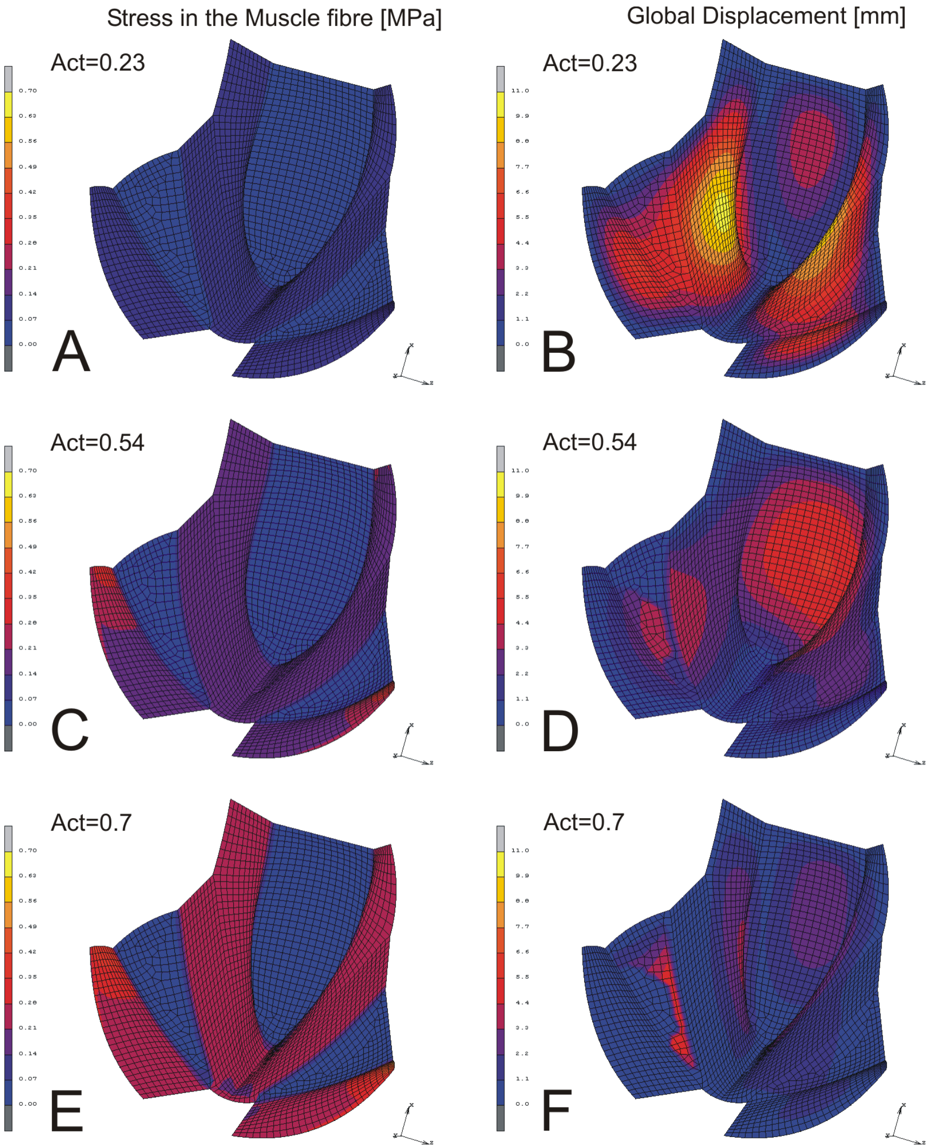

FIGURE 7.5: *Patient muscle activation and compliant connective tissue during all three conditions (see also Table 7.2). Connective tissue II. is used in all displayed conditions. The stress in the muscle fibre direction in MPa is displayed in the left column, displacement in millimetres in the right column. Load-cases P1b (Images A and B), P2b (Images C and D) and P3b (Images E and F) are displayed for three different levels of the muscle activation (23% - Rest condition, 54% - Max IAP condition, and 70% - Max ACT condition). The stress in the connective tissue is zero since it is not an active tissue. The same scale is used for all three load-cases.*

Summary

The present thesis was motivated by two main goals. The first research goal of the thesis was to understand the complex biomechanical behaviour of the pelvic floor muscles. The second goal was to study the mechanism of the pelvic organ prolapse (genital prolapse).

The pelvic floor in humans is a very complex muscular structure. It is largely responsible for supporting both pelvic and abdominal organs, and acts synergistically with the striated muscle of the anterior abdominal wall to generate the intra-abdominal pressure (IAP). It is hypothesized that if the levator ani is pathologically weakened or temporarily inactivated, or the connective tissue of the pelvic floor is not able to maintain support of the organs, a genital prolapse can occur. Genital prolapse is a major cause of morbidity in women.

Although the pelvic floor compartment and the pelvic floor pathology have received major attention, the biomechanical mechanisms determining the behaviour of the diaphragma pelvis (pelvic floor muscles and connective tissue) were not yet understood. The major problems are the complexity of the pelvic floor caused by the complex 3D shape of the pelvic floor, the relation between active muscle tissue and connective tissue, and the complex loading by the IAP and organs acting perpendicularly to the muscle fibres. It is expected that the pelvic floor muscles have a fundamental influence in disorders like genital prolapse.

The main loading of the pelvic floor muscles is due to IAP and the weight of the internal organs. Muscles in joint systems (e.g. in the upper or lower extremities) are activated to exert forces at the bones in line with their muscle line of action. In contrast, the pelvic floor muscles are loaded perpendicular to the muscle line of action by the IAP. A simple representation of the muscle action by a (one-dimensional) muscle line of action is not appropriate, but a more sophisticated approach using a finite-element (FE) model of the muscle is necessary. In a FE model the relationship between the loading and muscle forces in three dimensions can be represented. The model is able to predict the position of the pelvic floor depending on the load (e.g. IAP) and activation of the muscles, and to answer clinical questions by simulating possible failure mechanisms.

The strength of the FE model is the potential to predict the effect of surgical interventions and to give us insight into the fundamental behaviour of the diaphragma pelvis. The factors (e.g. compliant muscle and connective tissue) contributing to the development of the genital prolapse are described in Chapter 7, based on the simulations of the several load-cases arising from observations from the experimental measurements performed on healthy volunteers

and patients. The results from FE simulations are validated using the magnetic resonance imaging (MRI) and electromyography (EMG) data of healthy subjects obtained during three conditions (rest, max IAP and max activation (ACT) of the pelvic floor muscles) described in Chapters 4 and 5.

At the start of the development of the computer model, most of the necessary model parameters were missing. Particularly, the complete geometry of the pelvic floor was not exactly determined (i.e. direction of the muscle fibres, optimum muscle fibre length etc.). Also the material parameters of the muscle (foremost passive as well as active material properties) were unknown. The loading of the diaphragma pelvis during several specified conditions (i.e. rest, performing max IAP and performing max ACT) in both supine and erect position and the effect of loading of the pelvic floor by the weight of the internal organs were unknown, or not exactly determined. The loading of the diaphragma pelvis and the muscle activation are used as input variables for the model. The displacement and stress distribution of the pelvic diaphragma is the output of the model. Determining all these parameters has been described in the particular studies (Chapters 2 to 5):

In **Chapter 2**, the morphology of the pelvic floor is determined. Geometric parameters, as well as muscle parameters, of the pelvic floor muscles were measured on an embalmed female cadaver. A 3D geometric data set of the pelvic floor, including muscle fibre directions has been obtained using a palpator device. A 3D surface model based on the experimental data, needed for mathematical modelling of the pelvic floor, has been created. For all parts of the diaphragma pelvis, the optimal muscle fibre length has been determined by laser diffraction measurements of the sarcomere length. In addition, other muscle parameters such as physiological cross-sectional area and total muscle fibre length were determined. Apart from these measurements we obtained a data set of the pelvic floor structures based on MRI on the same cadaver specimen.

In **Chapter 3**, a new constitutive model for the passive elastic behaviour of human pelvic floor muscles has been developed. Since there was a lack of information concerning material properties of the pelvic floor muscles, we performed uniaxial and equibiaxial measurements. The data obtained are used to fit parameters of the Mooney-Rivlin (MR) constitutive model, which assumes the tissue to be isotropic and incompressible. The constants of the MR constitutive model are obtainable from experimental tests, which should be conducted with similar deformation modes to those appearing in vivo.

In **Chapter 4**, the difference in the displacement of the pelvic floor muscles between 10 patients and 10 healthy volunteers has been presented. The EMG activity, the displacement, the IAP and the width of the levator hiatus were measured. In order to obtain the pelvic floor muscles response, the EMG measurements and the IAP measurements were performed simultaneously.

Displacement was recorded separately using MRI. The study demonstrate: 1) significantly lower muscle activation (EMG activity) in the patient group; 2) no difference in the displacement in relation to the level of IAP; 3) larger width W of the levator hiatus in group of patients with cystocele but no difference in the depth D of the levator hiatus. No significant difference was found in the level of the IAP between groups. Performing MRI scanning in rest and during holding of the maximal level of the IAP provides the best information about the position and the displacement of the pelvic floor muscles. The combination of EMG, IAP and the width W of levator hiatus in these two conditions can be used for diagnostic purposes.

In **Chapter 5**, the effect of the loading of the pelvic floor by the weight of the internal organs in the erect and supine positions has been investigated. The experimental measurements were performed using FONAR, the Indomitable Stand-Up™ MRI machine. The effect of the loading of the pelvic floor (position, displacement and deformation of the diaphragma pelvis) was investigated in 12 female subjects (healthy volunteers) in the erect and supine positions. A highly significant effect in the position of the diaphragma pelvis was found between the erect and supine position. It is obviously caused due to the weight of internal organs. Present clinical MRI evaluation of the pelvic floor muscles performed on patients in the supine position cannot provide the correct information about the functional behaviour of the pelvic floor, since it is not loaded. Performing MRI scanning in supine position during holding the maximal level of the IAP provides diagnostic information about the position and the displacement of the pelvic floor muscles. Loading due to IAP and the weight of internal organs is related to the displacement and shape of the pelvic floor muscles.

In **Chapter 6**, the biomechanical behaviour of the pelvic floor muscles has been analyzed. The approach is to simulate the biomechanical behaviour of the pelvic floor muscles as a response to the loading by the IAP and muscle activation. We develop a FE model of the pelvic floor muscles based on cadaver morphology and a constitutive model for the passive elastic behaviour of human pelvic floor muscles. Thermal shortening in the muscle fibre direction is utilised to represent the muscle activation. One active and two passive layers are used in a multi-layer shell element, representing the active muscle fibres and passive tissue. This concept allows using an orthotropic active layer incorporated in a non-linear passive isotropic matrix formed of passive layers. The active muscle layer is modelled as an anisotropic material layer with defined stiffness in the muscle fibre direction. Three general conditions measured in healthy volunteers (Load-Case (LC) 1 - rest, LC2 maximal contraction of the pelvic floor muscles, and LC3 - holding the maximal level of IAP) are simulated and validated using the experimental data. The results show that the thermal shortening of the element, simulating a muscle force-length relationship, is a simple and effective method for modelling contractile properties of the muscle tissue. The FE analysis of the pelvic floor muscles results in the muscles' displacements in relation to the level of the IAP and muscle activation, which are qualitatively and quantitatively in line with the MRI measurements. The width of the levator hiatus and displacement of the muscle is in a good agreement with experimentally determined values in parenthesis: Width [mm] in LC1 39.4 (34 ± 3.6), LC2 47.6 (47 ± 7.5) and LC3 42.4 (41.9 ± 6.1); the displacement [mm] in LC1 3.28 (not determined), LC2 2.8 (3.2 ± 0.4) and LC3 2.32 (2.8 ± 0.5). It is concluded that the present model describes the muscle forces and displacements well, validated by experimental results. The FE model will be used to simulate the pathological behaviour of patients with a genital prolapse, and to predict the effect of surgical interventions.

Chapter 7 continues the approach from Chapter 6. The FE model is used to understand the development of the genital prolapse as a result of the biomechanical loading of the pelvic floor musculature. Twelve specific load-cases are analysed using a biomechanical model based on FE theory. These load-cases describe the effect of the level of the muscle activation and IAP on the shape and displacement of the pelvic floor. The load-cases could accurately be described by the FE model and validated using the experimental data. Width of the levator hiatus and displacement of the muscle are in a good agreement with experimentally determined values (healthy subject data used for validation: H1a - rest, H2a - max contraction of the pelvic floor muscles and H3a - holding the max level of IAP) in parenthesis: Width [mm] in H1a 39.4 (34 ± 3.6), H2a 47.6 (47 ± 7.5) and H3a 42.4 (41.9 ± 6.1); the displacement [mm] in H1a 3.28 (not determined), H2a 2.8 (3.2 ± 0.4) and H3a 2.32 (2.8 ± 0.5). The hypothesis was tested that genital prolapse might result from compliant connective tissue; Two types of connective tissue with different stiffness are tested. The results show, that the muscle tissue as the only active component in the pelvic floor, plays a major role in the support of the organs in the pelvic floor. When the muscle activation is increasing the upward muscle displacement is increasing as well. The levator hiatus is closing with increasing activation of the muscle tissues, if the pressure is constant. It leads to the conclusions, that: 1) Decreasing muscle activation leads to the increasing width of the levator hiatus, which is associated with the development of genital prolapse. 2) The compliance of the connective tissue of the levator hiatus does not have a significant effect on the width of hiatus, therefore, does not have a significant effect on the development of genital prolapse. 3) The muscle training is efficient since the muscle plays a crucial role in pelvic organ support. 4) Muscle activation is a major factor responsible for the enlargement of the levator hiatus. Therefore, the surgeon has to focus on the levator hiatus width, which should be reduced by use of mesh prosthesis in order to minimize the development of the genital prolapse. Design of a new biomaterial mesh prostheses for surgical repair of the genital prolapse can be based on predictions of the FE model.

Finally, **Chapter 8** discusses results presented in this thesis, and conclusions are drawn. The two main goals are discussed with respect to the validity of the mathematical model based on the FE theory used for studying the biomechanical behaviour of the pelvic floor, the mechanism of the pelvic organ prolapse, the fundamental principle of the behaviour of the pelvic floor muscles and the validity of the experimental data.

<u>This thesis concluded, that:</u>

- Decreasing muscle activation leads to the increasing width of the levator hiatus, which is associated with the development of genital prolapse.
- The compliance of the connective tissue of the levator hiatus has not a significant effect on the width of hiatus, therefore, has not a significant effect on the development of genital prolapse.
- A good quality of the muscle minimizes dispositions to the development of genital prolapse, even if there is a problem related to the compliant connective tissue of levator hiatus. The muscle training can improve the quality and function of the muscle tissue.
- Muscle activation is a major factor responsible for the enlargement of the levator hiatus. Therefore, the surgeon should to focus on the levator hiatus width, which should be reduced by use of mesh prosthesis in order to minimize the development of genital prolapse. Design of a new biomaterial mesh prostheses for surgical repair of the genital prolapse can be based on predictions of the FE model.
- Increased muscle activation resulted in an upward motion (dome shape) of the pelvic floor. Increased IAP (e.g. due to simultaneous activation of the abdominal and pelvic floor muscles) resulted in a downward motion of the pelvic floor (basin shape).
- The results of the FE simulations are in a good agreement with the experimental measurements for healthy subjects as well as for patients.
- The muscle tissue as the only active component in the pelvic floor plays a major role in the support of the organs in the pelvic floor.
- The model can be used for further studying of the function of the pelvic floor and for understanding the substance of disease such as genital prolapse.

Curriculum Vitae

PERSONAL INFORMATION

Name: Štěpán Janda
Nationality: Czech
Date of birth: 08 June 1975
Place of Birth: Jablonec nad Nisou, Czech Republic.

EDUCATION

•2004-	Crash test specialist, Car Development - Computation Department, Škoda-Auto a.s., Mladá Boleslav, Czech Republic.
•1999-2004	Ph.D.-student, BioMechanical Engineering Research Department, Faculty of Mechanical, Maritime and Materials Engineering, Delft University of Technology, The Netherlands. Dissertation on "Biomechanics of the pelvic floor musculature".
•1993-1999	Czech Technical University in Prague - Faculty of Mechanical Engineering, Department of Mechanics, Biomechanics of Man (Engineer degree - equivalent of MSc.). Master thesis on "Mathematical model of the lumbar spine".
•1995-1998	Masaryk Institute of Advanced Studies and Czech Technical University in Prague - Faculty of Teachers Training in Engineering (Bachelor study)
•1989-1993	Technical Engineering High School in Kolín
•1985-1989	2nd Elementary School in Kolín - Mathematics honours
•1981-1985	7th Elementary School in Kolín

OTHER COURSES

•October 2000	Course in vivo NMR, Wageningen University, The Netherlands

PREVIOUS RESEARCH AREAS

•1997-1999	Czech Technical University in Prague, Department of Mechanics. Development of the mathematical model of the lumbar spine.
•1995-1998	Institute of Thermomechanics, Academy of Science, Czech Republic - Development of the four compartment numerical model for hemodynamic effects simulation.
•1995-1996	Czech Technical University in Prague, Department of Mechanics - Mathematical modelling and simulation of the dynamic systems.

Acknowledgements

The work described in this thesis was carried out at the BioMechanical Engineering Research Department at Faculty of Mechanical, Maritime and Materials Engineering, Delft University of Technology. It formed part of the Minimally Invasive Surgery and Intervention Techniques (MISIT) research program. The experimental studies were conducted at the Academic Medical Center Amsterdam (AMC), and Onze Lieve Vrouwe Gasthuis (OLVG) in Amsterdam. I would like to gratefully acknowledge these institutions.

This research work involves multidiscipline studies in which clinical and physiological questions were addressed employing principles of solid mechanics. Therefore, this thesis is a result of a wonderful teamwork and it would never been completed otherwise. During this work, I had the privilege of being surrounded and interacting with a number of fantastic people, some of whom I wish to thank on these pages.

In the first place, I would like to express my gratitude to my promotor Frans van der Helm for his excellent supervision and his critical comments, which made this thesis a lot more valuable in scientific regards. Thank you for making me affiliated with the physiological aspects of the research and for helping me gain the skills of interpreting the results of mechanical analyses leading to physiological conclusions. Your never-ending enthusiasm for the research was most inspiring and encouraging for me. Thanks for keeping me motivated. I would also like to express my gratitude for support and concern in several situations, which made my experience in the Netherlands more pleasant and comfortable.

Henk Stassen, my promotor and the father of the MISIT project. Thank you for inspiring discussions and critical comments. Your enthusiasm for the multidisciplinary research and closing the gap between the engineers and doctors was very inspiring for me.

Sjoerd de Blok, my co-promotor, thank you for the years of pelvic floor surgery and clinical research knowledge and your sage advices. Your never-ending enthusiasm for the research in the pelvic floor was most inspiring and encouraging for me. Thanks for supporting me in the medical part of this research and keeping me motivated during this research. Thank you very much for teaching me all the medical stuff, taking me to the surgery and showing me the “real thinks”, for all your time, effort and insights.

All the AIOs, PostDocs and colleges: Petr, Hans, Martijn, Albert, Gabrielle, Just, Carolin, Evelien, Joanne, Ed, Dennis, Machteld, Mark, Sally, Paulus, David, Ruben, Alfred, Ervin, Richard, Niels, Jan, Magda and Dimitra. It was pleasure working together on a worthwhile project. For some of you, it was pleasure to share the cubicle.

To Albert Vossepoel, Frits Post, Fred van Keulen, for valuable discussions. I enjoyed going to MISIT meetings. Thank you for all the ideas, insight, comments and help.

W.H. Lamers and Kees de Jong from the Department of Anatomy and Embryology of the AMC Amsterdam, thank you for your support and offering the facilities to perform the specimen preparation. Jaap Stoker, from Department of Radiology of the AMC Amsterdam for co-operation and performing the MRI measurements.

Patrick Prendergast and Triona Lally from Bioengineering Group, Department of Mechanical Engineering, Trinity College Dublin, Ireland. Thank you for your support, help and offering the facilities to perform the bi-axial muscle tissue testing. Thank you Triona for a great time during my stay in Dublin.

Victor van der Hulst and Nelly de Jong from Department of Radiology, OLVG Amsterdam for support and offering the facilities to perform the MRI measurements. Marijke Cieremans and Ineke Ruyter-Liem from Department of Physiotherapy OLVG Amsterdam for co-operating during the EMG measurements and instructing subjects.

Robert Gort, Jos Hanraads, Sake Kroondijk and Ico Jongman from Medical Measurement Systems for offering the modular Solar Gold 4T urodynamics system and providing excellent support during our research measurements.

Malcolm Pope from Centre for Biomedical Functional Imaging, University of Aberdeen, Scotland for offering the facilities to perform the vertical MRI measurements. Andrew Bromiley, Tom Davidson for co-operation during MRI measurements and Beverly McLennan and Lindsey Christie for performing the MRI scanning.

Albert Konter from Netherlands Institute for Metals Research Nieuwegein for help and suggestions during using FORTRAN user subroutines within MARC finite-element software package. Thank you very much.

Joane, thank you for being my best fearless test subject during all pilot experiments. I would like to express my gratitude for your help.

Ed, Sally, Charl and Ruben, thank you for help and your endless patience with my English.

Charl for development and programming whatever I wanted for segmentation of the MRI scans. It was my pleasure to do beta testing of your new code.

To all my friends, Petr, Jirka, Jana, Pavel, Jirka, Honza, Leonie, Michal and Ilka. Thank you for doing what friends do.

Petr, I could have made a separate chapter to thank you for all the conversations, never-ending discussions, advices, support, trips, climbing experience, beery depths, Jameson evenings, and so much more, but instead, I would like just thank you for being such a great friend.

Jirka (alias doktor) and Honza (alias krizák), my two Czech friends, thank you for all the time we spent in Delft. It was great to play tennis and to do cycle trips, parties and other stuff together. Thank you for introducing genetic programming to me and trying to teach me Java.

Jirka a Jana, two keen climbers, thanks for all the time we spent together in Delft and Hen Haag. Thank you for the pleasure evenings and never-ending discussions. It was my pleasure and great experience to climb with you and to do all the crazy climbing trips (survivals) to Belgium, France and Luxemburg.

I would like to express my gratitude and thanks to my parents, brother and family who had done every sacrifice necessary to give me a good future. Thank you for always believing in me, encouraging me over the years and keeping reminding me the importance of achieving the goal. I hope that this work make you feel proud.

Finally, I would especially like to thank to my girlfriend Hana. We met in the very hectic period of my research, in the last phase. You gave me all I was looking for. Thanks to you, this hectic final stage was less difficult for me.